Energy, Exergy and Exergoeconomic Analyses of Gas-Turbine Based Systems

by

Khalid Altayib

A Thesis Submitted in Partial Fulfillment

of the Requirements for the Degree of

Master of Applied Science

in

The Faculty of Engineering and Applied Science

Mechanical Engineering Program

University of Ontario Institute of Technology

December 2011

Abstract

Gas turbines are the primary technology used for the purpose of power generation nearly everywhere. In this thesis, the Makkah Power Plant, running on a Brayton cycle, is considered for analysis. The peak demand for electric power in the City of Makkah occurs in the middle of the day during the summer and is almost double the off-peak demand. The plant employs turbines of two world renowned manufacturers. However, there are many mechanical and electrical issues related to the overall insufficient operation of the plant. From the balancing of mass, entropy, energy, exergy and cost equations, a greater understanding of the systems as well as their efficiencies is achieved. The parametric study and plant optimization are performed to investigate the effects of the variation of specific input parameters such as fuel mass flow rate, air volume flow rate and compressor inlet air temperature, on the overall operating efficiency of the system. Through this study, the overall plant energetic and exergetic efficiencies are increased by 20% and 12% respectively with cooling down the compressor inlet temperature to 10^{o}C. Furthermore, exergy and exergoeconomic analyses are conducted to obtain that the largest exergy destruction occurs in the combustion chamber, followed by the turbine. The optimization results demonstrate that CO_2 emissions can be reduced by increasing the exergetic efficiency and using a low fuel injection rate into the combustion chamber. Finally, this study will assist efforts to understand the thermodynamic losses in the cycle, and to improve efficiency as well as provide future recommendations for better performance, sustainability and lessen environmental impact.

Keywords: Gas turbine, Brayton Cycle, Energy, Exergy, Exergoeconomics, Efficiency, Optimization.

Acknowledgements

It gives me great pride to be in a position to thank all those who supported me and the work I performed. First and foremost, I would like to express my deepest gratitude to my supervisor Dr. Ibrahim Dincer. I am forever indebted to him for his constructive support and guidance. His thoughtful advice from the very beginning has always motivated me and given me the confidence to pursue and complete my research effort successfully.

I would also like to acknowledge my exam committee members, for their consideration and time in revising my thesis and their helpful recommendations. Also, I would like to express my deepest gratitude to the faculty and staff of the Faculty of Engineering and Applied Science at the University of Ontario Institute of Technology. I would also like to take the time to acknowledge the encouraging support of Professor Dincer's research group, in particular Dr. Calin Zamfirescu and Pouria Ahmadi. Their helpful insight made for a much more interesting journey in this research endeavour.

I am indebted to my brother and colleague, Musharaf Rabbani for having provided an educational, fun and simulating environment as well as for his great help and support. I would also like to express my deep and truthful thanks to Eng. Abdulhaleem Khan for providing the actual plant data and for his extreme help as well Eng. Faris Mirza for assistance and guidance.

Lastly, but certainly not least, I would like to thank my family. Without their encouragement and understanding it would have been impossible for me to finish this work. To them I dedicate this thesis as my success and accomplishments are a reflection of their love and support.

Table of Contents

List of Figures

List of Tables

Nomenclature

a_n	Coefficient of regression, n = 1,2,3,…,55
$\dot{C}$	Flow cost rate of stream, $/h
$\dot{C}_D$	Cost rate of exergy destruction, $/h
c	Cost per exergy unit, $/kJ
c_p	Heat capacity at constant pressure, kJ/kg K
c_v	Heat capacity at constant volume, kJ/kg K
c_f	Unit cost of fuel, US$
df	Degree of freedom
e	specific energy, kJ/kg
E	Energy, kJ
$\dot{E}$	Energy rate, kW
ex	Specific exergy, kJ/kg
ex^{ch}	Chemical exergy of element, kJ/kg
$\dot{E}x$	Exergy rate, kW
$\dot{E}x_{ch}$	Chemical exergy rate, kW
$\dot{E}x_{th}$	Thermal exergy rate, kW
$\dot{E}_{dest}$	Exergy destruction rate, kW
f	Exergoeconomic factor
G	Gibbs function, kJ
ΔG	Change in Gibbs function for a reaction, kJ
H	Total enthalpy, kJ
h	Specific enthalpy, kJ/kg
h_o	Specific enthalpy at reference state, kJ/kg
h_f	Specific enthalpy of formation, kJ/kmol
MM	Mean square value
$\dot{m}$	Mass flow rate, kg/s
MF	Mole fraction

N	Number of moles, kmol; Annual number of operation hours for the unit, h
P	Pressure, Pa
P_o	Reference-environment pressure, Pa
Q	Heat, kJ
$\dot{Q}$	Heat rate, kW
R	Gas constant, kJ/kg K
SS	Sum of squares
SI	Sustainability index
s	Specific entropy, kJ/kg K
s_o	Specific entropy at reference state, kJ/kg K
s_f	Specific entropy of formation, kJ/kg K
T_0	Reference-environment temperature, K
u	Specific internal energy, kJ/kg
V	Velocity, m/s
$\dot{V}$	Air volume flow rate, m^3/s
$\dot{W}$	Work rate, kW
y	Mole fraction of reactant in combustion chamber
ye	Mole fraction of reactant in environment
Z	Investment cost, US$
$\dot{Z}$	Capital cost rate ($/h)

Greek Letters

ε	CO_2 emission per unit net electricity output (kg_{CO2}/MWh)
φ	Maintenance factor
Δ	Finite change in quantity
η_{en}	Energy efficiency
η_{ex}	Exergy efficiency
η_{ov}	Overall energy efficiency

Subscripts

1,2,……,16 state points

f	Formation
i	Interest rate

Superscripts

$\dot{}$ (over dot)	Quantity per unit time
^{0}	Standard reference states

Acronyms

ABB	Asea Brown Boveri
AAC	Atomizing Air Compressor
ARF	Air to Fuel Ratio
ACFM	Actual Cubic Feet per Minute
CRF	Capital Recovery Factor
GT	Gas Turbine
GTIAC	Gas Turbine Inlet Air Cooling Technology
GE	General Electric
GW	Gigawatt
GWh	Gigawatt-hour
HAP	Hazardous Air Pollutants
HHV	High Heating Value
kVA	Kilo volt-ampere
LHV	Lower Heating Value
LCA	Life Cycle Assessment
MPP	Makkah Power Plant
NG	Natural Gas
RH	Relative Humidity
SOFC	Solid Oxide Fuel Cell
TWh	Terawatt-hour

Chapter 1

INTRODUCTION

1.1 Energy demand and usage in Saudi Arabia

The Kingdom of Saudi Arabia is located in the South Western corner of the Asian Continent. The Kingdom is neighboured by the countries Jordan, Iraq, Kuwait, Bahrain, Qatar, Emirates, Oman and Yemen. Saudi Arabia encompasses land and costal territories of 4431 km and 2640 km respectively, and covers an area of more than 2 million square kilometres [1].

In 2010, Saudi Arabia was listed as the world's largest producer and exporter of total petroleum liquids. They were also ranked the world's second largest crude oil producer, coming just behind Russia. To date, the Saudi economy is still heavily dependent on crude oil. Saudi oil export revenues account for 80-90 percent of total revenues and upwards of 40 percent of the country's gross domestic product (GDP) [2].

The hydrocarbon sector and crude oil industry of Saudi Arabia's is dominated by the state-owned oil company, Saudi Aramco. Saudi Aramco is considered the world's largest oil company with respect to proven reserves and production of hydrocarbons. Saudi Arabia's Ministry of Petroleum and Mineral Resources and the Supreme Council for Petroleum and Minerals have direct administrative control of the sector and Saudi Aramco. The Supreme Council administers policies related to petroleum and natural gas,

including contract review, and also Saudi Aramco's strategic planning. The Ministry's responsibilities relate to national planning in the area of energy and minerals, and include petrochemicals [2].

Not only Saudi Arabia is considered one of the world's major energy producers, it is also ranked among the world's largest energy consumers. Saudi's primary energy consumption was recorded as high as 100.5 Mtoe (Million Tons of Oil Equivalent) during 1998. This was an increase of 4.2 per cent, when compared to the 96.3 Mtoe of 1997[3]. In a study by Dincer and Alrashed [3], a linear regression trend line is applied to currently available data illustrating the future projected total energy consumption over the next two decades, Figure 1.1.

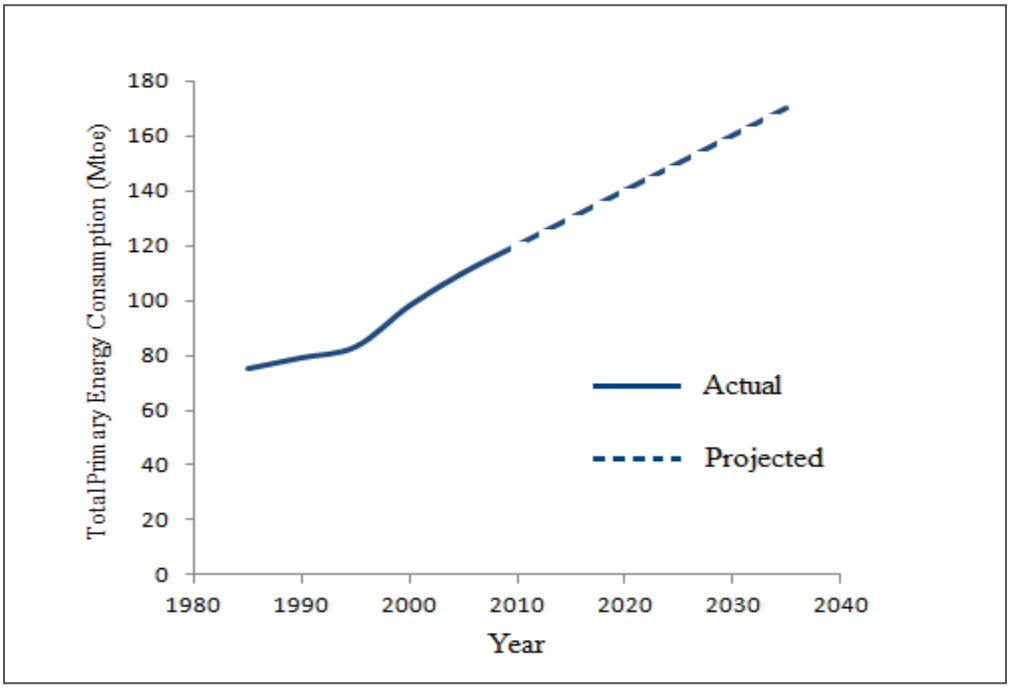

Figure 1.1 Total primary energy consumption of Saudi Arabia (Data from Ref. [3]).

In Saudi Arabia, they are specifically utilizing petroleum product in the areas of transportation fuels and direct burn for power generation [2]. Domestic consumption has been spurred by economic boom due to historically high oil prices and large fuel subsidies. In 2008, Saudi Arabia was ranked 15th largest consumer of total primary energy. Of their power consumption, almost 60 percent was petroleum-based and the rest natural gas. Saudi Arabia is moving forward with plans of nuclear reactors by 2020 in order to meet domestic power needs. This will free up oil and natural gas reserves for export and higher-end uses other than direct burn for power generation. At present, Saudi Arabia is participating in the Gulf Cooperation Council's efforts to link the power grids of member countries, with the goal of reducing shortages during peak periods. Figure 1.2 illustrates the total energy consumption of the year 2008.

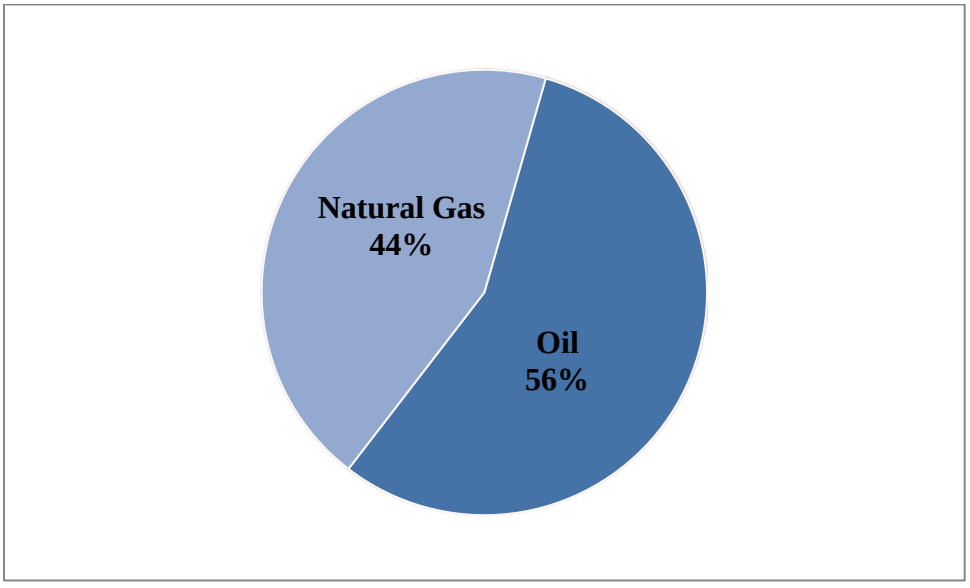

Figure 1.2 The total energy consumption in Saudi Arabia, 2008 (Data from Ref. [4]).

In this regard also, Saudi Arabia is shifting its focus beyond increasing its upstream oil production since Saudi Aramco said that it had reached its target production capacity of 12 million barrels per day. In addition, its spare oil production capacity is well above Saudi Arabia's stated target of 1.5-2 million barrels per day. Subsequently, Saudi Arabia is moving to diversify its economy by expanding its refining, petrochemicals, and mineral products industries [2]. Between the years 1999 to 2009, the Kingdom of Saudi Arabia experienced rapid growth of both its industrial base and population. These trends, along with the stimulus of low fuel costs and low electricity tariffs increased the electrical output demand of the power generating facilities of the country between 5% and 7% per annum. The number of electricity consumers rose by 64% to 5.7 million, peak demand by 82% to 40 GW and energy sales by 70% to 193 TWh [5].

The rates of energy consumption within different sectors are considered basic economic indices in the analysis of the economy’s growth and activities. The economy and individual sector expected growth in energy consumption, and the direction in each sector is considered in future development plans. In a study conducted in 1999, predictions were made on the growth of these sectors and the overall economy up to the year 2005 [6]. The values tabulated in Table 1.1 represent a rise in the cumulative energy consumption in all sectors from 418 mb equivalent (1146 thousand barrels per day) in 1986 to 616 mb equivalent (1688 thousand barrels per day) in 1996, denoting a rise of 4.1 per cent per year. It was expected that the cumulative energy consumption of the sectors

would increase by 7.3 per cent per year during the period between the years 1996-2005, reaching an estimated value of 1163 mb equivalent (3186 thousand barrels per day) in 2005.

Table 1.1 Saudi Arabia's sectoral energy consumption (thousand barrels crude oil equivalent).

Sector	1986	1991	1996	2000	2005
1. Transportation sector	144,059	148,154	161,120	174,106	191,663
• Land transport	764,68	103,258	128,307	140,873	155,783
• Air transport	16,250	28,434	19,107	20,167	22,192
• Sea transport	51,341	16,462	13,706	13,066	73,688
2. Agriculture sector	26,250	41,250	29,250	9,699	8,140
3. Service sector	131,776	169,661	226,562	308,431	360,566
4. Industrial sector	95,554	130,798	180,300	440,460	578,463
5. Commercial and residential sector	5,910	7,118	9,626	10,943	12,812
6. Construction sector	14,747	8,834	9,445	10,943	11,753
Total cumulative energy consumption	**418,296**	**505,815**	**616,303**	**954,582**	**1,163,401**

Source: [6]

The vast nation utilized little of its terrain for urban or agricultural needs, such that vast areas are uninhabited desert. The desert climate is harsh and dry with great temperature extremes. As a result, Saudi Arabia faces multiple environmental concerns, including desertification and the depletion of underground water resources. Statistical rainfall data available from the Ministry of Water and Electricity show that on average,

urban areas of Saudi Arabia receive just 10 mm of rain per month [1]. The lack of perennial rivers or permanent water sources has prompted the development of extensive seawater desalination facilities for domestic use. In 2007, demand for water in Saudi Arabia was more than 2 billion cubic meters; 54% of which was met from seawater desalination plants [1]. The limited supply of water has led Saudi industry to minimize its use of water to less than 3% of the total annual consumption of the country. Moreover, industries in the Kingdom have been searching for alternatives to the use of water in several applications. For example, Saudi industry has seen wide-spread use of less efficient air-cooled condensers instead of water-cooled condensers as a reaction to lessening water consumption.

Due to its harsh desert climate, Saudi Arabia faces large seasonal temperature variations. There are even extreme temperature variations depending on the time of day. As a consequence, electricity demand varies considerably from summer to winter and from day to night. The peak demand period for electric power occurs during the middle of the day in the summer, mainly due to the cooling loads required by air conditioning equipment [2]. The measured electric power consumption for a large facility in Riyadh during a summer's day is shown in Figure 1.3. For this facility, electric power consumption during peak times reaches almost 9 MW, which is twice as much as the consumption during off-peak times.

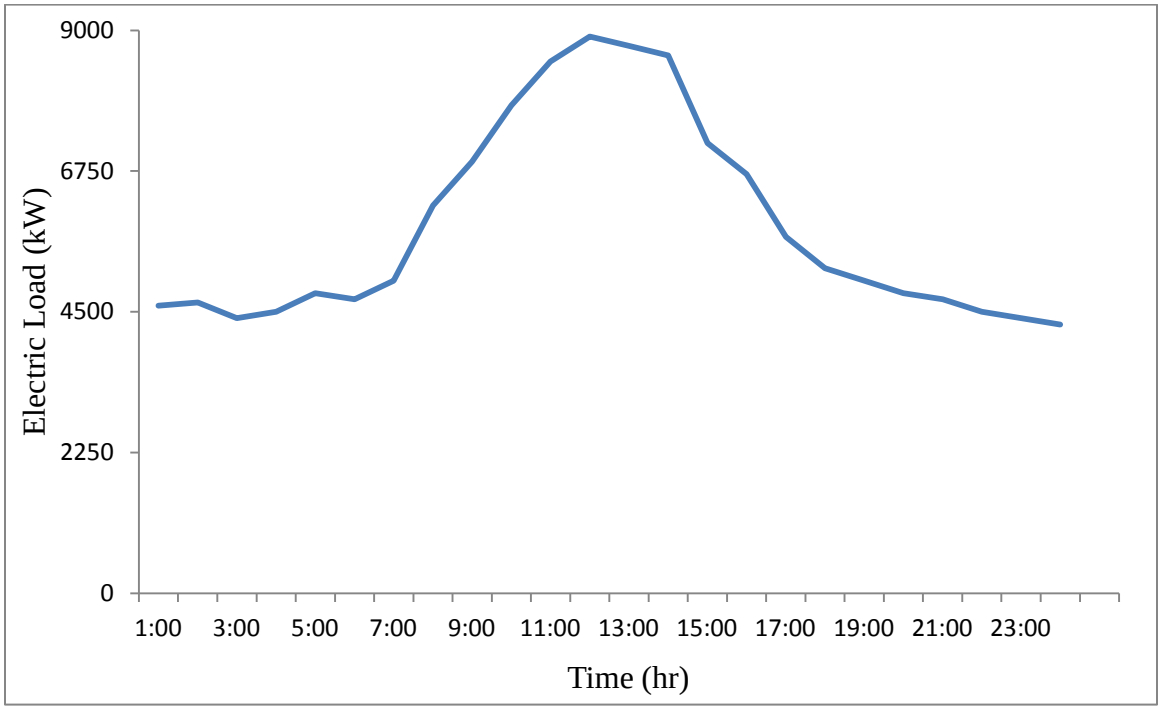

Figure 1.3 Electric power consumption for the King Abdulaziz City for Science and Technology Complex for Aug 22nd (Data from Ref. [1]).

In order to meet expected future energy demands, the Ministry of Water and Electricity of Saudi Arabia has plans to increase peak demand capacity to an additional 35 GW by 2023 at an estimated cost of $120 billion [1]. In addition to increasing energy demands, the Kingdom faces a rapidly increasing demand for desalinated water. Much of the increased demand stems from cogeneration plants that export excess power to the electricity grid. To meet this demand, the Saline Water Conversion Company is planning integrated power and water projects worth an estimated $50 billion by 2020 [1]. These enormous increases in demand will be met by investments in new power plants as well as in upgrading existing power infrastructures.

In 2008, the electric utility provider in Saudi Arabia, Saudi Electricity Company (SEC) produced a total of 178430 GWh of power. Of the total produced power, 79130 GWh (44.3%) was produced by simple cycle gas turbines, 15131 GWh (8.5%) produced by combined cycle gas turbines, 81770 GWh (45.8%) produced by steam turbines, and 2399 GWh (1.3%) produced by diesel engines [1]. However, the efficiency of gas turbines (GT) has been found to decrease with increased inlet-air temperature. This implies that as air-conditioning demand increases, the ability of the turbines to meet the demand decreases. Experience with simple cycle GT in the central Qaseem region of Saudi Arabia, shows that high midday ambient temperature during the summer can cause a 24% decrease in system capacity [1].

Saudi Electricity Company (SEC) has three major options in dealing with their GT efficiency issues. They can choose to install new GT to deal with peak demand and that would only be used during peak demand. The alternative to the expensive instillation of additional GT's is dealing with the issue itself. The intake air can be cooled prior to it proceeding through the GT by applying the various gas turbine inlet air cooling (GTIAC) systems. A coolant system ahead of the entering GT's is the more economic choice than first one. The last solution is to do a mathematical optimization of input parameter such as operating temperature, pressure and both fuel and air mass flow rate. Therefore and based on the given actual power production data of Makkah Power Plant (MPP), optimization was done using Design-Expert® Stat-Ease (*version 8.1.6*) in order to find optimum operating conditions. The goal was to find such processing conditions

which maximize energy efficiency, exergy efficiency and net work output. In addition the optimizing work, conceptual design has been conducted to examine the options open to SEC and identify key benefits and drawbacks in relation to the environmental conditions and generational requirements of Saudi Arabia.

1.2 Motivation and objectives

The gas turbine is by far the most commonly used power generation technology globally. This is especially true of oil producing nations such as the Kingdom of Saudi Arabia where gas or liquid fuel is readily available. In this study, the Makkah Power Plant, running a Brayton cycle is the case study being considered in this analysis.

This thesis presents an in-depth investigation into two different open gas turbines. The two gas turbines, despite having their own hardware design, are Brayton cycle turbines. The two systems are used for the analyses performed in this study. Figure 1.4 demonstrates the outline of the work done in this thesis.

The objective of this study is to define the system and its components as well as operational, economical and environmental conditions. Moreover, a comprehensive thermodynamic analysis using energy and exergy analyses is conducted, of a gas turbine based cycle.

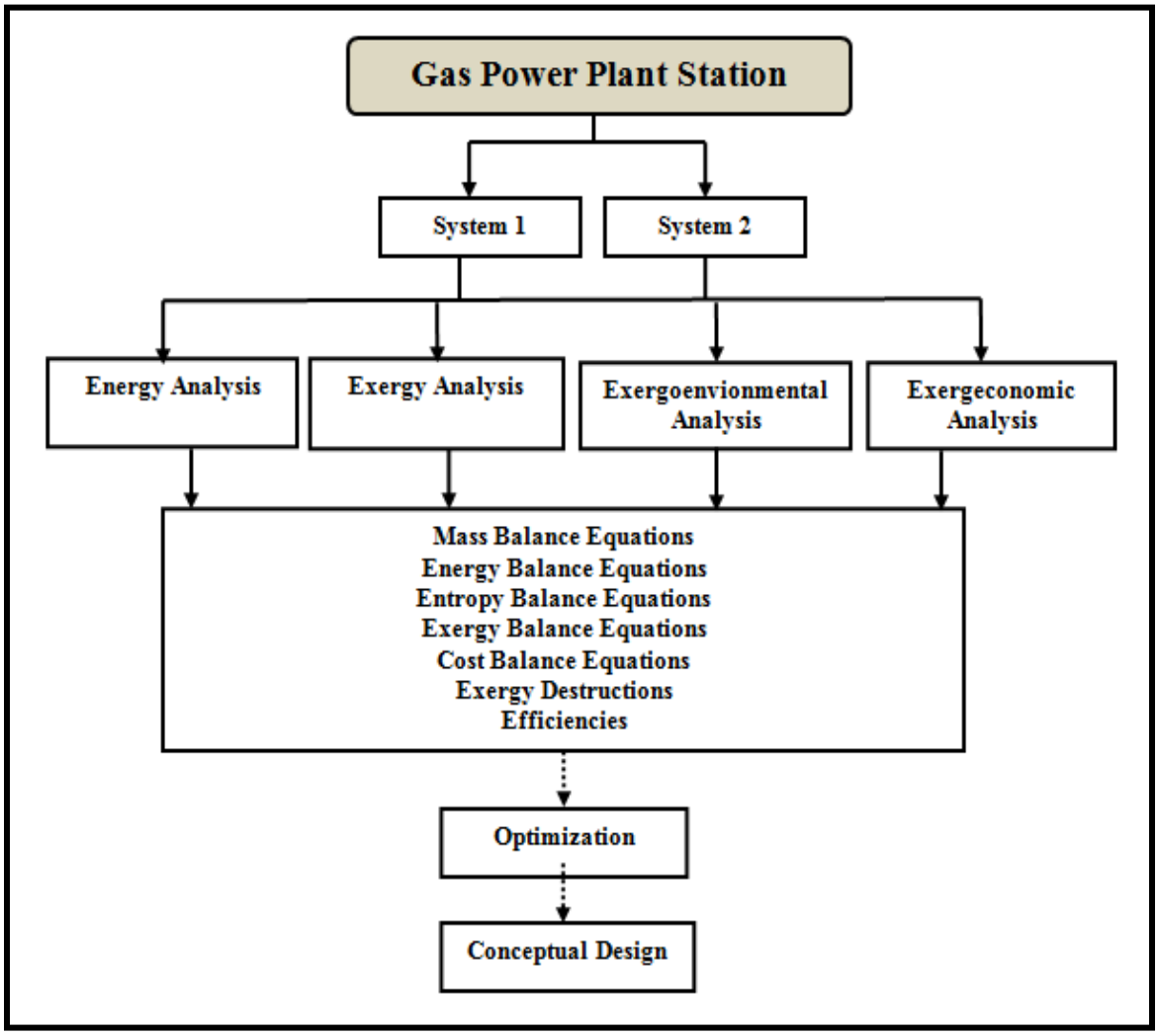

Figure 1.4 Elements of the thesis.

The first objective is two-fold to achieve the following tasks:

- To conduct an energy analysis of an industrial open gas turbine system.
- To conduct an exergy analysis of an industrial open gas turbine system.
- To determine the quantities and locations of exergy destructions in the open gas turbine.

The second objective is to do a parametric study of the enhancement of the turbine system via varying input parameter such as:

- Compressor air inlet temperature.
- Fuel flow rate.
- Air volume flow rate.

The third objective aims to conduct exergoeconomic analyses for each component to calculate:

- Cost of each stream of the system.
- Cost of exergy destruction of each component.
- Exergoeconomic factor for each component.

The forth objective is to perform the environmental impact assessment of the system to:

- Calculate the CO_2 emission of the system.
- Determine the sustainability index and find the relation between exergy and environmental impact.

Chapter 2

LITERATURE REVIEW

2.1 Energy and exergy studies

Total energy is the sum of available energy plus unavailable energy. The flow of energy in a system is comprised of both available and unavailable energies. The total energy of a system is simply called *energy*, while the available energy is termed *exergy*. Dincer and Rosen [13] elaborate on the concept of both energy and exergy. They discuss the fact that energy balance does not provide information regarding the degradation of energy or resources during a process. Nor does it quantify the usefulness or quality of the various forms of energy in the material streams flowing through a system that exists as products and wastes.

2.2 Exergy analyses and related aspects

Exergy is based on both the first and second law of thermodynamics. Dincer and Rosen [13] prove that exergy analysis clearly indicates the locations of energy degradation in a process. The results of such an analysis can lead to improved operation and improved technologies. Also, the analysis can quantify the quality of heat in a waste stream. Moreover, Hermann [14] defines exergy as a means of assessing and comparing the reservoir of theoretically extractable work we call energy resources. Resources are considered either matter or energy with properties that differ from the predominant

conditions in the environment. The differences can be physical, chemical, or even nuclear exergy.

Ganapathy et al. [15] perform an exergy analysis of a 50MW combined power plant located in India. They determined that major exergy losses were taking place in the condenser. In this case, the energy could not be used elsewhere. They also suggest modifications be made to the combustor due to high exergy loss. Horlock et al. [16] perform an exergy analysis for three different fossil fuel based power plants. They also find that irreversibility's take place during combustion. Dincer et al. [17-23] discuss exergy analysis of a variety of processes and system components. Sue et al. [24] also discuss application of exergy analysis for a gas combustion turbine based power generation system. Their results demonstrate that exergy analysis is a more accurate assessment of a plant's efficiency. Also, exergy destruction during combustion decreases with an increase in the pressure ratio. In the work of Haseli et al. [25], the thermodynamics analysis of a combined gas turbine power plant with a solid oxide fuel cell is discussed. The results of that analysis show that increasing the compressor inlet temperature decreases both energy and exergy efficiencies for both conventional and the solid oxide fuel cell (SOFC) power plants. However, a gas turbine with SOFC has a 26.6% better exergetic performance.

In a study performed by Bonnet et al. [26], the coupling of an Ericsson engine, with a system involving natural gas combustion. In designing this plant, they utilized energy, exergy and exergo-economic analyses. The study focused on the design and

performance of a real engine rather than a purely theoretical thermodynamic cycle. This allowed a balancing of energy performance with heat exchanger sizes, the plotting of Grassmann exergy diagrams, and the evaluation of costs of thermal and electrical energy production processes.

Energy and exergy analyses are applied by Camdali et al. [27] to a dry system rotary burner with pre-calcinations in an important Turkish cement plant using actual data. The rotary burner included thermal and chemical processes. The first and second-law efficiencies are determined. In South Africa, energy and exergy analyses of energy consumptions in the industrial sector are analyzed by Oladiran et al. [28].

Tatiana et al. [29] also consider the exergy analysis of a simply open gas turbine system. They demonstrate the importance of studying the thermodynamic performance of a system component in order to determine which component of the system is causing exergy destruction and how to avoid it.

The thermodynamic performance of a water electrolysis process for the purpose of producing hydrogen also is investigated by Rosen [30], using both energy and exergy analyses. Three cases are presented in which the principal driving energy inputs are (i) electricity, (ii) the high-temperature used to generate the electricity, and (iii) the heat source used to produce the high-temperature.

2.2.1 Exergy efficiency

The definition of an open cycle rational efficiency is defined by Horlock et al. [16]. He explicitly relates to the ratio of the actual shaft work output from a power plant to the maximum work that could be obtained in a reversible process between prescribed inlet and outlet states. However, since different constraints may be applied to such an ideal reversible process, the maximum work obtainable would be variable. As a consequence so would the value of the rational efficiency.

Dincer and Rosen [13] clearly differentiate energy and exergy efficiencies and outline the key features of exergy efficiency. They state that exergy efficiency frequently provides a finer understanding of performance than energy efficiency. Energetic efficiency does not differentiate different forms of energy, whether it is shaft work or a stream of low-temperature fluid. Also, energy efficiency is most concerned with reducing energy emissions to improve efficiency. In contrast, exergtic efficiency weights energy flows by accounting for each form of exergy present in the system. It deals with both waste emissions (external irreversibilities) and internal irreversibilities in order to improve performance. In many cases, it is the irreversibilities that are more significant and more difficult to address, such that a judgment has to be made as to what is the product, what is counted as a loss and what is the input. Different decisions about these lead to different efficiency expressions within the class.

For the reduction in consuming materials and energy, and to promote the use of renewable resources, Azouma et al. [31] prove that conclusions based on thermal efficiencies are not sufficient to attain best performance of the engine. Due to technical

constraints (e.g. incomplete combustion), from the viewpoint of the second law of thermodynamic, a combination of exergy analysis and gas emissions analysis was necessary in the proposal of a trade-off zone of engine load that could accommodate environmental concerns and engine efficiency. Though, exergetic efficiency takes into account not only quantity but also quality of energy flows.

2.2.2 Chemical exergy

The application of chemical exergy analysis, by many researchers, in the study of energy system efficiencies is documented frequently. Exergy analysis proves its usefulness in providing accurate insight into the efficiencies of many energy systems. Rivero et al. [32] revise the model proposed by Szargut for the calculation of the standard chemical exergy of elements, organic and inorganic substances. In Rivero's revision of Szargut's model, he compares his revised values of standard chemical exergy to those of Szargut [32]. In the work by Ertesvag [33], the variations of chemical exergy are investigated for gaseous fuels and atmospheric gases with reference-environment temperatures ranging from -30°C to 45°C, pressure from 0.6 bar to 1.1 bar and relative humidity from 10% to 100% using Szargut's model.

The exergy analysis performed by Gao et al. [34] on a coal-based polygeneration system for power and chemical production shows significant improvement in energy savings when compared to individual systems. The results of the analysis indicate that the combination of a power system with a chemical process results in 3.9% energy savings. Gao states that the "synthesis on the basis of thermal energy cascade utilization

is the main contribution to the performance benefit of the polygeneration system" [34]. A key criterion of a polygeneration system is the capacity ratio of the chemical process to the power system. This ratio strongly affects the matching of the two sides involved in the polygeneration system. Moreover, besides the thermal energy integration, the cascade utilization of the chemical exergy is likely to be a key issue in further studies of polygeneration systems.

The effect of variations in dead-state (a state that is in thermodynamic equilibrium with its surroundings) properties on energy and exergy analyses studied by Rosen et al. [35]. In that research, effort the sensitivities of energy and exergy values to the choice of the dead-state property is examined. Furthermore, the sensitivities of the results of energy and exergy analyses of complex systems and choice of dead-state property are also studied. A case study of a coal-fired electrical generating station was employed in order to illustrate the influence of dead state properties. It is demonstrated, however, that the effect of dead-state properties on energy and exergy values is dependent on intensive variations of the properties. Moreover, the main results of energy and exergy analyses are typically insensitive to reasonable variations in these properties.

2.2.3 Exergoecomonic analysis

Exergoecomonic analysis helps engineers to determine ways to improve the performance of a system in term of cost. This can play a crucial role in analyzing, designing and optimizing any thermal systems. Thermoeconomic optimization is an effective tool to

find out the best solutions between the two rival points, maximizing exergetic efficiency and minimizing economic costs.

Kwak et al. [36] perform exergetic and thermoeconomic analyses on a 500-MW power plant running a combined cycle system. In their analysis, they studied the conservation of mass and energy of each component in the system. They also consider the quantitative balance of exergy and exergetic cost (exergoeconomics) associated with each component, and for the system as a whole. In an exergoeconomic model, they represent the productive structure of the system to envision the cost associated with the formation process and the productive interaction between components. Kwak develops a computer program for the purpose of determining the production costs of power plants utilizing gas or steam turbines, or a combination of the two (cogeneration plant). The program could also be used to study plant characteristics, particularly thermodynamic performance and system sensitivity change. The sort of changes implied here are in process and/or component design variables.

In recent decades, interest in exergoeconomics (or thermoeconomics) has increased as researchers seek to bridge the concepts of thermodynamic principles with economics. A major contribution to the interest in the topics can be attributed to power generation and cogeneration plant development. Increasing demand for cheap, clean, efficient power around the world implies the need of effective trade-off studies. Rosen et al. [37] perform an exergoeconomic analysis of a coal-fired electricity generating station. In their analysis, they find the ratio of the rate of thermodynamic loss to capital cost to be

a significant factor in the evaluation of plant performance. The ratio was considered a potential measure of the trade-off bridging thermodynamic and economic concerns successfully in plant designs. In the work presented by Tsatsaronis [38], he introduces and defines several terms used in exergy analysis and exergy costing. He also discussed various options concerning symbols and parameters that could be used for exergy, including some exergoeconomic variables. He then continued to present the nomenclature for the remaining terms of his paper.

Ameri et al. [39] perform a study carrying out energy, exergy and exergoeconomic analyses of a steam power plant in Iran. In their study they considered the effect of the load variations and ambient temperature on component exergy destruction. The results of the energy analysis indicate energy losses to be mainly associated with the condenser. The rate of energy lost by the condenser to the environment is 307 MW, while the boiler's rate of energy loss is a mere 68 MW. Despite the relatively low energy loss, the irreversibility rate associated with the boiler is considerably higher than the irreversibility rate of the other components. Thermodynamic modeling, exergy and exergoeconomic analysis and optimization of a combined cycle power plant (CCPP) are performed by Ahmadi et al. [40]. Their study proves insightful. For instance, among their findings is the identification of the combustion chamber as being the most significant source of exergy destruction in the combined cycle power plant. The exergy destruction is ascribed to the irreversibility's associated with the combustion reaction and the heat transfer across large temperature

differences between the ignited gases and the working fluid. Furthermore, the exergoeconomic analysis identifies the combustion chamber as having the greatest cost associated with exergy destruction of all components. It is also determined that increasing the gas turbine inlet temperature (GTIT), effectively decreases the CCPP cost of exergy destruction.

Cziesla et al. [41] describe the calculation of avoidable cost rates associated with both exergy destruction and capital investment. The calculation is applied to the exergoeconomic evaluation of an externally fired combined cycle power plant. The avoidable and unavoidable exergy destructions and investment costs associated with each component in the system is calculated. The assumptions associated with the calculations were discussed. It is found that modified exergoeconomic variables assist in identifying the genuine prospect of improving a single plant component. In addition, some aspects of design and improvement of externally fired combined cycle systems was discussed. The results of this study illustrate the concept of avoidable exergy destruction and the associated avoidable investment costs are very useful in designing cost-effective energy conversion systems.

An exergoeconomic analysis and optimization carried out by Sahoo [42] to study a cogeneration system producing 50 MW of electricity and 15 kg/s of saturated steam at 2.5 bar. In his work, he optimizes the system by employing exergoeconomic principles and evolutionary programming. The results of his work, illustrate that the cost of

electricity production is 9.9% lower for the determined optimum case compared to the base case with regard to exergoeconomics.

In the research done by Tsatsaronis et al. [43], they demonstrate how exergy-related variables can be used to minimize the cost of a thermal system. These variables include, exergetic efficiencies, rates of exergy destruction, exergy loss, exergy destruction ratio, cost rates associated with exergy destruction, capital investment, operating and maintenance costs, relative cost difference of unit costs and exergoeconomic factor.

Toffolo et al. [44] propose a simple cogeneration system as an example to demonstrate the application of their iterative exergy-aided cost minimization method. Despite the value of exergy and exergoeconomic analyses, they alone cannot determine optimal design parameters in thermal systems. Using optimization procedures with thermodynamic laws and thermo-economics is therefore essential.

An exergoeconomic study of a geothermal district heating system is conducted via mass, energy, exergy and cost accounting analyses. The work, conducted by Ozgener [45] and associates, is based on the study of the Salihli Geothermal District Heating System (SGDHS) in Turkey. They investigate the relationships between capital cost and thermodynamic losses for the system components. The ratio of the rate of thermodynamic loss-to-capital cost was used to illustrate that each device and the overall system possess a systematic correlation between capital cost and exergy loss (total or internal). Apparently, however, there is no relation between capital cost and energy or external exergy loss. Furthermore, a parametric study is conducted in order to determine the effect

of changes to reference temperature on the ratio of the rate of thermodynamic loss to capital cost. Moreover, the parametric study provided the mean to develop a correlation that could be used for practical analyses. The correlation entails that the devices of SGDHS system are configured to achieve an overall optimal design. The design would be based on appropriately balancing the thermodynamic (exergy-based) and economic (cost) characteristics of the overall systems and their devices.

Sayyaadi [46] performs an exergoeconomic optimization of a light water nuclear power generation system, with an output rating of 1000 MW. In his optimization, he used a genetic algorithm that considers ten decision variables. His work shows that the fuel cost of the optimized system is greater than that for the base case. In other work was performed by Uhlenbruck [47] and associated, evolution strategy is combined with a particular exergoeconomic method to yield an optimization technique refers to as Exergo-economically-Aided Evolution Strategy. The newly developed method was applied to the optimization of a combined cycle power plant to demonstrate whether the exergoeconomic method could be employed to improve the evolutionary optimization technique. It is verified that there are benefits to the optimization progress under certain conditions. However, there are typically a large number of uncertainties associated with the exergoeconomic method. Therefore, the method is not recommended as a universal tool for wide spread use in computerized process optimization. The method, however, remains a promising tool as an interactive application to be used and perhaps improved by an experienced engineer.

2.2.4 Environmental concerns

Natural gas-fired turbines now dominate the field for several reasons. The reason the natural gas-fired turbine has gained popularity is due to the following issues:

- black start capabilities (to operate without relying on the external electric power transmission network)
- higher efficiencies
- lower capital costs
- shorter installation times
- better emission characteristics
- abundance of natural gas supplies

Conventional fossil-fuel steam power plants were the primary base-load power plants until the early 1980s [48]. The construction cost of a gas turbine power plant is approximately half that of a comparable conventional fossil-fuel steam power plant. Furthermore, it is forecasted that more than half of all power plants to be installed in the foreseeable future are gas-turbine or combined gas-steam turbine types [48].

Despite the fact that the Brayton cycle based stationary combustion turbine has many positive characteristics. Several hazardous air pollutants (HAP) are emitted into the atmosphere which is cause for concern. These HAP emissions are formed during combustion or result from HAP compounds contained in the fuel burn. In November of 2002, the U.S. Environmental Protection Agency [49] issued a report discussing the protection and enhancement of the quality of the nation's air resources. The report went

further to set national emission standards for HAPs. The report also evaluates the economic impact of pollution control requirements placed on stationary combustion turbines under these amendments. The control requirements are intended to reduce the release of HAPs into the atmosphere. The report highlighted concern over the discharge of HAP's in large quantity in the form of formaldehyde. Formaldehyde is a human carcinogen linked to human risk of cancer and can also cause symptoms such as irritated eyes and respiratory tract, coughing, dry throat, tightening of the chest, headache, heart palpitations and many other chronic diseases.

Al-Jeelani [48] performs a study that measured the levels of air pollutants, specifically NO_x, SO_2, CO, O_3, CH_4 and total hydrocarbons. Al-Jeelani identifies numerous serious issues in many cities and in particular the Holly City of Makkah. These serious issues should be of concern to scientific institutions and public health authorities.

Previous studies have shown that there are high concentrations of air pollutants in the atmosphere that exceed the standards that are attributed to traffic emission during the Hajj season in Makkah City, where about three million people gather in concentrated pockets. Also, many studies assessing the air quality inside the tunnels near the Holy Mosque show that there are very high concentrations that violate air quality standards [48]. Despite pollutant concentrations exceeding international guidelines are generally limited; the current air quality during Hajj could cause a potential hazard to pilgrims. Exposure to pollutant mixtures for long periods and combined with other pollutants (e.g. noise) can have serious consequences.

Al-Jeelani [50] also investigates and assesses the air quality of neighboring areas nearby to the Makkah Power Plant. His investigation sheds light on the effects of the hazardous gaseous emissions on Makkah City. His study has particular interest on the area located at the northern part of the Holy City of Makkah due to the concentrated levels of different pollutants.

Chapter 3

BACKGROUND AND THEORY

3.1 Exergy: as a thermodynamic analysis tool

Exergy analysis is tool employed in the development of efficient power plants. Exergy is not a thermodynamic quantity; however it depends on thermodynamic quantities (i.e. enthalpy and entropy). Since its inception in the early 60's, the concept has been used throughout different parts of the world [16]. The primary goal of exergy analysis in power plant applications is to identify and effectively minimize the irreversibility in each component of the plant. To date, the concept of exergy has been adopted by many researchers for a vast array of industrial processes.

Another attractive aspect of exergy analysis is that exergy is an effective tool used to achieve the development of energy efficient systems that have small environmental foot prints. In general, exergy analysis is applicable to any system involving heat and work transfer. Exergetic efficiency shows the actual effectiveness of the system. Moreover, combining exergy analysis and life cycle assessment can produce some useful results [13].

In addition, the exergy due to the concentration differences of varying species in most chemical fuels is lesser than the exergy of the involved chemical bonds. Concentration exergy is defined as the relative abundance of a species in a substance compared with the average concentration of those species in the reference state. The

concentration of various atoms and molecules vary widely across the globe depending on location. Therefore, making an exact universal determination of concentration exergy is impossible. Tables of standard chemical exergy have been published for a wide variety of species accounting for Gibbs free energy and an approximation of terrestrial concentration exergy [51].

3.2 Gas turbine technologies

Gas Turbines (GT) for electric power generation are manufactured in two basic sizes, specifically, industrial turbines and aero derivative turbines. An industrial GT, usually refers to a single-shaft heavy-duty GT. The industrial GT's power generating capability is typically rated between 20 MW to at least 130 MW. Also the turbine is most likely operated with dual-fuel units using natural gas or distillate oil.

Aero-derivative turbines (sometimes referred to as medium GT's) are modified aircraft engine turbines. They typically output within range of between 500 kW to at least 40 MW. This type of GT is most often operated with natural gas fuel only. They most commonly serve the needs of pipelines and industrial markets [53].

Production capacities of both types of turbines are rated by the International Standards Organization (ISO). ISO specifies the following operating conditions:

- Air inlet conditions: air temperature 15^{o}C (59^{o}F),
- Relative humidity 60%, and
- Absolute pressure (sea-level) 101.325 kPa (14.7 psia) at a power factor of 0.9.

Such conditions are rarely experienced in Saudi Arabia, especially during the summer months. A schematic of both an industrial GT and Aero-derivative turbines are shown in Figure 3.1

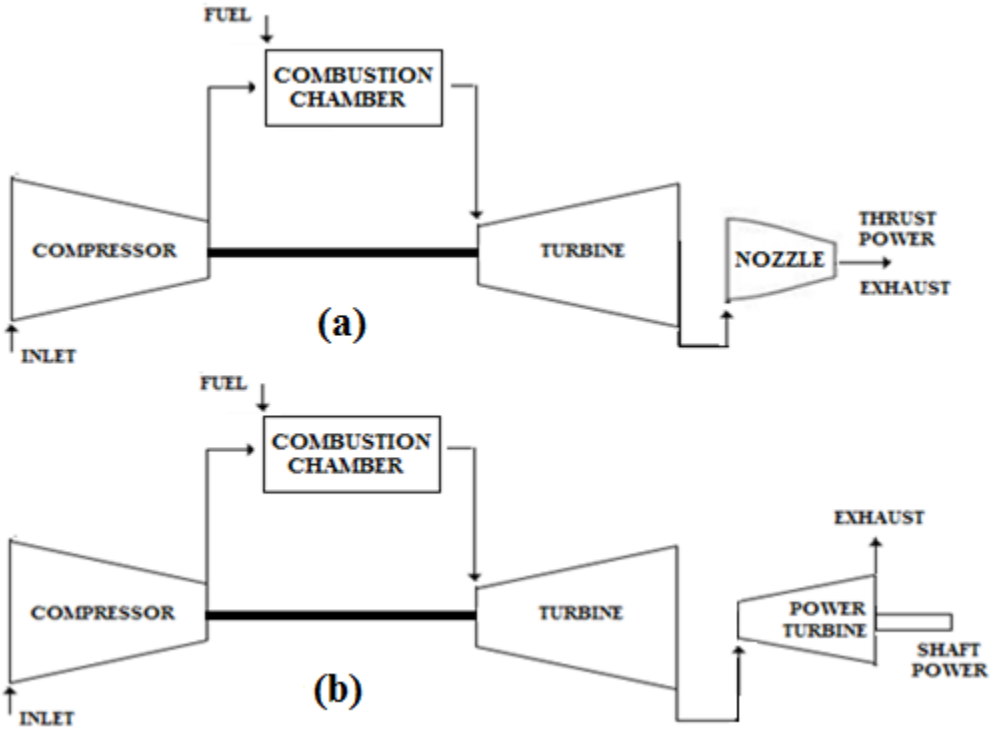

Figure 3.1 Schematic for a) an aircraft jet engine; and b) a land-based gas turbine (Modified from Ref. [54]).

Gas turbines such as the turbines in use at the Makkah Power Plant operate in the open Brayton thermodynamic cycle. The Brayton cycle CT was first proposed by George Brayton for use in the reciprocating oil-burning engine that he developed around 1870 [55]. In the modern world, the Brayton cycle turbine is used exclusively for gas turbines where both the compression and expansion processes take place in rotating machinery [12].

The turbine system begins with ambient fresh air entering the GT's compressor stage. As the ambient air passes through the compressor stage, the pressure is rapidly increased. The compressed air is then passed into the combustor where fuel is injected into the high-pressure stream and ignited. The now heated compressed air is released into the turbine, where work is produced. The work generated is used to drive the generator shaft generating electricity. A smaller part of the generated work is also used to drive the initial stage compressor. Usually, as the hot mixture (~500^{o}C) leaves the turbine, it is passed through a heat-recovery generator. This is done to recover some part of the wasted heat, after which the hot mixture is exhausted to the atmosphere [53]. The heat recovery system can be connected to a bottom cycle in cogeneration or combined cycle systems.

Gas turbines are constant-volume systems. Shaft power output is nearly proportional to the combustion air mass flow at base load. At base load, the mass flow rate of intake air into the GT determines its production capacity. Moreover, increasing fuel mass flow rate in the combustor also increases power output. However, an increase in fuel mass flow rate is not proportional to power output. The overall increase in power output is lesser than is achieved by increasing mass flow rate. Furthermore, increasing mass flow rate has an adverse effect on the heat rates (the ratio of fuel input rate to power produced). Increased mass flow rate causes a flow that is moving too quickly such that some of the injected fuel is not ignited. In worst case scenario, liquid fuel that was injected into the flow is actual ignited outside the combustor. Newly designed GT's

operate at lower air flow rates per unit of power produced. The lower flow rates decrease the cooling requirement for gas turbine inlet air-cooling technologies (GTIAC) systems and therefore increase the net benefit. Capacity increases, however, may be restricted by the maximum capacity of the GT, the maximum generator kVA rating, or lubrication oil cooling limitations [1].

The difference between the ISO standard conditions of 15^{o}C and the hot summer peak periods of approximately 40^{o}C, may result in a 20% drop in GT output. If, however, the inlet air flowing into the GT was cooled to 4^{o}C during these peak periods, a 27% increase would be achieved. Reducing the inlet air temperature of the GT has several advantages associated with the process [1]. A decrease in inlet air temperature has the potential to enhance capacity, improvement heat rates, extend turbine life, increase combustion turbine efficiency, and a delay the need to install additional GT's to deal with growing demand.

An additional factor influencing the performance of a gas turbine is relative humidity of the inlet ambient air. The effect has been simulated and multiple researchers have conducted and tested in a controlled environment were relative humidity was being controlled and temperature was held constant at 15^{o}C. The results of the test show that the compressor requires more energy to compress air of increasing humidity (higher density) [57]. Also, there is a decrease in the work generated at the turbine. The overall net effect is a reduction in the power output. Furthermore, it is proved that a reduction of

0.28 percentage points in the efficiency and of 2.7% in the electrical power output for an increase from 0% to 100% humidity (from totally dry to saturated air) [57].

3.3 Gas Turbine Inlet Air-Cooling Technologies (GTIAC)

A direct air conditioning system was the first application of the combustion turbine inlet air-cooling concept at a plant in Battle Creek, Michigan (USA) around the years 1987-88. In 1992, another example would appear in the form of an off-peak ice harvester system in Lincoln, Nebraska (USA) [1].

Theoretically gas turbines can attain efficiencies as high as 65%. However, most common simple open-cycle turbines only ever attain an efficiency of approximately 40%. There are several means of increasing efficiency such as reducing internal losses, increasing inlet temperatures, recycling waste heat from gas turbine exhausts, and the subject of this work, by decreasing ambient or compressor inlet temperatures [53].

To date, the ambient inlet air temperatures are typically reduced or cooled via the following methods:

- Wetted media evaporative cooling
- High-pressure fogging
- Absorption chiller cooling
- Refrigerative cooling
- Thermal energy storage

The techniques outlined above are amongst the most extensively studied. These methods of cooling are gaining increasing popularity and application globally. The

researchers Kitchen et al. [59] assess the potential capacity increase of various gas turbines with inlet cooling. Other researchers such as Giourof [60] , De Lucia et al. [61], ASHRAE [62], and Andrepont [63] also provide detailed discussion on the topic of turbine inlet air cooling techniques. The results of practical experience using exclusive cooling techniques or hybrid combinations, comparative studies and economic studies are the subject of the paper produced by the Energy Research Institute for Science and Technology in 2010, in the city of King Abdulaziz [1].

3.4 **The City of Makkah and its growing need for energy**

The city of Makkah (also known as Mekka or Mecca) is the holiest city in the Islamic world. The city is located in western region of the kingdom of Saudi Arabia. The city is the birth place of the founder of Islam, Mohammed and literally is the center of the Islamic world as the millions of Muslims across the world turn in the direction of the city for five daily prayers. One of the key tenets of Islam is the at least once in a life time pilgrimage to the city Makkah by every Muslim individual (Hajj). Each year, during the final month of the Islamic calendar nearly three million Muslims arrive in Makkah to perform the Hajj. Muslims are coming to the city all year round performing the ritual called Umrah. In overwhelming numbers that nearly rival those seen during Hajj, however, Muslims come for Umrah during the ninth month of the Islamic calendar also known as Ramadan. The influx of visitors during the two specific times of the Islamic calendar requires a great deal of logistical planning by the Saudi government. Services

such as accommodation and electricity become a logistical nightmare and stretch the limits of the city during these population booms twice a year.

3.4.1 Makkah Power Plant (MPP)

At present, gas turbines are the primary technology used for power generation in almost every part of the globe, including Saudi Arabia. This is especially true where gas or liquid fuel is readily available. In this study, the Brayton cycle based power plant in the city of Makkah is considered for analysis. Peak demand for electric power in the City of Makkah occurs in the middle of the day during the summer and is almost double the off-peak demand.

The power plant in Makkah consists of 18 gas turbine units with generating capacities ranging from 18 to 62 MW with 9 small diesel engines that range from 2 to 9 MW. The total installed generating capacity of plant is about 900 MW. This study describes a system of fifteen gas turbine units that are more cost effective and efficient. The system's benefits are proven through the thermodynamic analyses performed in this research as well as from the proven literature studied in this work. However, the first gas turbine unit installed at the power plant was an 18 MW Asia Brown Boveri (ABB) in 1975. The last gas turbine unit to be installed was a 50.990 MW in 1984.

Makkah Power Plant (MPP) is one of the largest gas turbine power plants in the western region of Saudi Arabia. Furthermore, MPP is linked into the main power network of the Saudi Electricity Company (SEC) and is also the backup power generation

plant for the holy city of “Makkah Almukaramah”. A satellite image of MPP is depicted in Figure 3.2.

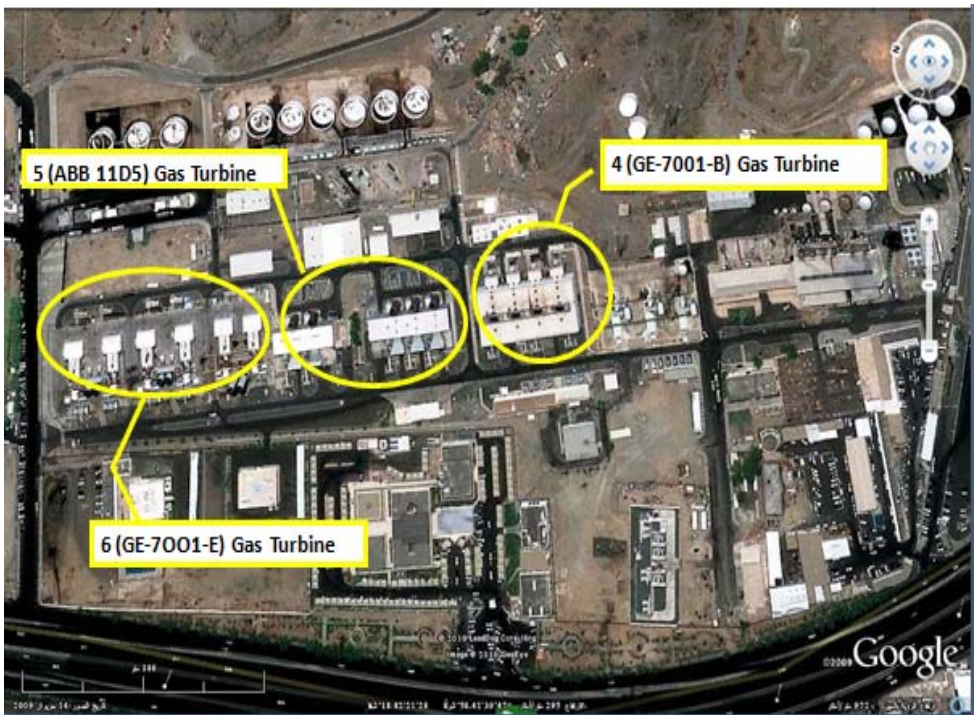

Figure 3.2 Satellite Image of MPP [65].

3.4.2 Technical details about Makkah Power Plant

As mentioned previously, the holy city of Makkah deals with a diverse set of demands. A city, 300 meters above sea-level, experiencing extreme peak temperatures and mass temporary migration of pilgrims poses a serious logistical challenge in so many required services. Paramount among these is power consumption requirements around peak demand periods. Periods of peak demand that tax the power systems of the holy city are during Hajj and Umrah seasons, when millions come to the city. The city is required to manage enough power resources to serve the large influx of people. If the large number

of pilgrims wasn't a great enough taxation on the power grid of MPP, there is the issue of weather and high temperatures. Generally, the weather in Makkah City is hot. Summer temperatures are considered very hot and often over-take the 50°C (122°F) mark by the middle of the afternoon. The evening often only finds itself dropping to a still very warm 37°C (99°F). In the winter, temperatures range between 17°C (63°F) at midnight and 25°C (77°F) in the afternoon.

Of particular concern during the period of peak demand during the holiest times of the year and due to extreme weather conditions, there exists the constant fear of power outages. Hence, the greatest challenge facing Makkah Power Plant is having sufficient provisions of power to meet the demands of the holy city during extreme peak energy demand period, and avoiding power shortages. Of equal concern in the operation of the Makkah Power Plant, are mechanical and electrical challenges, along with challenges in the cost effective and thermal efficient operation of the power generation systems. The mechanical problems are due to dirty turbine and compressor blades. Electrical problems are directly correlated to the malfunctioning of auxiliaries due to failure and outages. Moreover, this study is specifically interested and performed analyses of issues related thermo-mechanical problems.

Chapter 4

SYSTEMS STUDIED

4.1 Introduction

This section is intended to briefly depict an overall plant overview, describes the functional operation of a gas turbine, and introduces major turbine components in the turbine gas path from inlet to exhaust. The gas path is defined as the path gases flow through the gas turbine starting at the air inlet, into the compressor, then through the combustion chambers, into the turbine, and finally through the exhaust to the atmosphere.

As mentioned previously, MPP consists of 18 gas turbine units that have a generation capacity that ranges from 18 to 62.700 MW. The plant also possesses 9 small diesel engines that range from 2 to 9 MW power output. The total installed generating capacity of plant without the diesel engines is about 822 MW. However, this study covers only fifteen gas turbine units from two different manufacturers General Electric (GE) and Asia Brown Boveri (ABB). Both of them work under Brayton cycle based systems. In other word, the two turbines are simple cycle turbines that exhaust gases directly thrown into the atmosphere. Octane, $C_8H_{18,}$ is the used fuel in both systems. Total storage capacity of fuel oil is 58 million liters. The daily consumption of fuel during the summer season while the power plant is operating on a full load is approximately 7.2 to 7.5 million liters. Note that ABB and GE turbines will be named system 1 and system 2 respectively in this study.

4.2 Description of system 1

System or plant 1 consists of five gas turbine units. These gas turbines are designed to operate on distillate and crude oil, but are none the less operating on distillate. In fact, all the installed turbines at the plant are operating on distillate.

Fuel and air are used to produce shaft horsepower in the gas turbine. The turbine system includes a 17 stages axial flow compressor, a five stage turbine, combustion system components, starting equipments and all of the accessory devices necessary to support and keep the gas turbine operating. The compressor and gas turbine is directly connected with an in line, single shaft rotor supported by two pressure lubricated elliptical journal and thrust bearings.

The schematic of the system 1 is shown in Figure 4.1. There are two different loops in the system. The first one is the fuel loop and the second one is the air loop. The air circuit describes the path of the ambient air that is drawn in through the air filters (filter house), when the turbine system is activated. The air continues through the 17 stage axial flow compressor, where it eventually finds itself in the combustion chamber. The compressed air from the compressor flows in to the space surrounding the combustion chamber. From the space surrounding the combustion chamber the flow enters the combustion chamber through louvers. From the combustion chamber the now superheated flow is passed through the five stage turbine, which in turn drives the compressor and produces electricity. The flow is then finally exhausted into the atmosphere. In order to protect the system from pulsation during start up, 3^{rd}, 6^{th} and 9^{th}

stage extraction valves (compressor blow off or blow out valves) in the compressor are open.

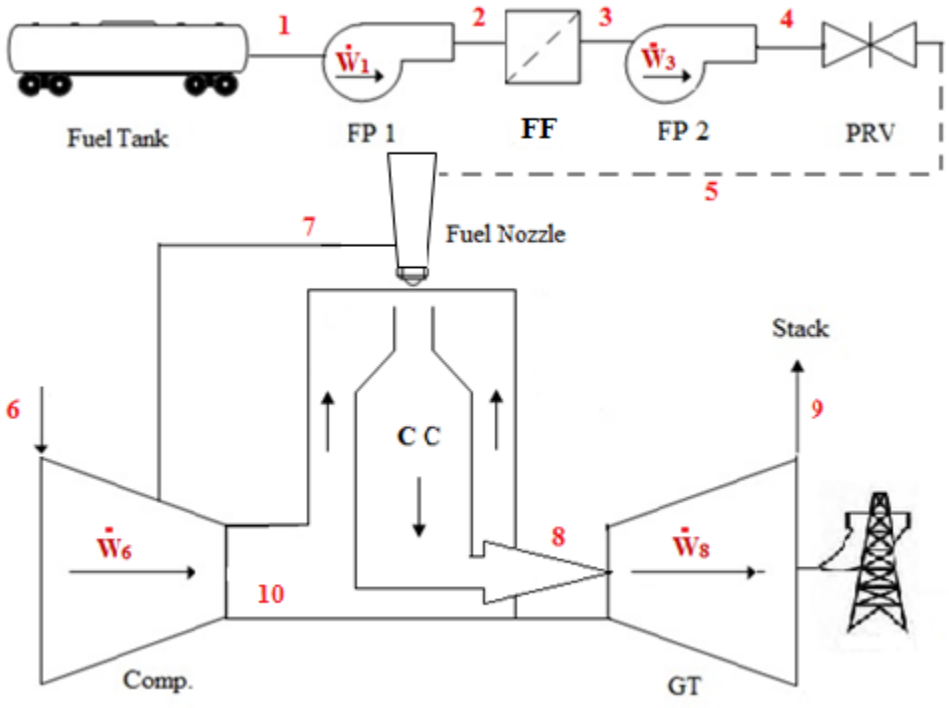

Figure 4.1 Schematic of system 1.

The filter house contains a duct and a filter net. The entire system is installed on a support structure, and mounted on the roof of turbine hall. Conical and cylindrical air filters are used. The filter houses are equipped with pulsing air system in order to remove dust and dirt from the filter house of turbine. The filtration system comes active when it is required.

The combustion chamber is equipped with a drainage false fuel drain valve. The purpose of this system is to remove any unburned fuel from the combustion chamber or lowest portion of the hot gas path. In other words, if any unburned fuel accumulates in

the combustion chamber, an indicator will appear and unit will not accept a start signal until the accumulated fuel manually drained. Cross sectional area drawing of system 1 is shown in Figure 4.2. Finally, gases are thrown through the stack in which the used gases to power the turbine shaft are redirected, cooled and released to atmosphere.

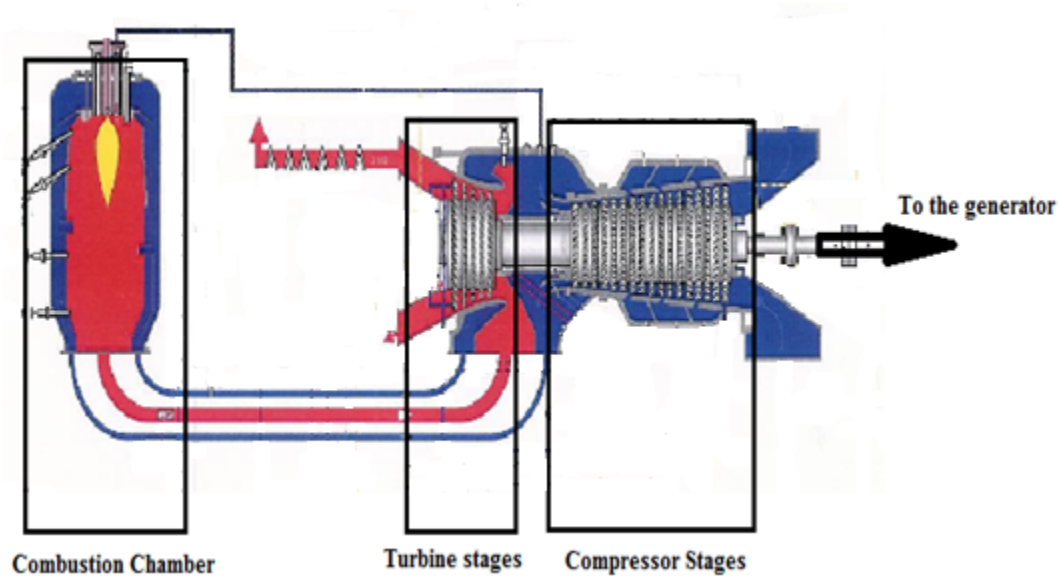

Figure 4.2 Cross sectional area of system 1 [66].

The fuel circuit is the system that provides fuel from the massive fuel reservoir to the combustion chamber. Liquid fuel is pumped, initially through a fuel filtration system by a 25 HP horizontal multistage centrifugal fuel pump at usually up to 80 psi. The filtration system removes certain impurities before the fuel is pumped once more by a 12 stages 200 HP horizontal centrifugal pump. The pumps are suitable in temperatures ranging from –50^{o}C to 180^{o}C and working pressures from 20 to 100 bars. Before the fuel is passed into the injector fuel nozzle, the fuel flow is regulated by a pressure regulating

valve. The main fuel pump and pressure regulating valve keep the required pressure sufficient for atomizing. The fuel injection nozzle is used to atomize liquid fuel for the gas turbine. The complete nozzle unit in reality consists of a combination of two nozzles concentrically arranged. These two nozzles work in a staggered mode in order to ensure a proper atomizing effect with largely varying fuel flow. This pressurized fuel then enters in to the combustion chamber where it is ignited into the compressed air. The whole system is monitored from a control room where the system's statistics are carefully monitored and corrective action can be taken if necessary.

4.3 Description of system 2

System or plant 1 consists of 10 gas turbine units. All the turbines installed at the power plant are 3600 rpm single shaft, simple cycle, heavy duty gas turbines, driving an air-cooled synchronous generator. The gas turbines are designed to operate on distillate or crude oil, but once again are operated on distillate at the location studied.

Fuel and air are used to produce shaft horsepower in the gas turbine. The turbine system includes a 17 stages axial flow compressor, a three stage turbine, combustion system components, starting equipment and all of the accessory devices necessary to support and keep the gas turbine operating. The compressor and gas turbine are directly connected with an in-line single shaft rotor supported by three pressure lubricated elliptical journal bearings. The inlet end of the rotor shaft is coupled to an accessory gear that drives the fuel, lubrication and other system pumps as well as the atomizing air compressor.

The schematic of the plant is shown in Figure 4.3. As with the system 1, there are two circuits that define this system, the first being the fuel circuit and the second the air circuit. When this system is activated and the clutch engaged, ambient air is drawn through the air inlet filters (filter house) and compressed in a 17 stage axial flow compressor. The filter house contains two parallel ducts and a filter house. The entire system is installed on a support structure that is over the control and accessory compartment. The system has a pulsing air system to remove dust and dirt from the filter house of the turbine and generator.

Compressed air from the compressor flows into the annular space surrounding the 10 combustion chambers. From the outer combustion liners, the flow enters the combustion zone through louvers in each of the combustion liners. The discharged air from the 17 stage compressor is divided into two different streams. One acts as atomizing air and the other is used to increase the kinetic energy of the combustion products. The atomizing air stream initially passes through pre-cooler heat exchanger before air goes to the main atomizing air compressor (AAC). The pre-cooler reduces the temperature of the air sufficiently to prevent thermal decomposition of the fuel at the fuel nozzle. It also prevents the main atomizing air compressor from overheating. It is, however, important to note that the air should not be over cooled as concerns of condensation arise and possible damage to the main atomizing air compressor may occur due to that formed condensation. The main atomizing air compressor is a centrifugal compressor. It is driven by its own gearbox by the accessory gear of the turbine.

The main function of the atomizing air manifold system is to break down the jet of fuel that is discharged from the fuel oil nozzle into a fine mist (small particles). This is done to ensure the fuel is completely burned in the combustion chamber. Also, the atomizing air manifold provides an equal pressure distribution of atomized air to ten individual fuel nozzles.

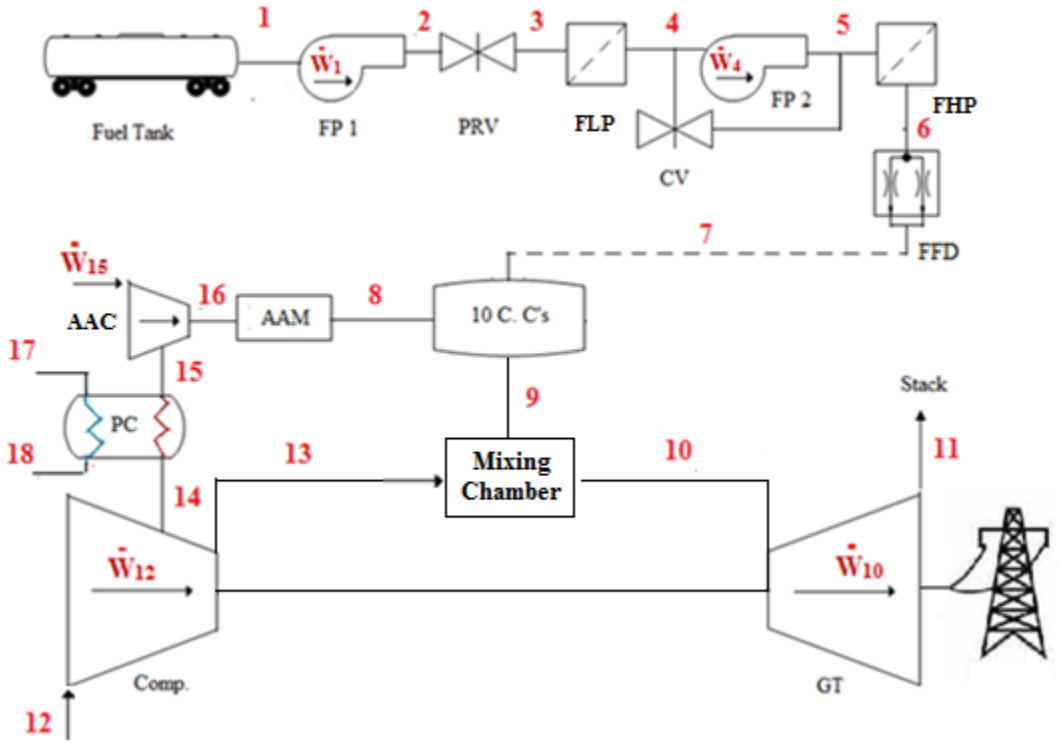

Figure 4.3 Schematic of system 2.

The fuel circuit is the system that provides fuel from the massive fuel reservoir to the combustion chamber. Liquid fuel is pumped, initially through a low pressure filter (LP) to remove certain impurities by a horizontal multistage centrifugal fuel pump at usually up to 120 psi.

The fuel then enters into the main displacement pump system, which has a capability roughly up to 350 psi. The fuel is pumped into a high pressure filter (HP) just before it continues into the 10 element circular flow divider. The filtered fuel is finally distributed into 10 equal flow lines, each being pumped into a nozzle centered in the end plate of a separate combustion chamber. The nozzle introduces the fuel in to each of the 10 combustion chambers, where it mixes with the atomizing air and ignited by spark plugs. The hot gases from the combustion chambers are expanded into the 10 separate exhaust paths attached to the end of the combustion chamber liners. At this point, the flow is passed through the three stage turbine section of the system.

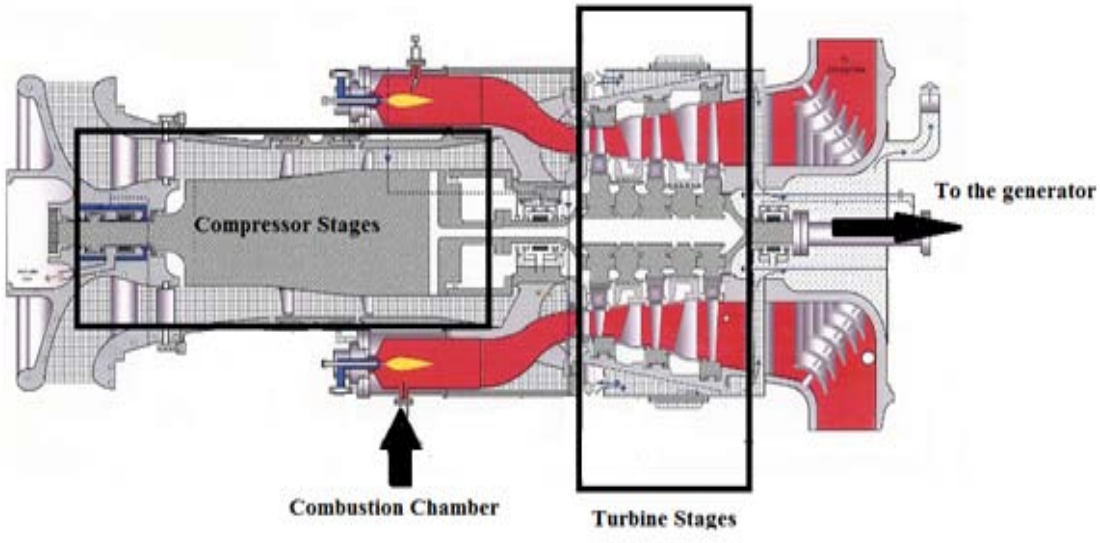

Figure 4.4 Cross sectional area of system 2 [66].

In order to increase the kinetic energy of combustion products, the airflow enters mixture case that are used to mix combustion products with air coming from the main turbine compressor. The airflow is then allowed to continue through the turbine stages. After passing through the third stage, the gases are directed into the exhaust hood and diffuser which contains a series of turning vanes to turn the gases from the axial direction to a radial direction. This is done so that the flow can pass into the exhaust system or stack. Cross sectional area of system 2 is shown in Figure 4.4. All the actual operating parameters for each state point (i.e. pressure, temperature and mass flow rate), are tabulated in Appendices A and B as provided by the site engineers of Makkah Power Plant.

Chapter 5

THERMODYNAMIC ANALYSES

5.1 Assumptions

This chapter is intended to detail the analysis of the overall system. The subsystems are dealt with in some detail in the following subsections. During these analyses, the following assumptions were made:

- Steady state operation for all components.
- All units are based on the Standard International unit system, e.g., kilopascal (kPa) for pressure, Kelvin (K) for temperature and kilojoules per kilogram (kJ/kg) for enthalpy.
- The heat exchanger, pumps, compressor and turbine are adiabatic and, hence, no heat transfer occurs between them and the surroundings.
- All kinetic and potential exergetic terms are negligible.
- The chemical exergetic term does not change in the turbine, pumps, compressor or the heat exchanger.
- The ambient temperature and pressure are held constant (T_0 and P_0) and any change in there value would obviously imply a change in system exergetic efficiency.
- The combination of a compressor and turbine as a turbocharger is used in this system. Therefore, a fraction of power produced by the turbine is used in the compressor and the rest is a useful power output.

- Molar flow rates for streams where any chemical reaction take place can be used in order to find the energy balance equations.
- Air is an ideal gas with a composition of 21 % oxygen and 79 % nitrogen.
- Isentropic operation is assumed for the compressor and the turbine.

5.2 Thermodynamic analysis of system 1

Each component in the plant was analyzed separately. Three balance equations were written for each component, including energy, entropy and exergy, see Figure 4.1. The basic exergy equation is

$$\dot{E}x = \dot{m}\big((h - h_o) - T_o(s - s_o)\big) \tag{5.1}$$

where h_o and s_o are represent the enthalpy and entropy at standard conditions.

State 1-2 (fuel transfers pump 25 HP)

$$\dot{m}_1\, h_1 \;+\; \dot{W}_1 \;=\; \dot{m}_2\, h_2 \tag{5.2a}$$

$$\dot{m}_1\, s_1 \;+\; \dot{S}_{g_1} \;=\; \dot{m}_2\, s_2 \tag{5.2b}$$

$$\dot{m}_1\, ex_1 \;+\; \dot{W}_1 \;=\; \dot{m}_2\, ex_2 + \dot{E}_{dest_{fp1}} \tag{5.2b}$$

State 2-3 (fuel filter)

$$\dot{m}_2\, h_2 \;=\; \dot{m}_3\, h_3 \tag{5.3a}$$

$$\dot{m}_2\, s_2 \;+\; \dot{S}_{g_2} \;=\; \dot{m}_3\, s_3 \tag{5.3b}$$

$$\dot{m}_2\, ex_2 \;=\; \dot{m}_3\, ex_3 + \dot{E}_{dest_{ff}} \tag{5.3c}$$

State 3-4 (fuel centrifugal pump, 12 stages, 25 HP)

$$\dot{m}_3\, h_3 \;+\; \dot{W}_3 \;=\; \dot{m}_4\, h_4 \tag{5.4a}$$

$$\dot{m}_3\, s_3 \;+\; \dot{S}_{g_3} \;=\; \dot{m}_4\, s_4 \tag{5.4b}$$

$$\dot{m}_3\, ex_3 \;+\; \dot{W}_3 \;=\; \dot{m}_4\, ex_4 + \dot{E}_{dest_{fp2}} \tag{5.4c}$$

State 4-5 (pressure regulating valve)

$$\dot{m}_4\, h_4 \;=\; \dot{m}_5\, h_5 \tag{5.5a}$$

$$\dot{m}_4\, s_4 \;+\; \dot{S}_{g_4} \;=\; \dot{m}_5\, s_5 \tag{5.5b}$$

$$\dot{m}_4\, ex_4 \;=\; \dot{m}_5\, ex_5 + \dot{E}_{dest_{prv}} \tag{5.5c}$$

State 6-7-10 (main 17 stages compressor)

$$\dot{m}_6\; h_6 \;+\; \dot{W}_6 \;=\; \dot{m}_7\; h_7 + \dot{m}_{10}\; h_{10} \tag{5.6a}$$

$$\dot{m}_6\;\; s_6 \;+\; \dot{S}_{g_5} \;=\; \dot{m}_7\; s_7 + \dot{m}_{10}\; s_{10} \tag{5.6b}$$

$$\dot{m}_6\; ex_6 \;+\; \dot{W}_6 \;=\; \dot{m}_7\, ex_7 + \dot{m}_{10}\, ex_{10} \;+\; \dot{E}_{dest_{comp.}} \tag{5.6c}$$

State 7-5-8 (combustion chamber)

$$\dot{m}_7\;\; h_7 \;+\dot{m}_5\;\; h_5 \;=\; \dot{m}_8\;\; h_8 \tag{5.7a}$$

$$\dot{m}_7\;\; s_7 \;+\; \dot{m}_5\;\; s_5 \;+\dot{S}_{g_6} \;=\; \dot{m}_8\;\; s_8 \tag{5.7b}$$

$$[\dot{m}_7\big(ex_7 + 0.79\, ex_{ch-N_2} + 0.21\, ex_{ch-O_2}\big) + \dot{m}_{10}(ex_{10} + 0.79 ex_{ch-N_2} +$$

$$0.21 ex_{ch-O_2})] + \dot{m}_5\,(ex_5 + exf_{ch}) = \dot{m}_8\, ex_8 + \dot{E}_{dest_{cc}} \tag{5.7c}$$

where ex_8 represent the exergy of combustion products at point 8. It is a summation of thermo-physical and chemical exergy of the combustion products. The thermo-physical exergy of the combustion products can be found as

$$\dot{E}x_{th_8} = N_{CO_2}\left[\left(h_{CO_2} - h_{0,CO_2}\right) - T_o\left(s_{CO_2} - s_{o,CO_2}\right)\right] + N_{H_2O}\left[\left(h_{H_2O} - h_{o,H_2O}\right) -\right.$$

$$TosH2O - so,H2O + NO2hO2 - ho,O2 - TosO2 - so,O2 + NN2[hN2 - ho,N2 -$$

$$\left.T_o\left(s_{N_2} - s_{o,N_2}\right)\right] \quad (5.7d)$$

and the chemical exergy for combustion is defined as

$$\dot{E}x_{ch_8} = R\,T_o\,(N_{CO_2}\ln(\frac{y_{CO_2}}{ye_{CO_2}}) + N_{H_2O}\ln\left(\frac{y_{H_2O}}{ye_{H_2O}}\right) + N_{O_2}\ln\left(\frac{y_{O_2}}{ye_{O_2}}\right) N_{N_2}\ln\left(\frac{y_{N_2}}{ye_{N_2}}\right) \quad (5.7e)$$

where y_{CO_2}, y_{H_2O}, $y_{O_2}$and y_{N_2} represent mole fraction of carbon dioxide, water, oxygen and nitrogen in combustion products respectively, and ye_{CO_2}, ye_{H_2O}, ye_{O_2} and ye_{N_2} represent the mole fraction of carbon dioxide, water, oxygen and nitrogen in environmental respectively and their values are:

$ye_{CO_2} = 0.0003$ $\quad mole\ fraction\ of\ carbon\ dioxide.$

$ye_{H_2O} = 0.0312$ $\quad mole\ fraction\ of\ water\ vapour.$

$ye_{O_2} = 0.2035$ $\quad mole\ fraction\ of\ oxygen.$

$ye_{N_2} = 0.7567$ $\quad mole\ fraction\ of\ nitrogen.$

Therefore, the total exergy at point 8 can be found as

$$\dot{E}x_8 = \dot{E}x_{th_8} + \dot{E}x_{ch_8} \quad (5.7f)$$

State 8-9 (5 stages turbine)

$$\dot{m}_8\ h_8 = \dot{m}_9\ h_9 + \dot{W}_8 \quad (5.8a)$$

$$\dot{m}_8\ s_8 + \dot{S}_{g_8} = \dot{m}_9\ s_9 \quad (5.8b)$$

$$\dot{m}_8\ ex_8 = \dot{m}_9\ ex_9 + \dot{W}_8 + \dot{E}_{dest_t} \quad (5.8c)$$

The net work output (in kW) of turbine work is calculated as

$$\dot{W}_{net} = \dot{W}_{turbine} - \sum \dot{W}_{pumps} - \sum \dot{W}_{compressors} \tag{5.9}$$

$$\dot{W}_{net} = \dot{W}_8 - \dot{W}_1 - \dot{W}_3 - \dot{W}_6 \tag{5.10}$$

The energy efficiency is defined as the ratio of net work over higher heating value below:

$$\eta_{en} = \frac{\dot{W}_{net}}{\dot{m}_1 \ HHV} \tag{5.11}$$

The exergy efficiency is defined as the ratio of net work over chemical content of the fuel below

$$\eta_{ex} = \frac{\dot{W}_{net}}{\dot{m}_1 \ ex_{ch_f}} \tag{5.12}$$

The analysis shows that the plant is currently running with thermal efficiency of 23.8% and exergy efficiency of 15.6%. Some of the calculated results are shown in Table 7.1Further results and discussion obtained in next chapter.

5.3 Thermodynamics analysis of system 2

Each component in the plant was analyzed separately. Three balance equations were written for each component, including energy, entropy and exergy, as shown in Figure 4.3. The basic exergy equation is same as the equation 5.1 where h_o and s_o are represent the enthalpy and entropy at standard conditions.

State 1-2 (fuel centrifugal pump)

$$\dot{m}_1 \, h_1 \ + \ \dot{W}_1 \ = \ \dot{m}_2 \, h_2 \tag{5.13a}$$

$$\dot{m}_1 \, s_1 \ + \ \dot{S}_{g_1} \ = \ \dot{m}_2 \, s_2 \tag{5.13b}$$

$$\dot{m}_1\, ex_1 + \dot{W}_1 = \dot{m}_2\, ex_2 + \dot{E}_{dest_{fp1}} \quad (5.13c)$$

State 2-3 (pressure regulating valve)

$$\dot{m}_2\, h_2 = \dot{m}_3\, h_3 \quad (5.14.a)$$

$$\dot{m}_2\, s_2 + \dot{S}_{g_2} = \dot{m}_3\, s_3 \quad (5.14b)$$

$$\dot{m}_2\, ex_2 = \dot{m}_3\, ex_3 + \dot{E}_{dest_{prv}} \quad (5.14c)$$

State 3-4 (fuel low pressure filter)

$$\dot{m}_3\, h_3 = \dot{m}_4\, h_4 \quad (5.15a)$$

$$\dot{m}_3\, s_3 + \dot{S}_{g_3} = \dot{m}_4\, s_4 \quad (5.15b)$$

$$\dot{m}_3\, ex_3 = \dot{m}_4\, ex_4 + \dot{E}_{dest_{flpf}} \quad (5.15c)$$

State 4-5 (fuel main displacement pump)

$$\dot{m}_4\, h_4 + \dot{W}_4 = \dot{m}_5\, h_5 \quad (5.16a)$$

$$\dot{m}_4\, s_4 + \dot{S}_{g_4} = \dot{m}_5\, s_5 \quad (5.16b)$$

$$\dot{m}_4\, ex_4 + \dot{W}_4 = \dot{m}_5\, ex_5 + \dot{E}_{dest_{fp2}} \quad (5.16c)$$

State 5-6 (fuel high pressure filter)

$$\dot{m}_5\, h_5 = \dot{m}_6\, h_6 \quad (5.17a)$$

$$\dot{m}_5\, s_5 + \dot{S}_{g_5} = \dot{m}_6\, s_6 \quad (5.17b)$$

$$\dot{m}_5\, ex_5 = \dot{m}_6\, ex_6 + \dot{E}_{dest_{fhp}} \quad (5.17c)$$

State 12-13-14 (main 17 stages compressor)

$$\dot{m}_{12}\, h_{12} + \dot{W}_{12} = \dot{m}_{13}\, h_{13} + \dot{m}_{14}\, h_{14} \quad (5.18a)$$

$$\dot{m}_{12}\, s_{12} + \dot{S}_{g_{12}} = \dot{m}_{13}\, s_{13} + \dot{m}_{14}\, s_{14} \quad (5.18b)$$

$$\dot{m}_{12}\ ex_{12}\ +\ \dot{W}_{12}\ =\ \dot{m}_{13}\ ex_{13} + \dot{m}_{14}\ ex_{14}\ +\ \dot{E}_{dest_{comp}} \tag{5.18c}$$

State 15-16 (air atomizing compressor)

$$\dot{m}_{15}\ h_{15}\ +\ \dot{W}_{15}\ =\ \dot{m}_{16}\ h_{16} \tag{5.19a}$$

$$\dot{m}_{15}\ s_{15}\ +\ \dot{S}_{g_{15}}\ =\ \dot{m}_{16}\ \ s_{16} \tag{5.19b}$$

$$\dot{m}_{15}\ ex_{15}\ +\ \dot{W}_{15}\ =\ \dot{m}_{16}\ ex_{16}\ +\ \dot{E}_{dest_{aac}} \tag{5.19c}$$

State 6-16-10 (combustion chamber)

$$\dot{m}_{16}\ \ h_{16}\ + \dot{m}_{6}\ \ h_{6}\ =\ \dot{m}_{10}\ \ h_{10} \tag{5.20a}$$

$$\dot{m}_{16}\ \ s_{16}\ +\ \dot{m}_{6}\ \ s_{6}\ + \dot{S}_{g_8}\ =\ \dot{m}_{10}\ \ s_{10} \tag{5.20b}$$

$$\dot{m}_{16}\ \left(ex_{16} +\ 0.79\ \ ex_{ch-N_2} +\ 0.21\ \ ex_{ch-o2}\right) +\ \dot{m}_{6}\ (ex_{6} +\ exf_{ch}) =$$

$$\dot{m}_{10}\ \ ex_{10} +\ \dot{E}_{dest_{CC}} \tag{5.20c}$$

where ex_{10} represent the exergy of combustion products at point 10. It is a summation of thermophysical and chemical exergy of the combustion products. The thermo-physical exergy of the combustion products can be found as

$$\dot{E}x_{th_{10}} = N_{CO_2}\left[\left(h_{CO_2} -\ h_{0,CO_2}\right) - T_o\left(s_{CO_2} -\ s_{o,CO_2}\right)\right] + N_{H_2O}\left[\left(h_{H_2O} -\ h_{o,H_2O}\right) -\right.$$

$$TosH2O - so,H2O + NO2hO2 - ho,O2 - TosO2 - so,O2 + NN2[hN2 - ho,N2 -$$

$$\left.T_o\left(s_{N_2} -\ s_{o,N_2}\right)\right] \tag{5.20d}$$

and the chemical exergy content for combustion becomes

$$\dot{E}x_{ch_{10}} = R\ T_o\ (N_{CO_2} \ln(\frac{y_{CO_2}}{ye_{CO_2}}) +\ N_{H_2O} \ln\left(\frac{y_{H_2O}}{ye_{H_2O}}\right) +\ N_{O_2} \ln\left(\frac{y_{O_2}}{ye_{O_2}}\right)\ N_{N_2} \ln\left(\frac{y_{N_2}}{ye_{N_2}}\right)$$

(5.20e)

where y_{CO_2}, y_{H_2O}, $y_{O_2}$and y_{N_2} represent mole fraction of carbondioxide, water, oxygen and nitrogen in combustion products respectively, and ye_{CO_2}, ye_{H_2O}, $ye_{O_2}$and ye_{N_2} represent the mole fraction of carbondioxide, water, oxygen and nitrogen in environmental respectively and their values are

$ye_{CO_2} = 0.0003$ $\quad mole\ fraction\ of\ carbon\ dioxide.$

$ye_{H_2O} = 0.0312$ $\quad mole\ fraction\ of\ water\ vapour.$

$ye_{O_2} = 0.2035$ $\quad mole\ fraction\ of\ oxygen.$

$ye_{N_2} = 0.7567$ $\quad mole\ fraction\ of\ nitrogen.$

Therefore, the total exergy at point 10 can be calculated as

$$\dot{E}x_{10} = \dot{E}x_{th_{10}} + \dot{E}x_{ch_{10}} \tag{5.20f}$$

State 10-11 (The 3 stages turbine)

$$\dot{m}_{10}\ h_{10} = \dot{m}_{11}\ h_{11} + \dot{W}_5 \tag{5.21a}$$

$$\dot{m}_{10}\ s_{10} + \dot{S}_{g_9} = \dot{m}_{11}\ s_{11} \tag{5.21b}$$

$$\dot{m}_{10}\ ex_{10} = \dot{m}_{11}\ ex_{11} + \dot{W}_{10} + \dot{E}_{dest_t} \tag{5.21c}$$

The net work output (in kW) of turbine work is calculated as

$$\dot{W}_{net} = \dot{W}_{turbine} - \sum \dot{W}_{pump} - \sum \dot{W}_{compressors} \tag{5.22}$$

$$\dot{W}_{net} = \dot{W}_{10} - \dot{W}_1 - \dot{W}_4 - \dot{W}_{12} - \dot{W}_{15} \tag{5.23}$$

The energy efficiency is defined as the ratio of net work over higher heating value below:

$$\eta_{en} = \frac{\dot{W}_{net}}{\dot{m}_1\ HHV} \tag{5.24}$$

The exergy efficiency is defined as the ratio of net work over chemical content of the fuel below:

$$\eta_{ex} = \frac{\dot{W}_{net}}{\dot{m}_1 \; exf_{ch}} \tag{5.25}$$

The analysis shows that the plant is currently running with thermal efficiency of 25.5% and exergy efficiency of 16.7%. Some of the calculated results are shown in Table 7.2. Further results and discussion will be presented in the next chapter.

5.4 Chemical exergy analysis

During a chemical reaction, the bonds between the molecules of reactants are broken. The atoms and electrons can then rearrange to form products. A physical requirement of chemical reactions is that mass is conserved. Therefore, the mass of the products must equal the mass of the reactants. The elements simply find themselves in different chemical compounds in the reactants, than they find themselves in the products. Despite the equality of mass between the reactants and products, the equality relation does not stand for the number of moles. The number of moles of the products may differ from the number of moles of reactants. Moreover, the chemical exergy is defined as the maximum useful work in a chemical process that brings the system into equilibrium with a heat reservoir. In some cases the ambient atmosphere is the reservoir of the system. Exergy, in this case, is the potential of that system to cause a change while achieving equilibrium with its environment. Exergy is the available energy for use in the system. Once the system and surroundings reach equilibrium, the exergy becomes zero.

The chemical exergy of a fuel is defined by the Gibbs free energy function and the chemical exergy of the individual element present in the fuel. For a given fuel the function takes the form

$$ex^{ch} = \Delta_f G^o + \sum_{elements} v \times ex^{ch}_{element} \text{ (kJ/mol)} \quad (5.26)$$

The Gibbs free energy ($\Delta_f G^o$) is a function of heating value and entropy of formation. It can be written as

$$\Delta_f G^o = \Delta_f H^o - T_o \Delta_f S^o \text{ (kJ/mol)} \quad (5.27)$$

where $\Delta_f H^o$ represents formation enthalpy (kJ/mol).

The formation enthalpy is dependent on standard entropy of fuel (i.e. entropy at reference temperature and pressure) and standard entropy of elements present in chemical equation. It is expressed as

$$\Delta_f S^o = s^o - \sum_{elements} v s^o_{f,element} \text{ (J/mol K)} \quad (5.28)$$

where v is the number of moles of the elements in the chemical equation in the formation of the substance. Usually standard (also called reference) thermo-physical properties are measured at a temperature of $298.15\ K$ and at pressure of 1 bar.

The selected fuel in the current study is Octane C_8H_{18}. The chemical equation of the combustion process can be written in the form

$$C_8H_{18} + 20\ (O_2 + 3.76N_2) \longrightarrow \mathcal{X}CO_2 + \mathcal{Y}H_2O + \mathcal{Z}O_2 + \mathcal{W}N_2 \quad (5.29)$$

The elements in parentheses represent the dry air involved in the combustion reaction that contains 1 kmol of O_2. The unknowns $\mathcal{X}, \mathcal{Y}, \mathcal{Z}, \mathcal{W}$ represent the mole numbers of the gases in the products. These unknowns are determined by applying the

mass balance to each of the elements. Hence, since the total mass or mole number of each element in the reactants must equal that in products

C:	$8 = \mathcal{X}$	$\longrightarrow$	$\mathcal{X} = 8$
H:	$18 = 2\mathcal{Y}$	$\longrightarrow$	$\mathcal{Y} = 9$
O:	$20 \times 2 = 2\mathcal{X} + \mathcal{Y} + 2\mathcal{Z}$	$\longrightarrow$	$\mathcal{Z} = 7.5$
N_2:	$(20)\ (3.76) = \mathcal{W}$	$\longrightarrow$	$\mathcal{W} = 75.2$

Substituting yields

$$C_8H_{18} + 20\ (O_2 + 3.76N_2) \longrightarrow 8CO_2 + 9H_2O + 7.5O_2 + 75.2N_2 \qquad (5.30)$$

The coefficient 20 in the balanced equation above represents the number of moles of oxygen, not the number of moles of air. The coefficient must be multiplied through the bracket contain the element representing dry air. Therefore, there would be 75.2 (20 × 3.76) moles of nitrogen and 20 moles of oxygen, for a total of 95.2 moles of air [67].

5.5 Exergoeconomic analysis

Exergoeconomic is a branch of study in engineering that combines economic constraints with exergy analysis providing an informative tool that is otherwise unavailable through conventional energy analysis and economic evaluation [40]. Exergoeconomic is a crucial tool in the design and operation of present and future cost effective systems. In the present study, several plant components were neglected in the exergoeconmics study of Makkah Power Plant. Their contribution to the overall study is deemed negligible in the greater scheme of the system. Components such as air /fuel filters, valves, fuel/air

dividers and atomizing manifolds are examples of the components deemed negligible. In the following subsections, an exergoeconomic study of components in both system 1 and 2 turbines will be presented including illustrations of the plant layout. Following the exergoeconomic study is the cost balance equations for each component.

5.5.1 Exergoeconomic analysis of system 1

The effect of exergy destruction can be quantified by combining exergoeconomic relations with the results of an exergy analysis. The components seen in Figure 5.1 are included in the exergoeconomic study.

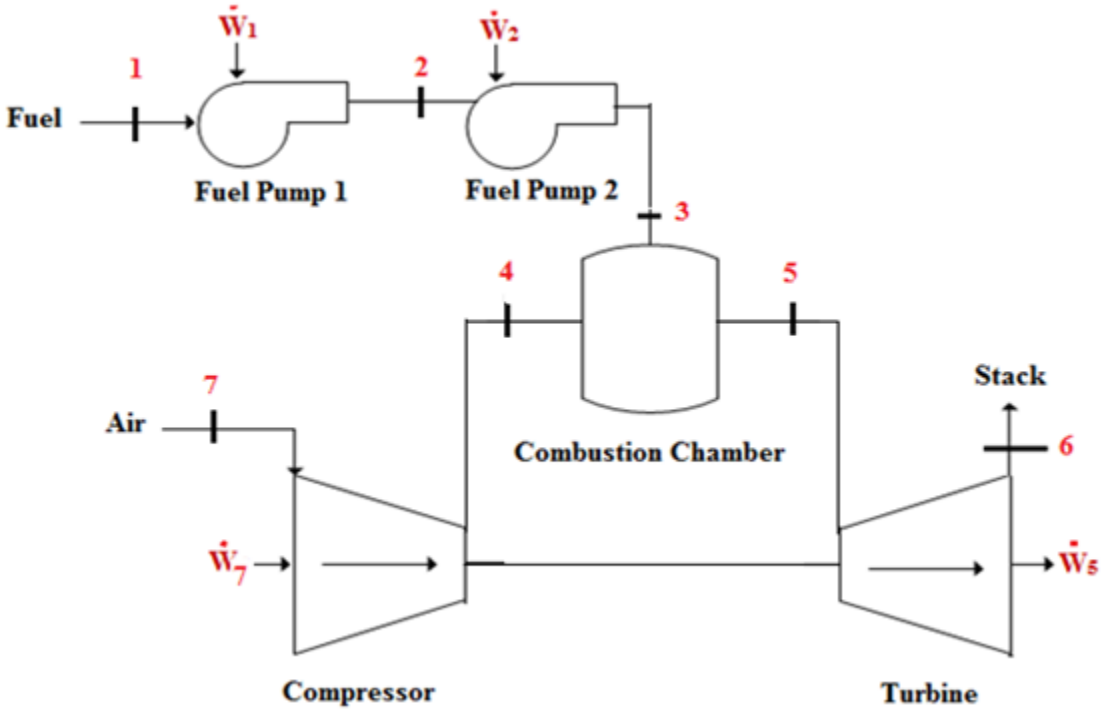

Figure 5.1 Exergoeconomic studied components of system 1

The exergoeconomic costs of all the flows that appear in the system 1 figure are obtained through exergy costing principles. The formulations of cost balance for each component and the required auxiliary equations are as followed. The exergoeconomic cost associated with ***fuel pump 1 and 2*** can be expressed by

$$\dot{C}_1 + \dot{Z}_p + \dot{C}_{w1} = \dot{C}_2 \tag{5.31a}$$

In above equation, $\dot{C}$ represents the flow cost rate of stream. Equation 5.31a can be expanded to [40]

$$c_1 \dot{E}x_1 + \dot{Z}_p + c_{w1} \dot{W}_{p1} = c_2 \dot{E}x_2 \tag{5.31b}$$

where $\dot{Z}_P$ is the cost function, or capital cost rate ($/h) of the centrifugal pump and can be expressed as

$$\dot{Z}_p = \left(c_{11} \times P_p^{0.71} \left(1 + \frac{0.2}{1 - \eta_s p} \right) \right) CRF * \frac{\varphi}{N * 3600} \tag{5.32}$$

where $c_{11} = 705.48$ $/kg s, *CRF* refers to capital recovery factor, φ is the maintenance factor, *N* is the annual number of operation hours for the unit and $\eta_s p$ is pump isentropic efficiency. Here, *CRF* depends on the interest rate and equipment life time, and is determined here as follows

$$\text{CRF} = \frac{\text{i} \times (1+\text{i})^{\text{n}}}{(1+\text{i})^{\text{n}} - 1} \tag{5.33}$$

Here, i denotes the interest rate and *n* the total operating period of the system in years [40].

An analogous approach will be followed for centrifugal fuel pump 2. The subscripts in Equation 5.31a will change from 1 and 2 to 2 and 3 respectively.

Compressor

Using a similar expression given in Equation 5.31a, for the exergoeconomic equation for the compressor takes the form

$$\dot{C}_7 + \dot{Z}_C + \dot{C}_{w7} = \dot{C}_4 \tag{5.34a}$$

or

$$c_7 \dot{E}x_7 + \dot{Z}_C + c_{w7} \dot{W}_{c7} = c_4 \dot{E}x_4 \tag{5.34b}$$

where $\dot{Z}_C$ is the cost function of the compressor and can be expressed as

$$\dot{Z}_C = (c_{11} \times \dot{m}_{air} \times \frac{1}{c_{12} - \eta_s c} \times P_r \times ln(P_r)) CRF * \frac{\varphi}{N*3600} \tag{5.35}$$

where c_{11}= 44.71 $/kg, c_{12}= 0.95, P_r is compressor pressure ratio and $\eta_s c$ is compressor isentropic efficiency.

Combustion Chamber

The exergoeconomic balance equation for the combustor takes the form

$$\dot{C}_3 + \dot{C}_4 + \dot{Z}_{CC} = \dot{C}_5 \tag{5.36a}$$

or

$$c_f \dot{m}_f LHV + \dot{Z}_{CC} + c_4 \dot{E}x_4 = c_5 \dot{E}x_5 \tag{5.36b}$$

where $\dot{Z}_{CC}$ is the cost function of the combustion chamber and can be expressed as

$$\dot{Z}_{CC} = \left(c_{21} \times \dot{m}_{air} \times \left(1 + e^{c_{22} \times (T_{out} - c_{23})}\right) \times \frac{1}{0.995 - {P_{out}}/{P_{in}}} \right) CRF * \frac{\varphi}{N*3600} \tag{5.37}$$

where c_{21}= 28.98 $/kg s, c_{22}= 0.015 K^{-1} and c_{23}= 0.015 K.

Turbine

The exergoeconomic balance equation of the turbine takes the form

$$\dot{C}_5 + \dot{Z}_{GT} = \dot{C}_6 + \dot{C}_{w5} \tag{5.38a}$$

or

$$c_5 \dot{E}x_5 + \dot{Z}_{GT} = c_6 \dot{E}x_6 + c_{w5} \dot{W}_{t5} \tag{5.38b}$$

where $\dot{Z}_{GT}$ is the cost function of the gas turbine and can be expressed as

$$\dot{Z}_{CC} = \left(c_{31} \times \dot{m}_{gas} \times \frac{1}{c_{32} - \eta_s T} \times \ln\left(\frac{P_{in}}{P_{out}}\right) \times \left(1 + e^{c_{33} \times (T_{in} - 1570\ K)}\right) \right) CRF * \frac{\varphi}{N * 3600} \tag{5.39}$$

where c_{31}= 301.45 \$/kg s, c_{32}= 0.94, c_{33}= 0.025 K^{-1} and $\eta_s T$ is turbine isentropic efficiency.

Some particular factors are associated with specific assumptions, such as the assumption that air is free. Therefore, the cost of the air stream ($\dot{C}_7$) passing through the system is assumed to be zero in this analysis. Another factor of great importance is the cost of the necessary fuel stream running into the system ($\dot{C}_1$). The fuel, octane, is taken as 0.07 \$/kg based on market price in Saudi Arabia.

Thus far, the number of equations is less than the number of unknowns. It is therefore necessary to employ an additional auxiliary relation assuming the same unit cost of exergy for the work produced or supplied to the system

$$c_{w1} \dot{W}_{p1} = c_{w2} \dot{W}_{p2} = c_{w7} \dot{W}_{c7} = c_{w5} \dot{W}_{t5} \tag{5.40}$$

The exergoeconomic parameters and the cost of the streams for each of the components of both plants are summarized in results and discussion chapter.

5.5.2 Exergoeconomic analysis of system 2

The cost balance equations for system 2 are along the same line as those for system 1. There are a few differences for the several components not contained in the system 1. Exergy and exergoeconomics can once again be correlated in the fashion described for system 1.

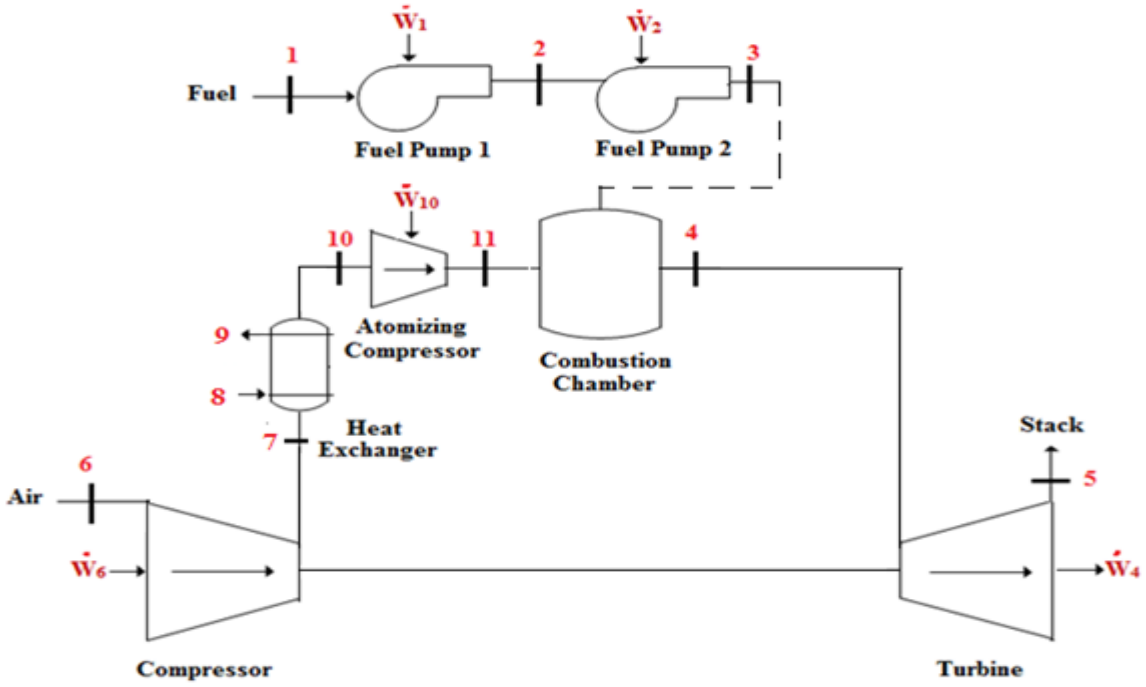

Figure 5.2 Exergoeconomic studied components of system 2

Figure 5.2 shows the major components included in the cost balance equation. As was the case for system 1 centrifugal pumps, the exergoeconomic cost associated with ***fuel pump 1 and 2*** can be expressed by

$$\dot{C}_1 + \dot{Z}_p + \dot{C}_{w1} = \dot{C}_2 \tag{5.41a}$$

or

$$c_1 \dot{E}x_1 + \dot{Z}_p + c_{w1} \dot{W}_{p1} = c_2 \dot{E}x_2 \tag{5.41b}$$

The subscripts in the above equations would be changed from 1 and 2 to 2 and 3 respectively for centrifugal fuel pump 2.

Compressor

Similar to the equation describing the compressor in the system 1, system 2 compressor takes the form

$$\dot{C}_6 + \dot{Z}_C + \dot{C}_w = \dot{C}_7 \tag{5.42a}$$

or

$$c_6 \dot{E}x_6 + \dot{Z}_C + c_{w6} \dot{W}_{c6} = c_7 \dot{E}x_7 \tag{5.42b}$$

Atomizing Compressor

This component, exclusive of the system 2 only, follows an identical formulation to the compressors of both systems

$$\dot{C}_{10} + \dot{Z}_C + \dot{C}_{w10} = \dot{C}_{11} \tag{5.43a}$$

or

$$c_{10} \dot{E}x_{10} + \dot{Z}_C + c_{w10} \dot{W}_{c10} = c_{11} \dot{E}x_{11} \tag{5.43b}$$

Heat Exchanger

The cost balance equation of the heat exchanger takes the form

$$\dot{C}_7 + \dot{C}_8 + \dot{Z}_{HE} = \dot{C}_9 + \dot{C}_{10} \quad (5.44a)$$

or

$$c_7 \dot{E}x_7 + c_8 \dot{E}x_8 + \dot{Z}_{HE} = c_9 \dot{E}x_9 + c_{10} \dot{E}x_{10} \quad (5.44b)$$

where $\dot{Z}_{HE}$ is the cost function of the heat exchanger and can be expressed as

$$\dot{Z}_{HE} = (c_{31} \times \frac{\dot{Q}_{HE}}{K - \Delta T_{ln}} + c_{62} \times \dot{m}_{CW} + 70.5 \times \dot{Q}_{HE} \times (-0.6936 \times \ln(\bar{T}_{CW} - T_{WB}) + 2.1898) \; CRF * \varphi N * 3600 \quad (5.45)$$

where c_{61}= 280.74 \$.m^{-2}, c_{62}= 746 \$. (m^2 K)$^{-1}$ and *K*= 2200 W. (m^2 K)$^{-1}$

Combustion Chamber

The combustion chamber cost balance equation becomes

$$\dot{C}_3 + \dot{C}_{11} + \dot{Z}_{CC} = \dot{C}_4 \quad (5.46a)$$

or

$$c_f \dot{m}_f LHV + \dot{Z}_{CC} + c_{11} \dot{E}x_{11} = c_4 \dot{E}x_4 \quad (5.46b)$$

Turbine

$$\dot{C}_4 + \dot{Z}_{GT} = \dot{C}_5 + \dot{C}_{w4} \quad (5.47a)$$

or

$$c_4 \dot{E}x_4 + \dot{Z}_{GT} = c_5 \dot{E}x_5 + c_{w4} \dot{W}_{t4} \quad (5.47b)$$

Due to a smaller number of equations relative to the number of unknowns, an additional auxiliary equation is once again required. Therefore, as in the case of system 1

a formulation assuming the same unit cost of exergy for the work produced or supplied to the system is defined as

$$c_{w1}\,\dot{W}_{p1} = c_{w2}\,\dot{W}_{p2} = c_{w6}\,\dot{W}_{c6} = c_{w10}\,\dot{W}_{c10} = c_{w4}\,\dot{W}_{t4} \tag{5.48}$$

The next step is to determine the costs of the unknown streams of the system. Information regarding the cost of required streams of the system helps in exergoeconomic evaluations. In the exergoeconomic evaluation of a thermal system, particular quantities called exergoeconomic variables, play a crucial role in the evaluation. The variables are defined by Sahoo [42] as the average unit cost of fuel (c_f), average unit cost of the product (c_p), the cost rate of exergy destruction ($\dot{C}_D$), the cost rate of exergy loss ($\dot{C}_L$), and the exergoeconomic factor (*f)*. In this study, the cost of exergy loss is taken as negligible such that it is very small. Moreover, the unit cost of fuel (c_f) represents the source that is consumed in generating the product. Mathematically, the cost rate of exergy destruction for each component is expressed as

$$\dot{C}_D = c_f\,\dot{E}_{dest} \tag{5.49}$$

and the exergoeconomic factor is expressed as

$$f = \frac{\dot{Z}}{\dot{Z} + \dot{C}_D} \tag{5.50}$$

The exergoeconomic parameters and the cost of the streams for each of the components of both plants are summarized in results and discussion chapter.

5.6 Exergoenvironmental analysis

A major objective of minimizing the environmental impact of a system is to increase the efficiencies of energy and exergy conversion processes, thereby decrease the fuel use. Recently, particular interest has been given to the releases of carbon dioxide. Since carbon dioxide is the main gas of concern in what is termed greenhouse gases, optimization of thermal systems based on this gas has received a great deal of attention. In this work, some effort is expended in consideration of CO_2 emissions since a large majority of reported approaches dealing with power plant optimization pay little attention to environmental impacts.

The effect of CO_2 emissions are of considerable significance, such that reduction of its harmful release is twofold. The first is obviously related to communal and environmental health. The second, as suggested in many references, is improvement in reduction of harmful emissions in the combustion chamber can lead to improvements of the cycle efficiency. Therefore, in order to provide a comprehensive optimization of the system, CO_2 emissions produced in the combustion chamber are considered as an objective function. Using the combustion equations, the normalized CO_2 emissions of the plant are expressed as

$$\varepsilon = \frac{\dot{m}_{co_2}}{\dot{W}_{net}} \tag{5.51}$$

where ε is the CO_2 emission per unit net electricity output (kg_{CO2}/MWh)

Reduction of the harmful emissions to the environment has proven its benefits in increasing system efficiency, which intern increases sustainability by lengthening the

lives of the fuel resources [19]. The relationships between sustainability versus exergy efficiency and environmental impact are documented in some detail by Connelly and Koshland [19]. They proposed that efficient fuel consumption could be characterized by a depletion number defined as

$$D_P = \frac{\dot{E}_{dest}}{\dot{E}x_{in}} \tag{5.52}$$

The formulation is meant to represent the relation between the exergy destruction ($\dot{E}_{dest}$) and the exergy input ($\dot{E}x_{in}$) by fuel consumption. The relationship between the depletion number and the exergy efficiency is described by

$$\eta_{ex} = 1 - D_P \tag{5.53}$$

Furthermore, the sustainability of the fuel resource can be expressed by a sustainability index (SI) as the inverse of the depletion number

$$SI = \frac{1}{D_P} \tag{5.54}$$

The octane is the fuel considered in the system as is show in Equation 5.30, the formulation describing the processes occurring in the combustor. The expression describing the environmental impact in terms of the amount of carbon dioxide emission and their mutual effect on sustainability is discussed in the chapter reserved for results and discussion.

Chapter 6

STATISTICAL ANALYSES

6.1 Stat-Ease Design-Expert and Analysis of Variance (ANOVA)

The Stat-Ease Design-Expert is a software package. It provides many powerful statistical tools to analyze the results using analysis of variation (ANOVA) , and to find the interaction between two input parameters and their mutual effect on the individual output and to find the regression (i. e. chosen output in term of input factors) to optimize the results for optimum operating conditions. The objective was to the determination of such processing conditions which maximize energy efficiency, exergy efficiency and output work with minimum fuel consumption [69].

ANOVA is a statistical method used to find statistical significance of factors. It consists of 4 main components namely sum of squares, degree of freedom, mean square vale and F-value [70].

6.1.1 Sum of squares

The total sum of squares (SS) is defined by two measures of variance. First, the total sum is defined as the sum of the squared deviation from the mean due to the effect of individual terms or the interaction between two terms. The second term of the Sum of Squares function represents the sum of the squared deviation that is not explained by the model [71].

$$SS_{Total} = SS_{Model\ terms} + SS_{Residual} \tag{6.1}$$

where $SS_{Residual}$ have two components [71] as follows

$$SS_{Residual} = \mathrm{SS}_{\mathrm{LOF}} + \mathrm{SS}_{\mathrm{Pure\ Error}} \tag{6.2}$$

$\mathrm{SS}_{\mathrm{LOF}}$ is the portion of the residual $SS_{Residual}$ that is due to the model not fitting the data. It is the weighted sum of squared deviations between the mean response at each factor level and the corresponding fitted value.

The pure error sum of squares ($\mathrm{SS}_{\mathrm{Pure\ Error}}$) is a measure of the effect of the error contribution associated with repeatability. It is the corrected sum of squares of the repeat observations at each level of input and then pooled over all the levels of input.

6.1.2 Degree of freedom (df)

The degree of freedom (df) in an ANOVA analysis is defined as the minimum number of values required to specify all data points in a sample. Hence, N data points have N degrees of freedom. If the mean of the data is known and N data points in the statistical population then df is considered N-1 [72]. Total df for a given model is defined as

$$df_{total} = df_{Model\ Terms} + df_{Residual} \tag{6.3}$$

where each model term is considered to have one df. The degree of freedom associated with the residual portion of the above equation is defined as

$$df_{Residual} = df_{\mathrm{LOF}} + df_{\mathrm{Pure\ Error}} \tag{6.4}$$

The term $\mathrm{df}_{\mathrm{LOF}}$ varies depending on model of choice. Linear models for scattered data have higher df while quadratic or cubic model's have smaller df for same scattered

data. This is due to the increase in the number of points captured by the estimated model regression.

6.1.3 Mean square value

The mean square value is defined as the ratio of the sum of squares to the degree of freedom [73]. Mathematically it is expressed as

$$MM = SS/df \tag{6.5}$$

6.1.4 F-value

The F-value of a model term is the test for comparing the variance related with that term with the residual variance. It is the ratio between mean square value of the term and mean square value of the error [74]. It is defined as

$$F_{Term} = \frac{MM_{term}}{MM_{residual}} = \frac{\frac{SS_{term}}{df_{term}}}{\frac{SS_{residual}}{df_{residual}}} \tag{6.6}$$

The larger the F-value of a given term signifies a greater significance of that term in the model. However, the F-value associated with LOF (Lack of Fit) should be small; a large value implies greater error for the model term.

6.1.5 P-value

The P-value is the probability of a term that is associated with the F-value for the term. It is the probability of getting a given F-value for a term if the term did not have an effect on the response. In general, based on 95% confidence level, a term that has a probability

value less than 0.05 would be considered a significant effect. A probability value which is greater than 0.10, is generally regarded as not significant [73].

6.2 Regression calculation

The factors involved in calculation of ANOVA terms would either be quantitative or qualitative [72]. Quantitative factors are termed categoric factors e.g. colors on different plastic production lines, Grade of color produced for a given line etc. The qualitative factors are termed numeric factors e.g. inlet air temperature, fuel mass flow rate and air volume flow rate.

The empirical model equation has constants associated with them and these constant can be determined by using given output data. The general approach to calculating the constants of the empirical model equation is a regression calculation.

In a regression calculation, the least square method is used to calculate the coefficients of the model equation [70]. If the calculated regression captures all empirical data points, the residual is 1 (no error). A calculated residual of less than one implies the regression fails to capture all data points and the model has associated error in its predictive capability.

A simple three input linear predictive model can be expressed as

$$y = a_0 + a_1x_1 + a_2x_2 + a_3x_3 \tag{6.7}$$

where y represents the output and $x_1, x_2, and\ x_3$ represent the inputs of the model [70]. Linear models of greater complexity include the interactions between two and even all three terms. Such a model may take the form,

$$y = a_0 + a_1x_1 + a_2x_2 + a_3x_3 + a_4x_1x_2 + a_5x_2x_3 + a_6x_3x_1 + a_7x_1x_2x_3 \quad (6.8)$$

In similar fashion quadratic and cubic model regressions can be calculated. Calculation of quadratic and cubic terms will also include square and cubic input terms. For example, a cubic regression model can be calculated as

$$y = a_0 + a_1x_1 + a_2x_2 + a_3x_3 + a_4x_1x_2 + a_5x_2x_3 + a_6x_3x_1 + a_7x_1x_2x_3 + a_9x_2^2 + a_{10}x_3^2 + a_{11}x_1^2x_2 + a_{12}x_2^2x_3 + a_{13}x_3^2x_1 + a_{14}x_1^2x_1 + a_{15}x_2^2x_1 + a_{16}x_3^2x_2 + a_{17}x_1^3 + a_{18}x_2^3 + a_{19}x_3^3 \quad (6.9)$$

In general, the addition of more terms can improve the accuracy of the model (residual closer to unity), but this also increases complexity and the need for more empirical data. Generally, the usefulness of a model is dependent the minimal amount of constants among other factors.

6.3 Response surface methodology

The response surface methodology (RSM) is a useful method by which interactions between two input variables and their mutual effect on output can be determined. The results are presented in terms of contours graphs, where the two inputs are on the X and Y axis and the output is on the Z-axis [75]. A contour surface is constructed representing the inputs to the output in three dimensions. In the case of more than 2 inputs, the relation between the inputs and the response can be represented by multiple response surfaces. The response surfaces of two particular inputs can be found by holding the remaining inputs constant. Consider the case of three input variables (x_1, x_2, x_3) as described earlier. Response surfaces can be plotted for three different combinations of

inputs. The combinations include (x_1, x_2, y), (x_1, x_3, y) and (x_2, x_3, y). For each of the combinations two inputs are allowed to vary while one is held constant, such as the response surface representing$(x_1, x_{2,}\, y)$, the input x_3 is held constant [76].

Chapter 7

RESULTS AND DISCUSSION

7.1 Current operating parameters

The current operating conditions are determined by analyzing the thermodynamics of each system using the current plant operating parameters as indicated in Appendices A and B.

Table 7.1 Current operating parameters of system 1.

Volume flow rate of air (m^3/s)	$\dot{V}_6$	232
Mass flow rate of fuel (kg/s)	$\dot{m}_1$	3.61
Total work (kW)	$\dot{W}_{net}$	62,700
Work of Fuel transfer pump (kW)	$\dot{W}_1$	42.86
Work of fuel centrifugal pump (kW)	$\dot{W}_3$	94.56
Work of Main 17 stages compressor (kW)	$\dot{W}_6$	2,065
Work of turbine (kW)	$\dot{W}_8$	60,497
Exergy destruction across fuel transfer pump (kW)	$\dot{E}_{dest_{fp1}}$	38.11
Exergy destruction across fuel centrifugal pump (kW)	$\dot{E}_{dest_{fp2}}$	40
Exergy destruction across fuel filter (kW)	$\dot{E}_{dest_{ff}}$	0
Exergy destruction across pressure regulating valve (kW)	$\dot{E}_{dest_{prv}}$	0
Exergy destruction across main 17 stages compressor (kW)	$\dot{E}_{dest_{comp}}$	1,383
Exergy destruction across main 5 stages turbine (kW)	$\dot{E}_{dest_t}$	22,907
Exergy destruction across combustion chamber (kW)	$\dot{E}_{dest_{cc}}$	6.12E+04
Energetic Efficiency	η_{en}	0.23
Exergetic Efficiency	η_{ex}	0.17

Table 7.2 Current operating parameters of system 2.

Volume flow rate of air (m^3/s)	$\dot{V}_{12}$	194.4
Mass flow rate of fuel (kg/s)	$\dot{m}_1$	3.80
Total work (kW)	$\dot{W}_{net}$	50,900
Work of fuel centrifugal pump (kW)	$\dot{W}_1$	130.7
Work of Fuel main displacement pump (kW)	$\dot{W}_4$	93.82
Work of main 17 stages compressor (kW)	$\dot{W}_{12}$	2,608
Work of atomizing compressor work (kW)	$\dot{W}_{15}$	55.78
Turbine work (kW)	$\dot{W}_{10}$	48,157
Exergy destruction across centrifugal fuel pump (kW)	$\dot{E}_{dest_{fp1}}$	78.01
Exergy destruction across main displacement pump (kW)	$\dot{E}_{dest_{fp2}}$	123.8
Exergy destruction across pressure regulating valve (kW)	$\dot{E}_{dest_{prv}}$	1.686
Exergy destruction across LP filter (kW)	$\dot{E}_{dest_{flp}}$	0
Exergy destruction across HP filter (kW)	$\dot{E}_{dest_{fhp}}$	0
Exergy destruction across main 17 stages compressor (kW)	$\dot{E}_{dest_{comp}}$	406.4
Exergy destruction across main 3 stages turbine (kW)	$\dot{E}_{dest_t}$	13,934
Exergy destruction across combustion chamber (kW)	$\dot{E}_{dest_{cc}}$	3.77E+03
Energetic Efficiency	η_{en}	0.25
Exergetic Efficiency	η_{ex}	0.16

Using the thermodynamic principles introduced earlier and the software Design-Expert® Stat-Ease (version 8.1.6), optimization of the system was performed. Optimization is defined by processing conditions which maximize energy efficiency, exergy efficiency and work output. The Stat-Ease uses a method developed by Derringer and Suich [77]. The specifics of their method are out of the scope of this thesis and will

not be discussed. Specifics of their method can be found in literature. Specifics pertaining to the plant operating parameters for system 1 and 2 are tabulated in Table 7.1 and Table 7.2 respectively.

7.2 Results of energy analysis

The fifth order regression model used to calculate energy efficiency to input variables of air-inlet temperature, fuel mass flow rate and air volume flow rate for both systems is

$$\sqrt{\eta_{en}} = a_0 + a_1A + a_2B + a_3C + a_4AB + a_5AC + a_6BC + a_7A^2 + a_8B^2 + a_9C^2 + a_{10}ABC + a_{11}A^2B + a_{12}A^2C + a_{13}AB^2 + a_{14}AC^2 + a_{15}B^2C + a_{16}C^2B + a_{17}A^3 + a_{18}B^3 + a_{19}C^3 + a_{20}A^2B^2 + a_{21}A^2BC + a_{22}A^2C^2 + a_{23}AB^2C + a_{24}ABC^2 + a_{25}B^2C^2 + a_{26}A^3B + a_{27}A^3C + a_{28}AB^3 + a_{29}AC^3 + a_{30}B^3C + a_{31}BC^3 + a_{32}A^4 + a_{33}B^4 + a_{34}C^4 + a_{35}A^2B^2C + a_{36}A^2BC^2 + a_{37}AB^2C^2 + a_{38}A^3B^2 + a_{39}A^3BC + a_{40}A^3C^2 + a_{41}A^2B^3 + a_{42}A^2C^3 + a_{43}AB^3C + a_{44}ABC^3 + a_{45}B^3C^2 + a_{46}B^3C^3 + a_{47}A^4B + a_{48}A^4C + a_{49}AB^4 + a_{50}AC^4 + a_{51}B^4C + a_{52}BC^4 + a_{53}A^5 + a_{54}B^5 + a_{55}C^5 \quad (7.1)$$

where **A** represents air inlet temperature (K), **B** represents mass flow rate of fuel (kg/s) and **C** represents volume flow rate of air (m^3/s). The regression coefficients a_0 - a_{55} are model fitting factors.

In Figures 7.1-7.2, and Figures 7.3-7.4 for systems 1 and 2 respectively show similar trends as those observed for exergy efficiency, the interaction between mass flow rate of fuel and inlet air temperature and their mutual effect on energy efficiency at different air flow rates. Air inlet temperature also plays an important role. By increasing

air inlet temperature, efficiency decreases and by decreasing air inlet temperature efficiency increases.

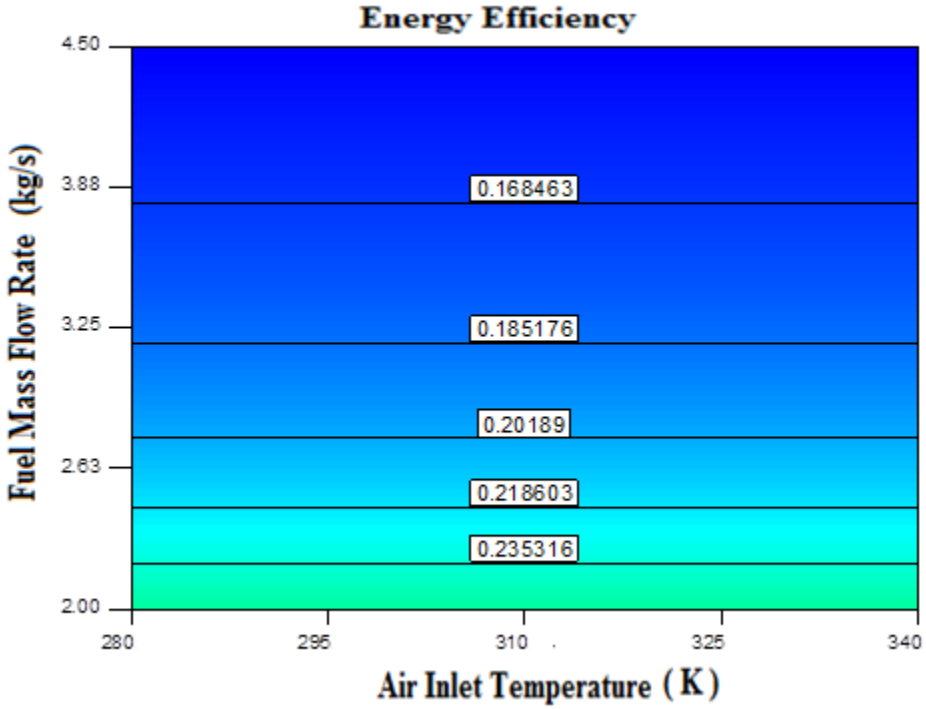

Figure 7.1 Relationship between air inlet temperature and fuel mass flow rate and their mutual effect on the energy efficiency of system 1 at 180 m^3/s volumetric air flow rate.

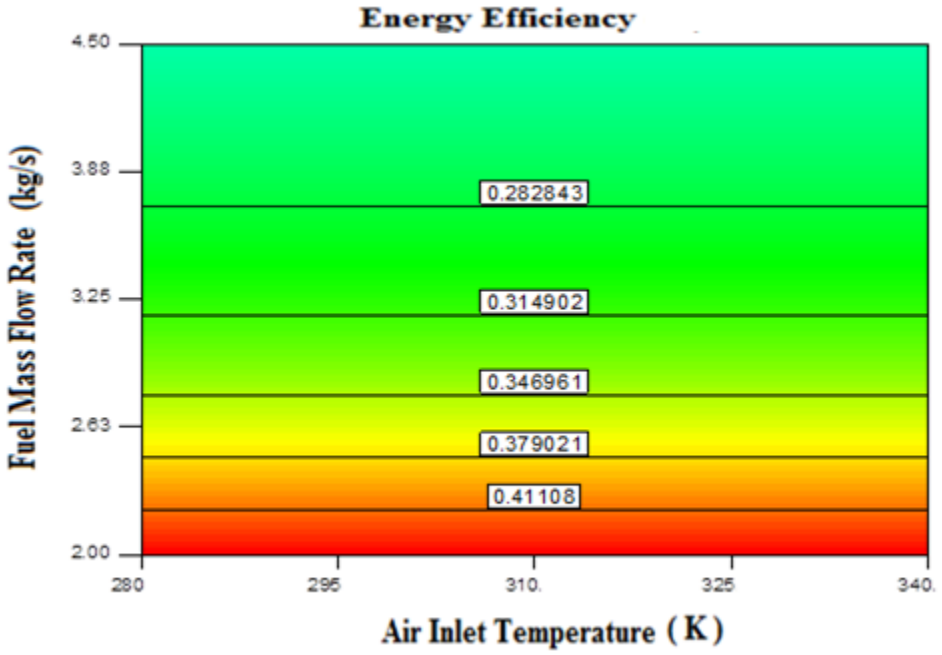

Figure 7.2 Relationship between air inlet temperature and fuel mass flow rate and their mutual effect on the energy efficiency of system 1 at 250 m^3/s volumetric air flow rate.

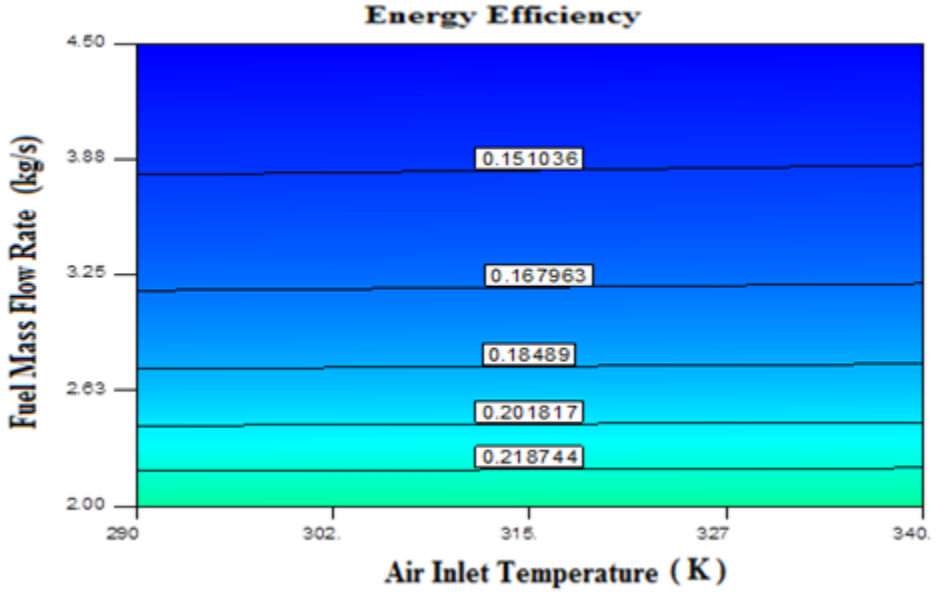

Figure 7.3 Relationship between air inlet temperature and fuel mass flow rate and their mutual effect on the energy efficiency of system 2 at 180 m^3/s volumetric flow rate of air.

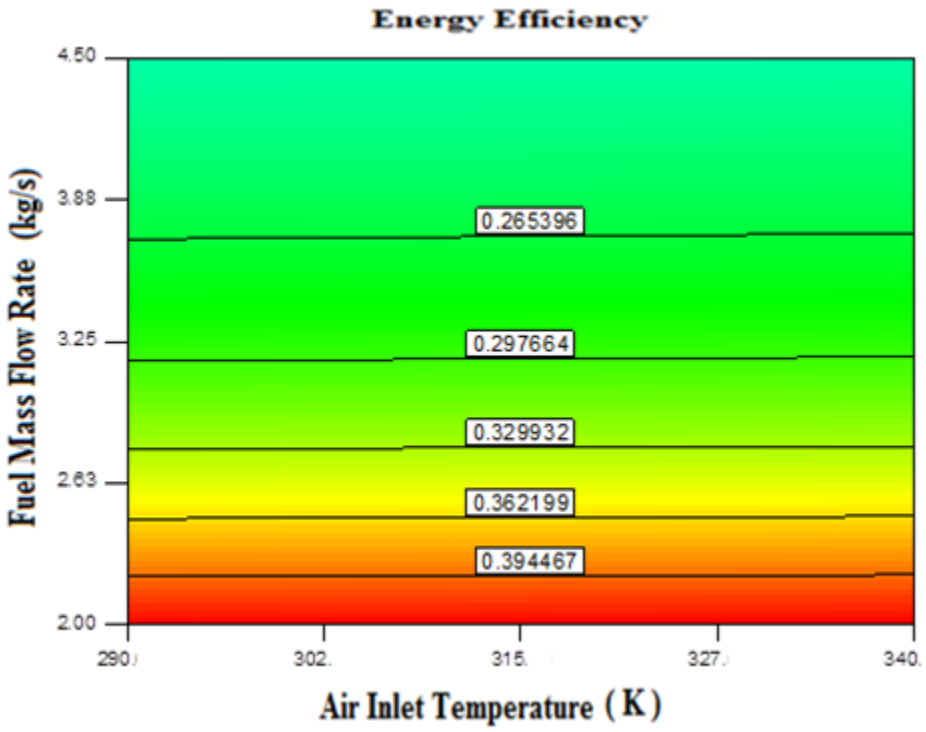

Figure 7.4 Relationship between air inlet temperature and fuel mass flow rate and their mutual effect on the energy efficiency of system 2 at 250 m^3/s volumetric air flow rate.

Table 7.3 represents the analysis of variance of the energy efficiency of system 1. The F-value of the models for the system is 31676781.51, which implies the models are significant. There is only a 0.01% chance that a "Model F-Value" this large could occur due to noise. Values of "Prob > F" less than 0.0500 indicate model terms are significant. In this case, B, C, BC, B^2, C^2, B^2C, BC^2, B^3, B^3C, B^4,C^4, B^3C^2, B^2C^3, B^4C, B^5 are significant model terms. The values greater than 0.1000 indicate the model terms are not significant.

Table 7.3 ANOVA results of system 1 for energy efficiency.

Source	Sum of Squares	df	Mean Square	F Value	p-value Prob > F
Model	1.508113	55	0.02742	31676782	< 0.0001
A-Air Inlet Temperature	0	1	0	0	1.0000
B-Fuel Flow Rate	0.007822	1	0.007822	9035825	< 0.0001
C-Volume Flow rate of Air	0.011144	1	0.011144	12874199	< 0.0001
AB	0	1	0	0	1.0000
AC	0	1	0	0	1.0000
BC	0.001762	1	0.001762	2035801	< 0.0001
A^2	0	1	0	0	1.0000
B^2	0.001159	1	0.001159	1339216	< 0.0001
C^2	4.74E-05	1	4.74E-05	54762.85	< 0.0001
ABC	0	1	0	0	1.0000
A^2B	0	1	0	0	1.0000
A^2C	0	1	0	0	1.0000
AB^2	0	1	0	0	1.0000
AC^2	0	1	0	0	1.0000
B^2C	4.58E-05	1	4.58E-05	52924.74	< 0.0001
BC^2	2.36E-06	1	2.36E-06	2725.573	< 0.0001
A^3	0	1	0	0	1.0000
B^3	1.45E-05	1	1.45E-05	16763.1	< 0.0001
C^3	1.86E-09	1	1.86E-09	2.151109	0.1436
A^2B^2	0	1	0	0	1.0000
A^2BC	0	1	0	0	1.0000
A^2C^2	0	1	0	0	1.0000
AB^2C	0	1	0	0	1.0000
ABC^2	0	1	0	0	1.0000
B^2C^2	4.21E-06	1	4.21E-06	4860.696	< 0.0001
A^3B	0	1	0	0	1.0000
A^3C	0	1	0	0	1.0000
AB^3	0	1	0	0	1.0000
AC^3	0	1	0	0	1.0000
B^3C	8.85E-05	1	8.85E-05	102231.4	< 0.0001
BC^3	1.86E-10	1	1.86E-10	0.214418	0.6437
A^4	0	1	0	0	1.0000

Table 7.3 (Continued).

Source	Sum of Squares	df	Mean Square	F Value	p-value Prob > F
B^4	5.86E-05	1	5.86E-05	67685.48	< 0.0001
C^4	1.89E-11	1	1.89E-11	0.02188	0.8825
A^2B^2C	0	1	0	0	1.0000
A^2BC^2	0	1	0	0	1.0000
AB^2C^2	0	1	0	0	1.0000
A^3B^2	0	1	0	0	1.0000
A^3BC	0	1	0	0	1.0000
A^3C^2	0	1	0	0	1.0000
A^2B^3	0	1	0	0	1.0000
A^2C^3	0	1	0	0	1.0000
AB^3C	0	1	0	0	1.0000
ABC^3	0	1	0	0	1.0000
B^3C^2	1.8E-07	1	1.8E-07	208.1586	< 0.0001
B^2C^3	7.89E-11	1	7.89E-11	0.091164	0.7629
A^4B	0	1	0	0	1.0000
A^4C	0	1	0	0	1.0000
AB^4	0	1	0	0	1.0000
AC^4	0	1	0	0	1.0000
B^4C	2.76E-06	1	2.76E-06	3193.412	< 0.0001
BC^4	1.56E-09	1	1.56E-09	1.802239	0.1805
A^5	0	1	0	0	1.0000
B^5	1.11E-06	1	1.11E-06	1285.237	< 0.0001
C^5	6.46E-10	1	6.46E-10	0.746705	0.3883
Residual	2.42E-07	280	8.66E-10		
Cor Total	1.508114	335			

The regression coefficients for a_0-a_{55} of system 2 energy efficiency, η_{en} are tabulated in Table 7.4

Table 7.4 Coefficients of regression of system 1 for energy efficiency.

Coefficients for Energy Efficiency							
a_0	0.458357	a_{14}	2.11E-16	a_{28}	4.69E-17	a_{42}	9.8E-23
a_1	1.06E-10	a_{15}	0.000675	a_{29}	-1.3E-19	a_{43}	-3.8E-19
a_2	-0.15863	a_{16}	-4.5E-06	a_{30}	-0.0001	a_{44}	-2.9E-22
a_3	-0.0033	a_{17}	1.65E-15	a_{31}	1.41E-08	a_{45}	1.29E-08
a_4	-3.1E-12	a_{18}	-0.0355	a_{32}	-2.3E-18	a_{46}	-1.3E-10
a_5	-2.2E-13	a_{19}	-3.2E-07	a_{33}	0.005824	a_{47}	2.49E-20
a_6	-0.00159	a_{20}	-1.4E-17	a_{34}	7.1E-10	a_{48}	1.21E-21
a_7	-5.9E-13	a_{21}	-2.1E-18	a_{35}	-3E-20	a_{49}	3.34E-18
a_8	0.101397	a_{22}	-5.5E-19	a_{36}	6.28E-22	a_{50}	7.97E-23
a_9	7.35E-05	a_{23}	2.97E-17	a_{37}	-1.6E-20	a_{51}	5.73E-06
a_{10}	5.53E-16	a_{24}	-8.1E-20	a_{38}	2.31E-20	a_{52}	-1.5E-11
a_{11}	1.49E-14	a_{25}	-4.9E-08	a_{39}	2.2E-21	a_{53}	1.25E-21
a_{12}	9.27E-16	a_{26}	-3.2E-17	a_{40}	5.21E-22	a_{54}	-0.00036
a_{13}	6.52E-16	a_{27}	-1.7E-18	a_{41}	4.63E-21	a_{55}	-6.2E-13

From Table 7.5, ANOVA for system 2 energetic efficiency,$\boldsymbol{\eta_{en}}$, indicates that F-value of the models for the system is 83579566.21, which implies the models are significant. There is only a 0.01% chance that a "Model F-Value" this large could occur due to noise. Values of "Prob > F" less than 0.0500 indicate model terms are significant. In this case, B, C, BC, B^2, C^2, B^2C, BC^2, B^3, B^3C, B^4,C^4, B^3C^2, B^2C^3, B^4C, B^5 are significant model terms. Values greater than 0.1000 indicate the model terms are not significant.

Table 7.5 ANOVA results of system 2 for energy efficiency.

Source	Sum of Squares	df	Mean Square	F Value	p-value Prob > F
Model	2.308901	55	0.04198	83579566	< 0.0001
A-Air Inlet Temperature	0	1	0	0	1.0000
B-Fuel Mass Flow Rate	0.013325	1	0.013325	26528469	< 0.0001
C-Air Volume Flow Rate	0.01929	1	0.01929	38404260	< 0.0001
AB	0	1	0	0	1.0000
AC	0	1	0	0	1.0000
BC	0.00104	1	0.00104	2071330	< 0.0001
A^2	0	1	0	0	1.0000
B^2	0.001364	1	0.001364	2716633	< 0.0001
C^2	5.14E-08	1	5.14E-08	102.3017	< 0.0001
ABC	0	1	0	0	1.0000
A^2B	0	1	0	0	1.0000
A^2C	0	1	0	0	1.0000
AB^2	0	1	0	0	1.0000
AC^2	0	1	0	0	1.0000
B^2C	1.54E-05	1	1.54E-05	30693.77	< 0.0001
BC^2	4.26E-09	1	4.26E-09	8.478687	0.0039
A^3	0	1	0	0	1.0000
B^3	1.3E-05	1	1.3E-05	25875.31	< 0.0001
C^3	1.19E-09	1	1.19E-09	2.365868	0.1251
A^2B^2	0	1	0	0	1.0000
A^2BC	0	1	0	0	1.0000
A^2C^2	0	1	0	0	1.0000
AB^2C	0	1	0	0	1.0000
ABC^2	0	1	0	0	1.0000
B^2C^2	1.12E-10	1	1.12E-10	0.223664	0.6366
A^3B	0	1	0	0	1.0000
A^3C	0	1	0	0	1.0000
AB^3	0	1	0	0	1.0000
AC^3	0	1	0	0	1.0000
B^3C	1.91E-05	1	1.91E-05	38005.49	< 0.0001
BC^3	1.55E-10	1	1.55E-10	0.308119	0.5793
A^4	0	1	0	0	1.0000
B^4	3.49E-05	1	3.49E-05	69542.36	< 0.0001

Table 7.5 (Continued)

C^4	2.49E-09	1	2.49E-09	4.962326	0.0267
A^2B^2C	0	1	0	0	1.0000
A^2BC^2	0	1	0	0	1.0000
AB^2C^2	0	1	0	0	1.0000
A^3B^2	0	1	0	0	1.0000
A^3BC	0	1	0	0	1.0000
A^3C^2	0	1	0	0	1.0000
A^2B^3	0	1	0	0	1.0000
A^2C^3	0	1	0	0	1.0000
AB^3C	0	1	0	0	1.0000
ABC^3	0	1	0	0	1.0000
B^3C^2	2.82E-09	1	2.82E-09	5.609473	0.0185
B^2C^3	2.25E-08	1	2.25E-08	44.72228	< 0.0001
A^4B	0	1	0	0	1.0000
A^4C	0	1	0	0	1.0000
AB^4	0	1	0	0	1.0000
AC^4	0	1	0	0	1.0000
B^4C	5.49E-07	1	5.49E-07	1093.428	< 0.0001
BC^4	1.3E-09	1	1.3E-09	2.580635	0.1093
A^5	0	1	0	0	1.0000
B^5	5.1E-07	1	5.1E-07	1015.525	< 0.0001
C^5	8.66E-10	1	8.66E-10	1.724867	0.1901
Residual	1.41E-07	280	5.02E-10		
Cor Total	2.308901	335			

The regression coefficients for a_0-a_{55} of system 2 energy efficiency, η_{en} are tabulated in Table 7.6

Table 7.6 Coefficients of regression of system 2 for energy efficiency.

Coefficients for Energy Efficiency							
a_0	-0.24272	a_{14}	4.98E-16	a_{28}	-4.9E-16	a_{42}	2.29E-22
a_1	8.98E-11	a_{15}	0.001086	a_{29}	-1.3E-19	a_{43}	-2.9E-19
a_2	-0.04641	a_{16}	2.51E-06	a_{30}	-0.00013	a_{44}	-6.3E-22
a_3	0.012885	a_{17}	4.52E-16	a_{31}	3.35E-09	a_{45}	1.54E-08
a_4	-2.1E-12	a_{18}	-0.03753	a_{32}	2.26E-19	a_{46}	1.52E-09
a_5	-6.4E-13	a_{19}	2.71E-07	a_{33}	0.006319	a_{47}	1.39E-20
a_6	-0.00366	a_{20}	-2.4E-17	a_{34}	-6.6E-10	a_{48}	3.68E-21
a_7	-3.5E-13	a_{21}	-6.2E-18	a_{35}	-1.8E-20	a_{49}	1.63E-17
a_8	0.087644	a_{22}	-1.5E-18	a_{36}	1.67E-21	a_{50}	-1.5E-23
a_9	-5.9E-05	a_{23}	1.96E-17	a_{37}	-1.1E-20	a_{51}	7.62E-06
a_{10}	1.95E-15	a_{24}	-5.3E-19	a_{38}	2.55E-20	a_{52}	-1.5E-11
a_{11}	9.32E-15	a_{25}	-1.1E-06	a_{39}	6.05E-21	a_{53}	-6.9E-22
a_{12}	2.74E-15	a_{26}	-1.9E-17	a_{40}	1.42E-21	a_{54}	-0.0004
a_{13}	7.26E-15	a_{27}	-5.2E-18	a_{41}	5.65E-19	a_{55}	6.8E-13

7.3 Results of exergy analysis

A similar analysis is performed for energy, as was performed for energy efficiency, the fifth order regression model used to calculate exergy efficiency to input variables of air inlet temperature, fuel mass flow rate and air volume flow rate for both systems is

$$\sqrt{\eta_{ex}} = a_0 + a_1A + a_2B + a_3C + a_4AB + a_5AC + a_6BC + a_7A^2 + a_8B^2 + a_9C^2 + a_{10}ABC + a_{11}A^2B + a_{12}A^2C + a_{13}AB^2 + a_{14}AC^2 + a_{15}B^2C + a_{16}C^2B + a_{17}A^3 + a_{18}B^3 + a_{19}C^3 + a_{20}A^2B^2 + a_{21}A^2BC + a_{22}A^2C^2 + a_{23}AB^2C + a_{24}ABC^2 + a_{25}B^2C^2 + a_{26}A^3B + a_{27}A^3C + a_{28}AB^3 + a_{29}AC^3 + a_{30}B^3C + a_{31}BC^3 + a_{32}A^4 + a_{33}B^4 + a_{34}C^4 + a_{35}A^2B^2C + a_{36}A^2BC^2 + a_{37}AB^2C^2 + a_{38}A^3B^2 + a_{39}A^3BC + a_{40}A^3C^2 + a_{41}A^2B^3 + a_{42}A^2C^3 + a_{43}AB^3C + a_{44}ABC^3 + a_{45}B^3C^2 + a_{46}B^3C^3 + a_{47}A^4B + a_{48}A^4C + a_{49}AB^4 + a_{50}AC^4 + a_{51}B^4C + a_{52}BC^4 + a_{53}A^5 + a_{54}B^5 + a_{55}C^5 \quad (7.2)$$

where **A** represents air inlet temperature (K), **B** represents mass flow rate of fuel (kg/s) and **C** represents volume flow rate of air (m^3/s). The regression coefficients a_0 - a_{55} are model fitting factors.

In the analysis of exergy, energy and net work, three parameters are varied parametrically. They are air inlet temperature (T), fuel mass flow rate ($\dot{m}_f$) and air volume flow rate ($\dot{V}$). The analysis of variance (ANOVA) is applied and the results showed that the selected parameters have considerable effect on the efficiency of the different systems (System 1 and 2). A square root transformation is applied to the three input parameters assisting the fitting of fifth order regression model chosen to model the relation between inputs and outputs for exergy and energy efficiency and net work analysis.

The results of both turbine systems indicate decreasing air flow and increasing fuel flow actually decreases efficiency. The trend can be explained as improper burning. In term of improper burring, we will not be able to get a desire combustion temperature which leads to decrease the efficiency of the system. Higher efficiency is observed at low air flow and low mass flow of fuel. Moreover, increasing the air flow increases the overall plant efficiency at low fuel flow. Figures 7.5 - 7.6 and Figures 7.7 - 7.8 show the interaction between mass flow rate of fuel and inlet air temperature, and their mutual effect on exergy efficiency at different air flow rates for the system 1 and 2 turbines respectively.

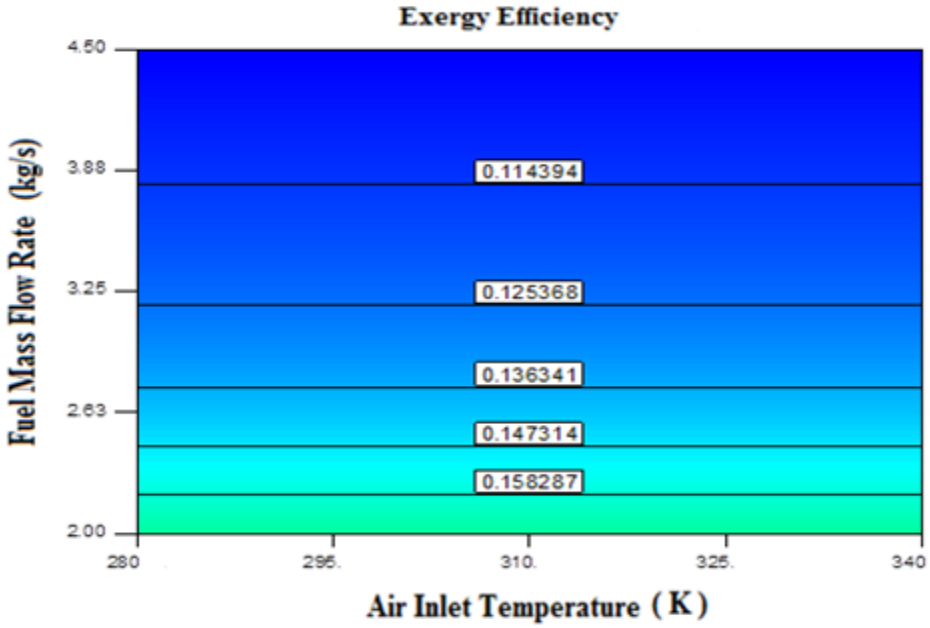

Figure 7.5 Relationship between air inlet temperature and fuel mass flow rate and their mutual effect on the exergy efficiency of system 1 at 180 m^3/s volumetric air flow rate.

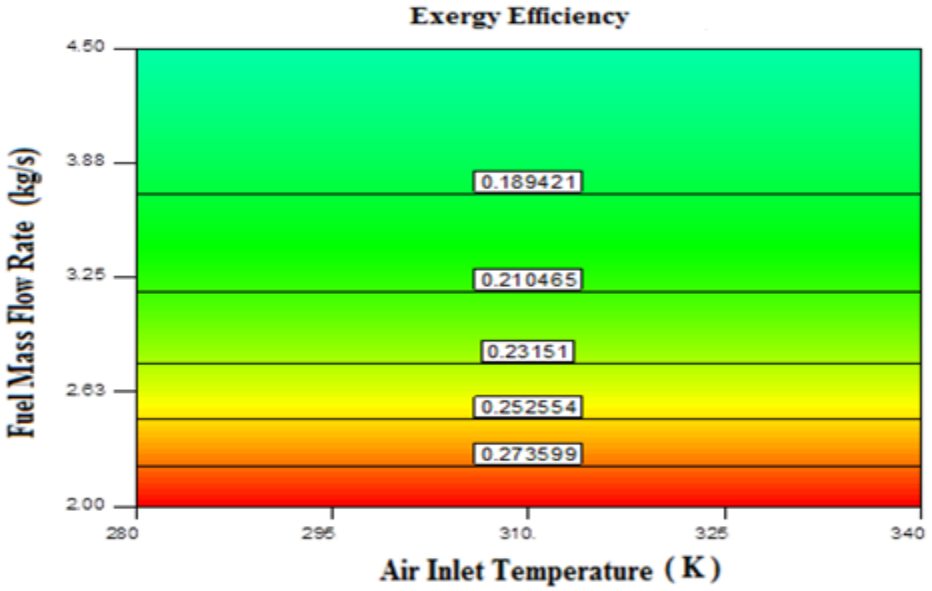

Figure 7.6 Relationship between air inlet temperature and fuel mass flow rate and their mutual effect on the exergy efficiency system 1 at 250 m^3/s volumetric air flow rate.

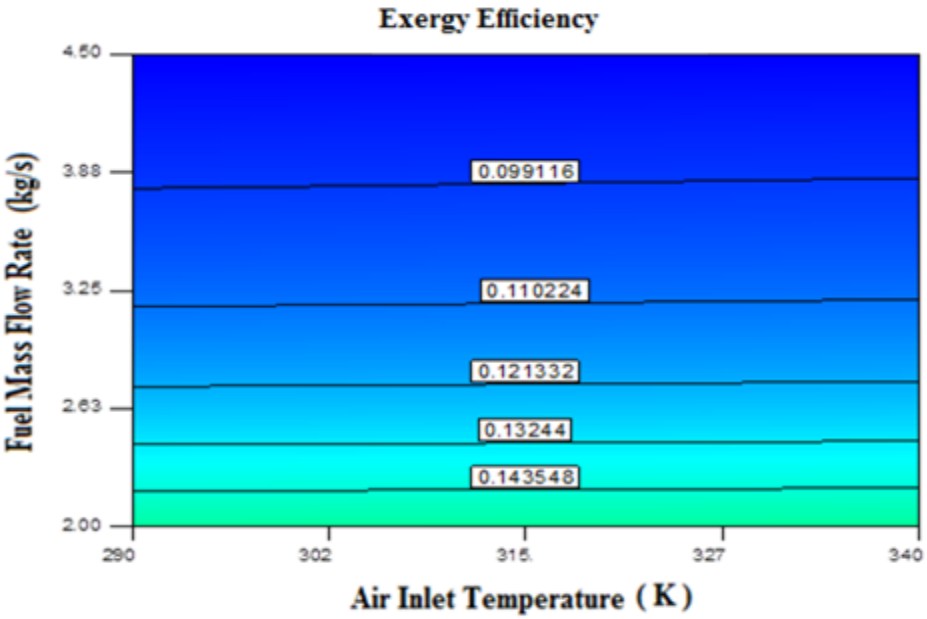

Figure 7.7 Relationship between air inlet temperature and fuel mass flow rate and their mutual effect on the exergy efficiency of system 2 at 180 m^3/s volumetric air flow rate.

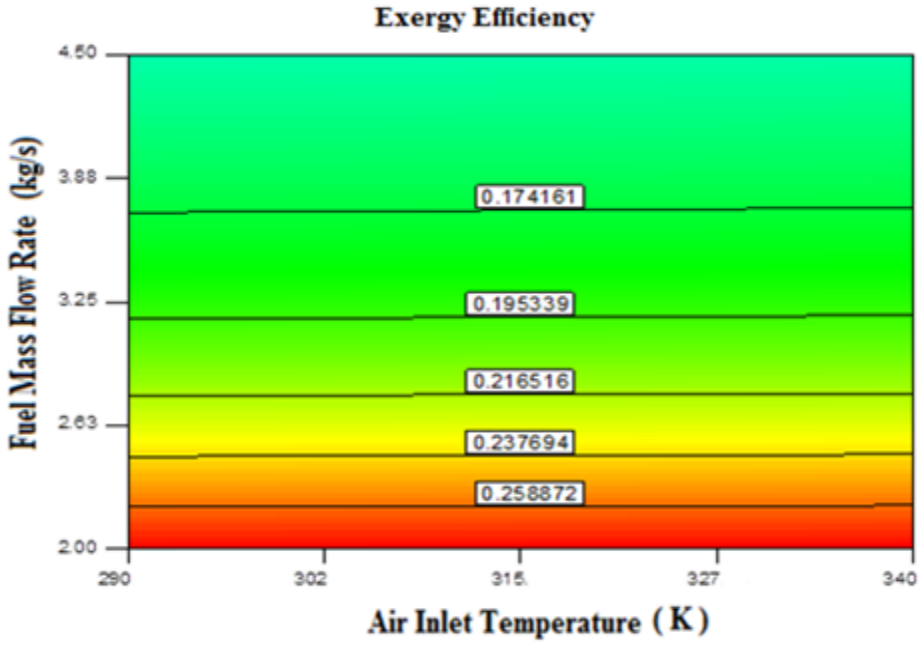

Figure 7.8 Relationship between air inlet temperature and fuel mass flow rate and their mutual effect on the exergy efficiency of system 2 at 250 m^3/s volumetric air flow rate.

The exergy efficiency, η_{ex}, ANOVA results of the system 1 is given in Table 7.7. The Model F-value for exergy efficiency is 17936046.09, implying the models are significant. There is only a 0.01% chance that a "Model F-Value" this large could occur due to noise. Values of "Prob > F" less than 0.0500 indicate model terms are significant. In this case B, C, BC, B^2, C^2, B^2C, BC^2, B^3, C^3, B^2C^2, B^3C, BC^3, B^4, C^4, B^3C^2, B^4C, BC^4, B^5, C^5 are significant model terms. Values greater than 0.1000 indicate the model terms are not significant

Table 7.7 ANOVA results of system 1 for exergtic efficiency.

Source	Sum of Squares	df	Mean Square	F Value	p-value Prob > F
Model	0.979654	55	0.017812	17936046	< 0.0001
A-Air Inlet Temperature	0	1	0	0	1.0000
B-Fuel Flow Rate	0.005679	1	0.005679	5718790	< 0.0001
C-Volume Flow rate of Air	0.008113	1	0.008113	8169895	< 0.0001
AB	0	1	0	0	1.0000
AC	0	1	0	0	1.0000
BC	0.000434	1	0.000434	436881.9	< 0.0001
A^2	0	1	0	0	1.0000
B^2	0.000585	1	0.000585	589080.5	< 0.0001
C^2	1.31E-07	1	1.31E-07	131.6711	< 0.0001
ABC	0	1	0	0	1.0000
A^2B	0	1	0	0	1.0000
A^2C	0	1	0	0	1.0000
AB^2	0	1	0	0	1.0000
AC^2	0	1	0	0	1.0000
B^2C	5.85E-06	1	5.85E-06	5892.737	< 0.0001
BC^2	8.93E-09	1	8.93E-09	8.995404	0.0029
A^3	0	1	0	0	1.0000
B^3	5.97E-06	1	5.97E-06	6006.902	< 0.0001
C^3	1.18E-08	1	1.18E-08	11.8764	0.0007
A^2B^2	0	1	0	0	1.0000

Table 7.7 (Continued).

Source	Sum of Squares	df	Mean Square	F Value	p-value Prob > F
A^2BC	0	1	0	0	1.0000
A^2C^2	0	1	0	0	1.0000
AB^2C	0	1	0	0	1.0000
ABC^2	0	1	0	0	1.0000
B^2C^2	1.85E-08	1	1.85E-08	18.615	< 0.0001
A^3B	0	1	0	0	1.0000
A^3C	0	1	0	0	1.0000
AB^3	0	1	0	0	1.0000
AC^3	0	1	0	0	1.0000
B^3C	7.37E-06	1	7.37E-06	7417.859	< 0.0001
BC^3	7.36E-09	1	7.36E-09	7.408053	0.0069
A^4	0	1	0	0	1.0000
B^4	1.49E-05	1	1.49E-05	15017.27	< 0.0001
C^4	3.12E-08	1	3.12E-08	31.39289	< 0.0001
A^2B^2C	0	1	0	0	1.0000
A^2BC^2	0	1	0	0	1.0000
AB^2C^2	0	1	0	0	1.0000
A^3B^2	0	1	0	0	1.0000
A^3BC	0	1	0	0	1.0000
A^3C^2	0	1	0	0	1.0000
A^2B^3	0	1	0	0	1.0000
A^2C^3	0	1	0	0	1.0000
AB^3C	0	1	0	0	1.0000
ABC^3	0	1	0	0	1.0000
B^3C^2	1.19E-08	1	1.19E-08	11.97823	0.0006
B^2C^3	1.95E-09	1	1.95E-09	1.967825	0.1618
A^4B	0	1	0	0	1.0000
A^4C	0	1	0	0	1.0000
AB^4	0	1	0	0	1.0000
AC^4	0	1	0	0	1.0000
B^4C	4.37E-07	1	4.37E-07	439.8399	< 0.0001
BC^4	1.21E-08	1	1.21E-08	12.13522	0.0006
A^5	0	1	0	0	1.0000
B^5	1.46E-07	1	1.46E-07	146.7914	< 0.0001
C^5	6.53E-09	1	6.53E-09	6.577724	0.0108
Residual	2.78E-07	280	9.93E-10		
Cor Total	0.979655	335			

The regression coefficients for a_0-a_{55} of system 1 exergy efficiency, η_{ex} are tabulated in Table 7.8.

Table 7.8 Coefficients of regression of system 1 for exergy efficiency.

Coefficients for Exergy Efficiency							
a_0	1.371845	a_{14}	1.13E-17	a_{28}	-1E-16	a_{42}	1.09E-23
a_1	-7E-11	a_{15}	0.000428	a_{29}	-1.4E-19	a_{43}	1.98E-19
a_2	-0.1922	a_{16}	-1.6E-05	a_{30}	-9.1E-05	a_{44}	1.76E-21
a_3	-0.02462	a_{17}	-1.6E-15	a_{31}	4.24E-08	a_{45}	-3.2E-08
a_4	-1E-12	a_{18}	-0.01657	a_{32}	2.59E-18	a_{46}	-4.5E-10
a_5	-3E-14	a_{19}	-1E-06	a_{33}	0.002958	a_{47}	5.68E-21
a_6	0.000661	a_{20}	-8E-18	a_{34}	2.22E-09	a_{48}	2.95E-22
a_7	4.69E-13	a_{21}	-4.5E-18	a_{35}	2.37E-20	a_{49}	1.66E-18
a_8	0.053651	a_{22}	1.22E-19	a_{36}	2.36E-21	a_{50}	1.47E-22
a_9	0.000245	a_{23}	-2.4E-17	a_{37}	1.74E-20	a_{51}	6.8E-06
a_{10}	2.04E-15	a_{24}	-2.7E-18	a_{38}	2.83E-21	a_{52}	-4.7E-11
a_{11}	4.13E-15	a_{25}	6.24E-07	a_{39}	3.62E-21	a_{53}	-1.7E-21
a_{12}	1.28E-16	a_{26}	-7.8E-18	a_{40}	-1.5E-22	a_{54}	-0.00022
a_{13}	5.27E-15	a_{27}	-3.2E-19	a_{41}	7.71E-20	a_{55}	-1.9E-12

From Table 7.9, the Model F-value for system 2's exergy efficiency is 39311324.13, implying the models are significant. There is only a 0.01% chance that a "Model F-Value" this large could occur due to noise. Values of "Prob > F" less than 0.0500 indicate model terms are significant. In this case B, C, BC, B^2, C^2, B^2C, BC^2, B^3, C^3, B^2C^2, B^3C, BC^3, B^4, C^4, B^3C^2, B^4C, BC^4, B^5, C^5 are significant model terms. The values greater than 0.1000 indicate the model terms are not significant.

Table 7.9 ANOVA results of system 2 for exergy efficiency.

Source	Sum of Squares	df	Mean Square	F Value	p-value Prob > F
Model	1.515996	55	0.027564	39311324	< 0.0001
A-Air Inlet Temperature	0	1	0	0	1.0000
B-Fuel Mass Flow Rate	0.008768	1	0.008768	12505559	< 0.0001
C-Air Volume Flow Rate	0.01264	1	0.01264	18026832	< 0.0001
AB	0	1	0	0	1.0000
AC	0	1	0	0	1.0000
BC	0.000684	1	0.000684	976001.3	< 0.0001
A^2	0	1	0	0	1.0000
B^2	0.000898	1	0.000898	1280457	< 0.0001
C^2	4.63E-08	1	4.63E-08	66.01506	< 0.0001
ABC	0	1	0	0	1.0000
A^2B	0	1	0	0	1.0000
A^2C	0	1	0	0	1.0000
AB^2	0	1	0	0	1.0000
AC^2	0	1	0	0	1.0000
B^2C	1.1E-05	1	1.1E-05	15734.9	< 0.0001
BC^2	4.37E-09	1	4.37E-09	6.229465	0.0131
A^3	0	1	0	0	1.0000
B^3	7.99E-06	1	7.99E-06	11399.69	< 0.0001
C^3	1.84E-08	1	1.84E-08	26.20646	< 0.0001
A^2B^2	0	1	0	0	1.0000
A^2BC	0	1	0	0	1.0000
A^2C^2	0	1	0	0	1.0000
AB^2C	0	1	0	0	1.0000
ABC^2	0	1	0	0	1.0000
B^2C^2	1.22E-08	1	1.22E-08	17.45302	< 0.0001
A^3B	0	1	0	0	1.0000
A^3C	0	1	0	0	1.0000
AB^3	0	1	0	0	1.0000
AC^3	0	1	0	0	1.0000
B^3C	1.25E-05	1	1.25E-05	17794.59	< 0.0001
BC^3	1.31E-09	1	1.31E-09	1.868887	0.1727
A^4	0	1	0	0	1.0000
B^4	2.31E-05	1	2.31E-05	32907.82	< 0.0001

Table 7.9 (Continued).

C^4	6.51E-09	1	6.51E-09	9.280892	0.0025
A^2B^2C	0	1	0	0	1.0000
A^2BC^2	0	1	0	0	1.0000
AB^2C^2	0	1	0	0	1.0000
A^3B^2	0	1	0	0	1.0000
A^3BC	0	1	0	0	1.0000
A^3C^2	0	1	0	0	1.0000
A^2B^3	0	1	0	0	1.0000
A^2C^3	0	1	0	0	1.0000
AB^3C	0	1	0	0	1.0000
ABC^3	0	1	0	0	1.0000
B^3C^2	2.68E-09	1	2.68E-09	3.820565	0.0516
B^2C^3	8.73E-09	1	8.73E-09	12.44682	0.0005
A^4B	0	1	0	0	1.0000
A^4C	0	1	0	0	1.0000
AB^4	0	1	0	0	1.0000
AC^4	0	1	0	0	1.0000
B^4C	2.08E-07	1	2.08E-07	296.2664	< 0.0001
BC^4	5.64E-09	1	5.64E-09	8.04786	0.0049
A^5	0	1	0	0	1.0000
B^5	4.5E-07	1	4.5E-07	641.3093	< 0.0001
C^5	2.83E-08	1	2.83E-08	40.35212	< 0.0001
Residual	1.96E-07	280	7.01E-10		
Cor Total	1.515996	335			

The regression coefficients for a_0-a_{55} of system 2 exergy efficiency, η_{ex} are tabulated in Table 7.10

Table 7.10 Coefficients of regression of system 2 for exergy efficiency.

Coefficients for Exergy Efficiency							
a_0	2.047611	a_{14}	-1.8E-16	a_{28}	-2.5E-16	a_{42}	-1.8E-22
a_1	-9.5E-11	a_{15}	0.000643	a_{29}	2.06E-19	a_{43}	1.68E-19
a_2	-0.19551	a_{16}	-5.3E-06	a_{30}	-7.5E-05	a_{44}	6.62E-22
a_3	-0.04003	a_{17}	-1.8E-15	a_{31}	2.15E-08	a_{45}	-1.5E-08
a_4	-1.4E-12	a_{18}	-0.04127	a_{32}	2.71E-18	a_{46}	9.48E-10
a_5	1.3E-13	a_{19}	-1.9E-06	a_{33}	0.006288	a_{47}	9.32E-21
a_6	-0.00145	a_{20}	-2.2E-17	a_{34}	4.31E-09	a_{48}	-6.9E-22
a_7	5.76E-13	a_{21}	-3.2E-18	a_{35}	1.39E-20	a_{49}	7.92E-18
a_8	0.121931	a_{22}	3.58E-19	a_{36}	1.44E-21	a_{50}	-1.1E-22
a_9	0.000414	a_{23}	-1.4E-17	a_{37}	9.6E-21	a_{51}	4.69E-06
a_{10}	1.31E-15	a_{24}	-1.4E-18	a_{38}	1.92E-20	a_{52}	-3.2E-11
a_{11}	6.09E-15	a_{25}	-4.9E-07	a_{39}	2.7E-21	a_{53}	-1.7E-21
a_{12}	-5.2E-16	a_{26}	-1.2E-17	a_{40}	-2.7E-22	a_{54}	-0.00038
a_{13}	9.24E-15	a_{27}	9.6E-19	a_{41}	2.01E-19	a_{55}	-3.9E-12

7.4 Work output results

The total output work of the system increases with an increase in mass flow of fuel and at low inlet temperature. An increase in temperature decreases net work, due to the decrease of either of the other two efficiencies discussed earlier. In Figures 7.9 - 7.10 and Figures 7.11 - 7.12 for systems 1 and 2 respectively show the interaction between mass flow rate of fuel and inlet air temperature and their mutual effect on net work output at different air flow rates. Once again, a fifth order regression model is employed and a transformation is applied. The calculated regression for net work in terms of air-inlet temperature, mass flow of fuel and volume flow of air is

$$\dot{W}_{net} = a_0 + a_1A + a_2B + a_3C + a_4AB + a_5AC + a_6BC + a_7A^2 + a_8B^2 + a_9C^2 + a_{10}ABC + a_{11}A^2B + a_{12}A^2C + a_{13}AB^2 + a_{14}AC^2 + a_{15}B^2C + a_{16}C^2B + a_{17}A^3 + a_{18}B^3 + a_{19}C^3 +$$

$$a_{20}A^2B^2 + a_{21}\,A^2BC + a_{22}A^2C^2 + a_{23}AB^2C + a_{24}ABC^2 + a_{25}B^2C^2 + a_{26}A^3B + a_{27}A^3C + a_{28}\,AB^3 + a_{29}AC^3 + a_{30}B^3C + a_{31}BC^3 + a_{32}A^4 + a_{33}B^4 + a_{34}C^4 + a_{35}A^2B^2C + a_{36}A^2BC^2 + a_{37}\,AB^2C^2 + a_{38}A^3B^2 + a_{39}\,A^3BC + a_{40}A^3C^2 + a_{41}A^2B^3 + a_{42}A^2C^3 + a_{43}AB^3C + a_{44}ABC^3 + a_{45}B^3C^2 + a_{46}\,B^3C^3 + a_{47}A^4B + a_{48}A^4C + a_{49}AB^4 + a_{50}AC^4 + a_{51}B^4C + a_{52}BC^4 + a_{53}A^5 + a_{54}B^5 + a_{55}C^5 \quad (7.3)$$

where **A** represents air inlet temperature (K), **B** represents mass flow rate of fuel (kg/s) and **C** represents volume flow rate of air (m^3/s). The regression coefficients a_0 - a_{55} are model fitting factors.

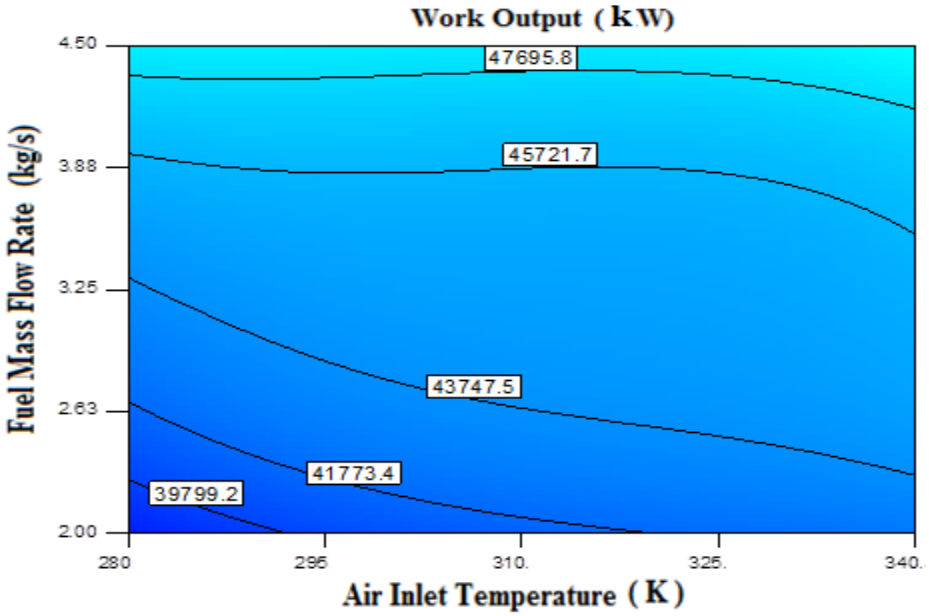

Figure 7.9 Relationship between air inlet temperature and fuel mass flow rate and their mutual effect on the net work of system 1 at 180 m^3/s volumetric air flow rate.

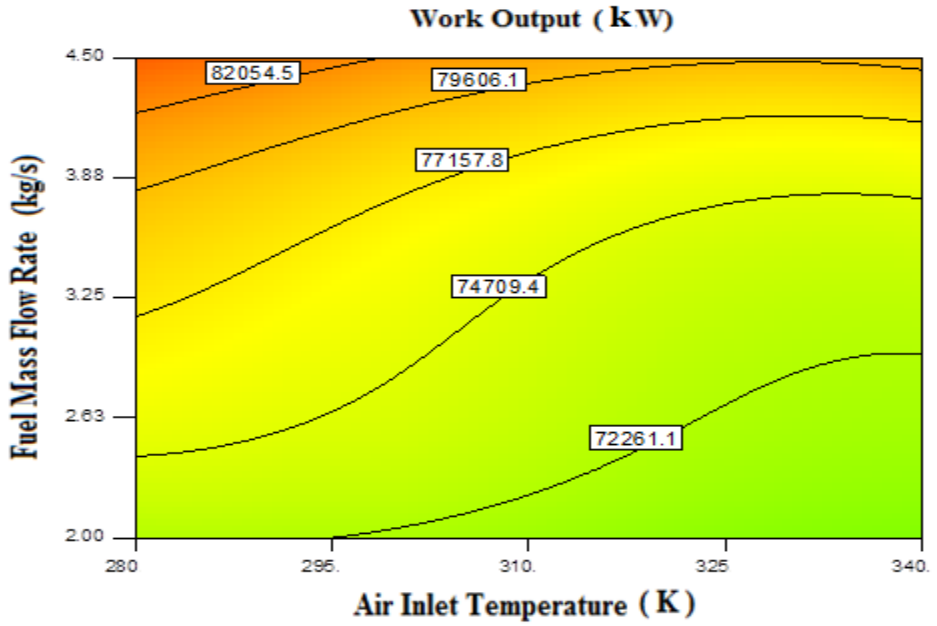

Figure 7.10 Relationship between air inlet temperature and fuel mass flow rate and their mutual effect on the net work of system 1 at 250 m^3/s volumetric air flow rate.

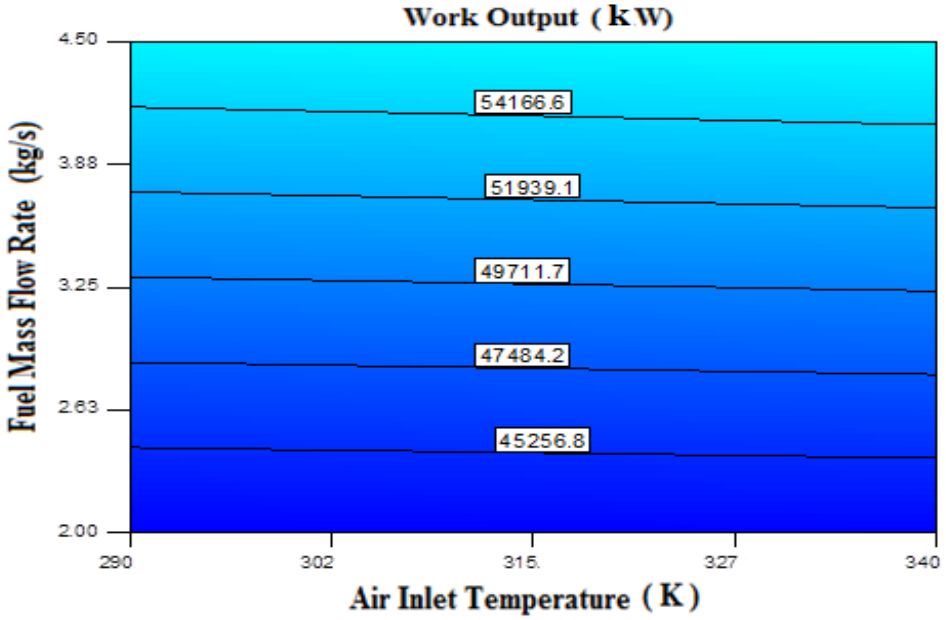

Figure 7.11 Relationship between air inlet temperature and fuel mass flow rate and their mutual effect on the net work of system 2 at 180 m^3/s volumetric air flow rate.

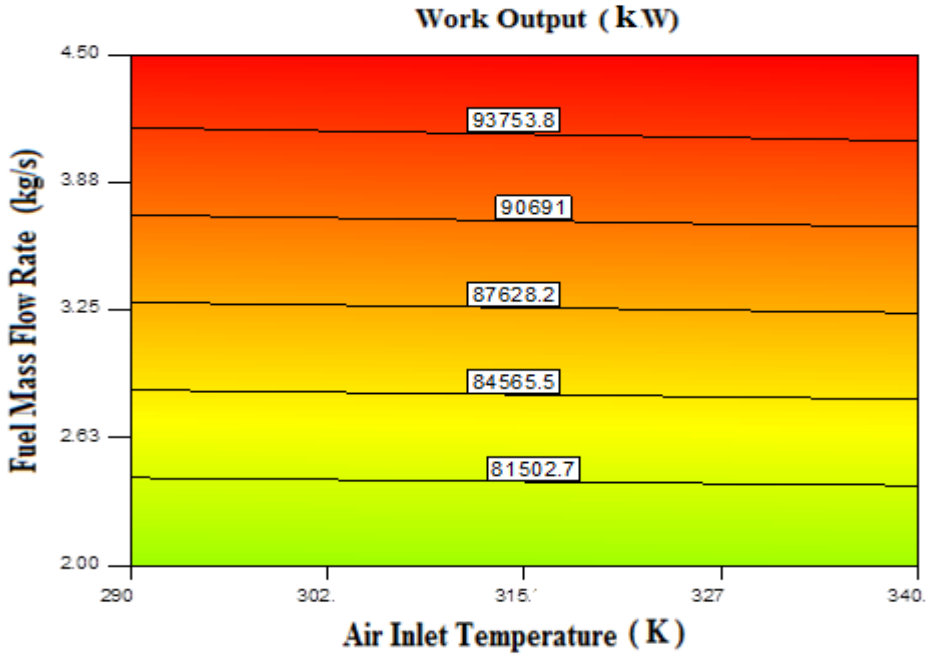

Figure 7.12 Relationship between air inlet temperature and fuel mass flow rate and their mutual effect on the net work of system 2 at 250 m^3/s volumetric air flow rate.

The analysis of variance (ANOVA) results of system 1 for $\dot{W}_{net}$ are shown in Table 7.11. The Model F-value of the system is 25723703492.92, implying the models are significant. There is only a 0.01% chance that a "Model F-Value" this large could occur due to noise. Values of "Prob > F" less than 0.0500 indicate model terms are significant. In this case B, C, BC, B^2, C^2, B^2C, BC^2, C^3, BC^3, B^4, B^3C^2, B^4C, BC^4, C^5 are significant model terms. Values greater than 0.1000 indicate the model terms are not significant.

Table 7.11 ANOVA results of system 1 for work output.

Source	Sum of Squares	df	Mean Square	F Value	p-value Prob > F
Model	6.14E+10	55	1.12E+09	2.57E+10	< 0.0001
A-Air Inlet Temperature	0	1	0	0	1.0000
B-Fuel Flow Rate	1.27E+08	1	1.27E+08	2.94E+09	< 0.0001
C-Volume Flow rate of Air	9.95E+08	1	9.95E+08	2.29E+10	< 0.0001
AB	0	1	0	0	1.0000
AC	0	1	0	0	1.0000
BC	6903608	1	6903608	1.59E+08	< 0.0001
A^2	0	1	0	0	1.0000
B^2	866.4998	1	866.4998	19974.03	< 0.0001
C^2	4233639	1	4233639	97591276	< 0.0001
ABC	0	1	0	0	1.0000
A^2B	0	1	0	0	1.0000
A^2C	0	1	0	0	1.0000
AB^2	0	1	0	0	1.0000
AC^2	0	1	0	0	1.0000
B^2C	0.944458	1	0.944458	21.77107	< 0.0001
BC^2	1.708366	1	1.708366	39.38023	< 0.0001
A^3	0	1	0	0	1.0000
B^3	0.004028	1	0.004028	0.092858	0.7608
C^3	1.041374	1	1.041374	24.00513	< 0.0001
A^2B^2	0	1	0	0	1.0000
A^2BC	0	1	0	0	1.0000
A^2C^2	0	1	0	0	1.0000
AB^2C	0	1	0	0	1.0000
ABC^2	0	1	0	0	1.0000
B^2C^2	0.012405	1	0.012405	0.285962	0.5932
A^3B	0	1	0	0	1.0000
A^3C	0	1	0	0	1.0000
AB^3	0	1	0	0	1.0000
AC^3	0	1	0	0	1.0000
B^3C	0.039124	1	0.039124	0.901852	0.3431
BC^3	0.985229	1	0.985229	22.71091	< 0.0001
A^4	0	1	0	0	1.0000

Table 7.11 (Continued).

Source	Sum of Squares	df	Mean Square	F Value	p-value Prob > F
B^4	0.78125	1	0.78125	18.0089	< 0.0001
C^4	0.047356	1	0.047356	1.091614	0.2970
A^2B^2C	0	1	0	0	1.0000
A^2BC^2	0	1	0	0	1.0000
AB^2C^2	0	1	0	0	1.0000
A^3B^2	0	1	0	0	1.0000
A^3BC	0	1	0	0	1.0000
A^3C^2	0	1	0	0	1.0000
A^2B^3	0	1	0	0	1.0000
A^2C^3	0	1	0	0	1.0000
AB^3C	0	1	0	0	1.0000
ABC^3	0	1	0	0	1.0000
B^3C^2	3.972458	1	3.972458	91.5707	< 0.0001
B^2C^3	0.053352	1	0.053352	1.229846	0.2684
A^4B	0	1	0	0	1.0000
A^4C	0	1	0	0	1.0000
AB^4	0	1	0	0	1.0000
AC^4	0	1	0	0	1.0000
B^4C	1.251495	1	1.251495	28.84871	< 0.0001
BC^4	0.198868	1	0.198868	4.58418	0.0331
A^5	0	1	0	0	1.0000
B^5	0.03125	1	0.03125	0.720356	0.3968
C^5	1.180023	1	1.180023	27.20118	< 0.0001
Residual	12.14677	280	0.043381		
Cor Total	6.14E+10	335			

The regression coefficients for a_0-a_{55} of system 1 turbine's net work, $\dot{W}_{net}$ are tabulated in below Table 7.12

Table 7.12 Coefficients of regression of system 1 for work output.

Coefficients for Work Output							
a_0	-9478.56	a_{14}	1.56E-12	a_{28}	-1.7E-11	a_{42}	2.28E-18
a_1	1.97E-07	a_{15}	-1.38921	a_{29}	-3.4E-15	a_{43}	1.94E-14
a_2	-823.957	a_{16}	-0.06471	a_{30}	0.099912	a_{44}	3.82E-17
a_3	226.5011	a_{17}	2.56E-12	a_{31}	0.000155	a_{45}	-0.00058
a_4	-1E-08	a_{18}	13.14683	a_{32}	-3.4E-15	a_{46}	2.34E-06
a_5	-6.9E-10	a_{19}	0.011106	a_{33}	-3.89087	a_5	-6.9E-10
a_6	41.07509	a_{20}	-1.1E-12	a_{34}	-2.6E-05	a_6	41.07509
a_7	-9.7E-10	a_{21}	-7.7E-14	a_{35}	1.14E-15	a_7	-9.7E-10
a_8	76.8597	a_{22}	-1.2E-15	a_{36}	4.94E-17	a_8	76.8597
a_9	-1.24077	a_{23}	-1.3E-12	a_{37}	9.66E-16	a_9	-1.24077
a_{10}	4.2E-11	a_{24}	-6.2E-14	a_{38}	7.11E-16	a_{10}	4.2E-11
a_{11}	2.78E-11	a_{25}	0.004098	a_{39}	5.09E-17	a_{11}	2.78E-11
a_{12}	2.01E-12	a_{26}	-3.4E-14	a_{40}	-5.3E-19	a_{12}	2.01E-12
a_{13}	5.67E-10	a_{27}	-3.5E-15	a_{41}	1.56E-14	a_{13}	5.67E-10

From Table 7.13, the ANOVA results of system 2 work output,$\dot{W}_{net}$, indicates that F-value of the models for the system is 14050934484.75, implies the model is significant. There is only a 0.01% chance that a "Model F-Value" this large could occur due to noise. Values of "Prob > F" less than 0.0500 indicate model terms are significant. In this case B, C, BC, B^2, C^2, BC^2, B^3, C^4, B^2C^3, BC^4, B^5 are significant model terms. The values greater than 0.1000 indicate the model terms are not significant.

Table 7.13 ANOVA results of system 2 for work output.

Source	Sum of Squares	df	Mean Square	F Value	p-value Prob > F
Model	4.61E+10	55	8.39E+08	1.41E+10	< 0.0001
A-Air Inlet Temperature	0	1	0	0	1.0000
B-Fuel Mass Flow Rate	88177260	1	88177260	1.48E+09	< 0.0001
C-Air Volume Flow Rate	7.59E+08	1	7.59E+08	1.27E+10	< 0.0001
AB	0	1	0	0	1.0000
AC	0	1	0	0	1.0000
BC	4824483	1	4824483	80793368	< 0.0001
A^2	0	1	0	0	1.0000
B^2	652.4038	1	652.4038	10925.5	< 0.0001
C^2	3379401	1	3379401	56593250	< 0.0001
ABC	0	1	0	0	1.0000
A^2B	0	1	0	0	1.0000
A^2C	0	1	0	0	1.0000
AB^2	0	1	0	0	1.0000
AC^2	0	1	0	0	1.0000
B^2C	0.137062	1	0.137062	2.295315	0.1309
BC^2	0.823143	1	0.823143	13.78479	0.0002
A^3	0	1	0	0	1.0000
B^3	0.373169	1	0.373169	6.249287	0.0130
C^3	0.013008	1	0.013008	0.217841	0.6411
A^2B^2	0	1	0	0	1.0000
A^2BC	0	1	0	0	1.0000
A^2C^2	0	1	0	0	1.0000
AB^2C	0	1	0	0	1.0000
ABC^2	0	1	0	0	1.0000
B^2C^2	0.001984	1	0.001984	0.033219	0.8555
A^3B	0	1	0	0	1.0000
A^3C	0	1	0	0	1.0000
AB^3	0	1	0	0	1.0000
AC^3	0	1	0	0	1.0000
B^3C	0.18148	1	0.18148	3.039168	0.0824
BC^3	0.001511	1	0.001511	0.025298	0.8737
A^4	0	1	0	0	1.0000
B^4	0.125	1	0.125	2.093317	0.1491

Table 7.13 (Continued).

Source	Sum of Squares	df	Mean Square	F Value	p-value Prob > F
C^4	1.280304	1	1.280304	21.44066	< 0.0001
A^2B^2C	0	1	0	0	1.0000
A^2BC^2	0	1	0	0	1.0000
AB^2C^2	0	1	0	0	1.0000
A^3B^2	0	1	0	0	1.0000
A^3BC	0	1	0	0	1.0000
A^3C^2	0	1	0	0	1.0000
A^2B^3	0	1	0	0	1.0000
A^2C^3	0	1	0	0	1.0000
AB^3C	0	1	0	0	1.0000
ABC^3	0	1	0	0	1.0000
B^3C^2	0.000923	1	0.000923	0.01546	0.9011
B^2C^3	0.789139	1	0.789139	13.21534	0.0003
A^4B	0	1	0	0	1.0000
A^4C	0	1	0	0	1.0000
AB^4	0	1	0	0	1.0000
AC^4	0	1	0	0	1.0000
B^4C	0.005951	1	0.005951	0.099657	0.7525
BC^4	1.200645	1	1.200645	20.10665	< 0.0001
A^5	0	1	0	0	1.0000
B^5	0.347221	1	0.347221	5.814755	0.0165
C^5	0.034187	1	0.034187	0.572519	0.4499
Residual	16.71988	280	0.059714		
Cor Total	4.61E+10	335			

The regression coefficients for a_0-a_{55} of system 2 net work, $\dot{W}_{net}$ are tabulated in Table 7.14.

Table 7.14 Coefficients of regression of system 2 for work output.

Coefficients for Work Output							
a_0	4887.349	a_{14}	3.78E-13	a_{28}	-2.3E-12	a_{42}	3.98E-19
a_1	6.49E-09	a_{15}	1.302566	a_{29}	-2.8E-16	a_{43}	1.92E-15
a_2	-284.568	a_{16}	-0.0906	a_{30}	-0.01164	a_{44}	4.34E-18
a_3	-120.982	a_{17}	6.72E-13	a_{31}	0.000342	a_{45}	8.82E-06
a_4	4.62E-09	a_{18}	35.50705	a_{32}	-1.6E-15	a_{46}	9.02E-06
a_5	1.38E-10	a_{19}	-0.00353	a_{33}	-5.50397	a_{47}	-4E-17
a_6	33.99713	a_{20}	-6.3E-14	a_{34}	6.52E-06	a_{48}	-2.2E-18
a_7	-1.1E-10	a_{21}	3.09E-15	a_{35}	2.88E-17	a_{49}	5.47E-14
a_8	-188.333	a_{22}	-8.9E-16	a_{36}	2.92E-18	a_{50}	1.84E-20
a_9	1.842786	a_{23}	-9.9E-14	a_{37}	1.37E-16	a_{51}	0.000794
a_{10}	6.39E-13	a_{24}	-5.6E-15	a_{38}	4.02E-17	a_{52}	-4.7E-07
a_{11}	-2.3E-11	a_{25}	-0.00589	a_{39}	-5E-18	a_{53}	1.45E-18
a_{12}	-9.4E-13	a_{26}	4.98E-14	a_{40}	6.67E-19	a_{54}	0.333333
a_{13}	4.26E-11	a_{27}	2.43E-15	a_{41}	1.74E-15	a_{55}	-4.3E-09

Figures 7.13 - 7.16 can be utilized to determine the optimal input parameters of the system by utilizing the observable effect of the interacting system inputs. The inputs of the system mass flow rate of fuel, inlet air temperature and air volumetric flow rate are varied to determine the optimum system condition. It is evident that by running both turbines at a 250 m^3/s air volumetric flow rate, 2 kg/s mass flow rate of fuel and 283^{o}k inlet air temperature, results in a desirability value of 90%.

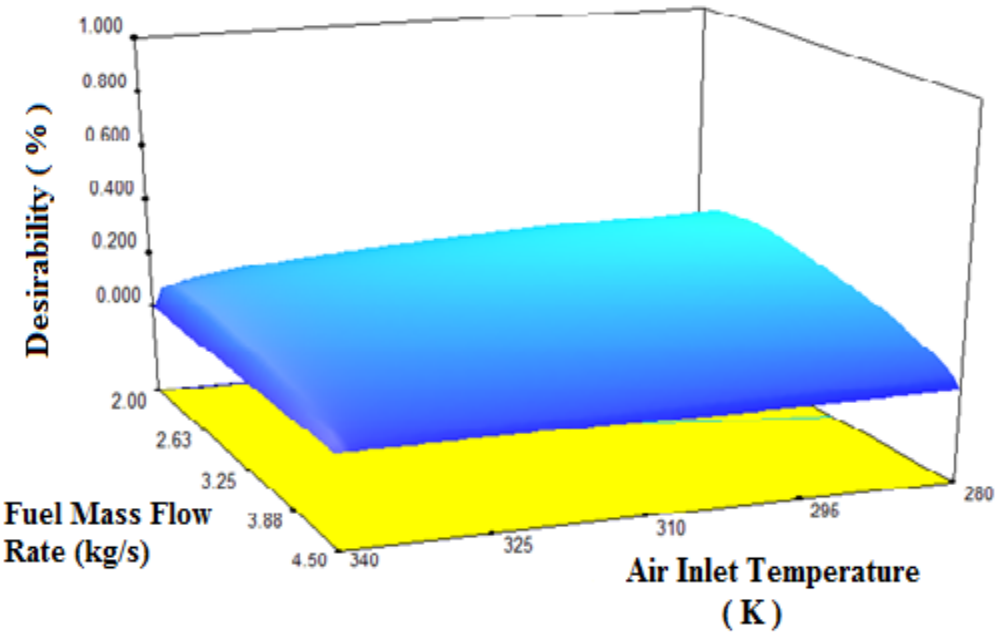

Figure 7.13 System 1 and the desirable operating conditions with interacting fuel flow rate and air inlet temperature at 180 m^3/s volumetric air flow rate.

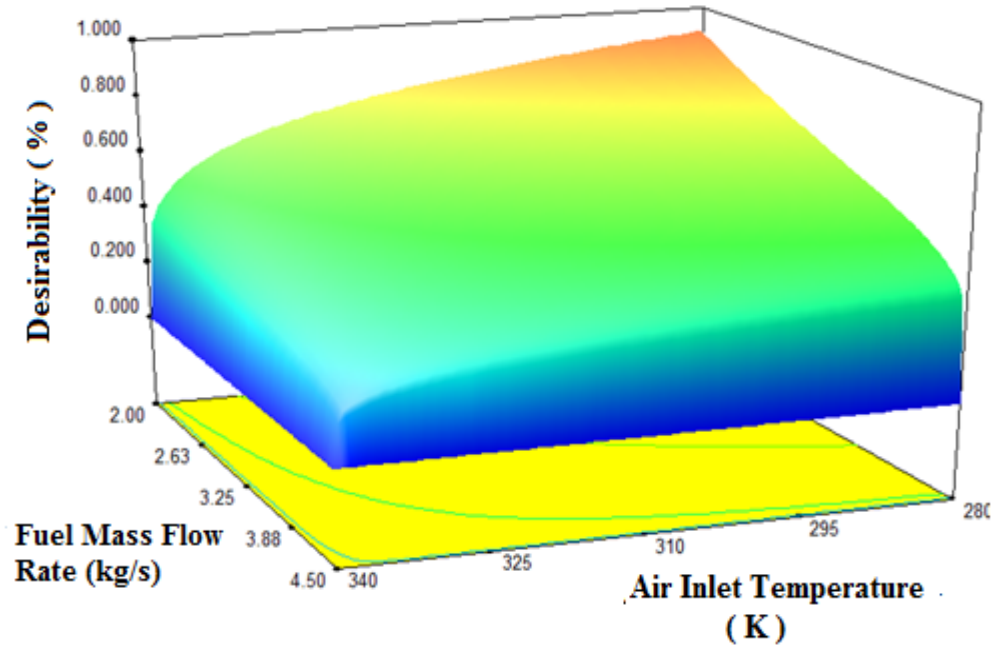

Figure 7.14 System 1 and the desirable operating conditions with interacting fuel flow rate and air inlet temperature at 250 m^3/s volumetric air flow rate.

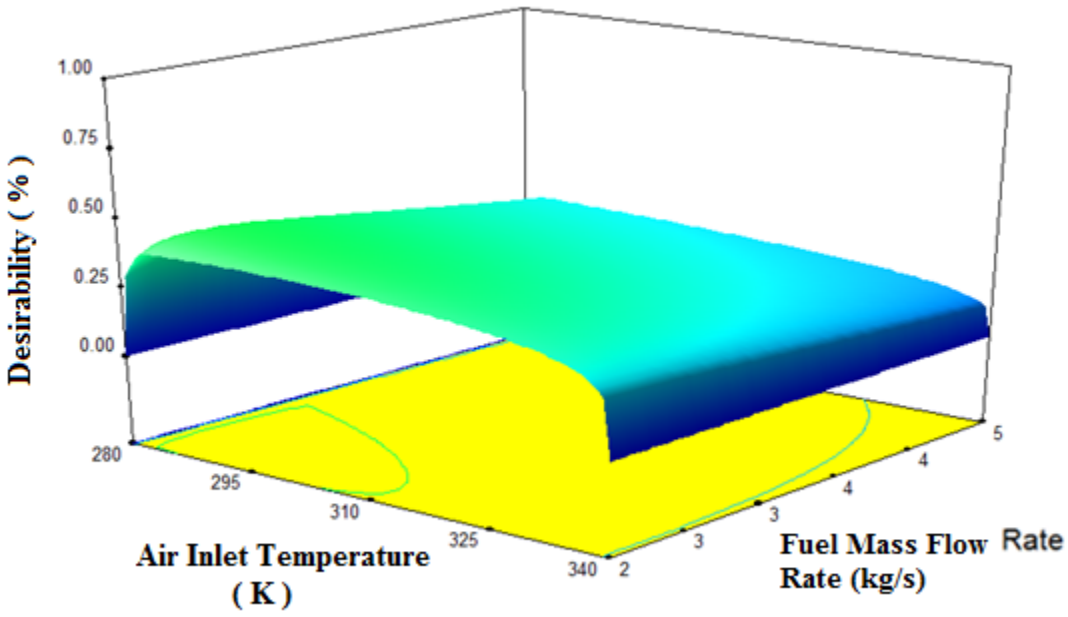

Figure 7.15 System 2 and the desirable operating conditions with interacting fuel flow rate and air inlet temperature at 180 m^3/s volumetric air flow rate.

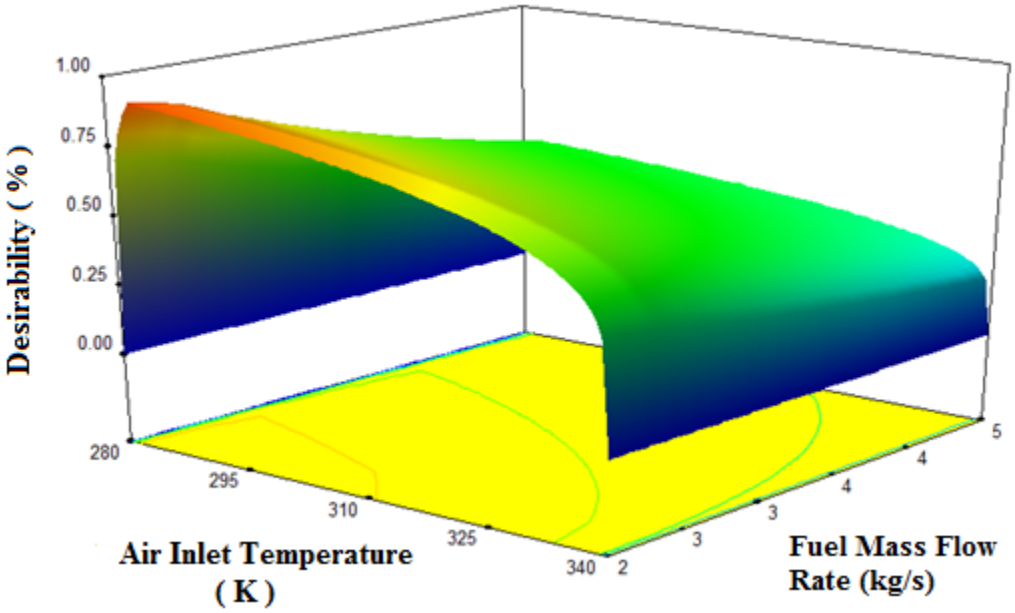

Figure 7.16 System 2 and the desirable operating conditions with interacting fuel flow rate and air inlet temperature at 250 m^3/s volumetric air flow rate.

Table 7.15 illustrate other optimal operating condition details for system1 in which it can be detect how these optimal operating factors have a major effect on both energy and exergy efficiencies.

Table 7.15 Optimal operating conditions of system 1. m^3/s

Air Inlet Temperature (K)	Mass Flow Fuel (kg/s)	Volume Flow Air (m^3/s)	Energy-Eff	Exergy-Eff	Net Work (kW)	Desirability (%)
283.01	2.19	250	0.42697	0.280188	85,026	86.9483
283.00	2.30	250	0.426898	0.280140	82,206	86.9314
284.05	2.00	249.99	0.426851	0.280112	80,655	86.9209
283.12	2.00	250	0.426777	0.280071	79,070	86.9053
283.00	2.42	249.99	0.426746	0.280055	78,446	86.8988
287.00	2.00	249.99	0.426712	0.280037	78,441	86.8915
283.63	2.12	249.53	0.425498	0.279221	78,213	86.5979
285.33	2.00	249.37	0.424729	0.278739	78,078	86.4206
283.00	2.08	249.99	0.411931	0.270333	78,070	86.0646
283.02	2.00	248.36	0.421812	0.27680	77,538	85.7174
283.00	2.04	248.39	0.421629	0.276707	77,509	85.6787
292.92	2.08	249.99	0.416080	0.259997	76,864	85.1629
286.27	2.00	246.53	0.4082318	0.273048	76,486	84.3305
283.00	2.19	249.99	0.396221	0.249925	78,463	84.1593
283.00	2.38	250	0.380877	0.242911	81,187	83.3592
283.71	2.00	244.00	0.370162	0.267901	75,042	82.3967
288.00	2.00	250	0.354678	0.232729	78,471	82.2344
283.45	2.00	250	0.316161	0.207470	78,484	78.7237

Similar optimal operating parameters are shown in Table 7.16. The table shows more details about the optimal operating conditions for system 2 in which it can be seen that the optimal operating factors that directly affect both energy and exergy efficiencies.

Table 7.16 Optimal operating conditions of system 2.

Air Inlet Temperature (K)	Fuel Mass Flow Rate (kg/s)	Air Volume Flow Rate (m^3/s)	Energy-Eff.	Exergy-Eff.	Net Work (kW)	Desirability (%)
283.00	2.00	250.00	0.444382	0.295495	72,185	92.3398
283.28	2.00	250.00	0.444370	0.295495	72,184	92.2525
283.00	2.01	250.00	0.441927	0.293885	72,264	92.1486
283.63	2.00	250.00	0.444383	0.295496	72,182	92.1452
283.00	2.03	250.00	0.440081	0.292673	72,323	92.0033
284.45	2.00	250.00	0.444373	0.295489	72,178	91.8891
283.00	2.00	249.17	0.441731	0.293746	71,852	91.8532
283.00	2.00	248.88	0.440858	0.293171	71,729	91.6837
285.71	2.00	250.00	0.444382	0.295496	72,170	91.4895
283.00	2.00	248.30	0.439021	0.291959	71,480	91.3319
283.00	2.08	250.00	0.43108	0.286766	72,605	91.2761
286.61	2.00	250.00	0.444382	0.295495	72,162	91.1981
283.63	2.09	250.00	0.429747	0.285892	72,642	90.9733
287.93	2.00	250.00	0.444382	0.295495	72,147	90.7611
283.00	2.00	247.36	0.43607	0.290014	71,066	90.7543
283.00	2.00	246.61	0.433746	0.288482	70,721	90.2841
291.13	2.00	250.00	0.444381	0.295495	72,099	89.6586

In conclusion, employing the thermodynamic concepts and based software package introduced in prior sections of this thesis assisted the determination of optimal operating conditions for systems 1 and 2 as shown in Tables 7.15 and Table 7.16 respectively. The application of the determined optimal operating conditions of both systems led to an increase of overall plant work output by 28% from the base case. This increase is illustrated in Figure 7.17.

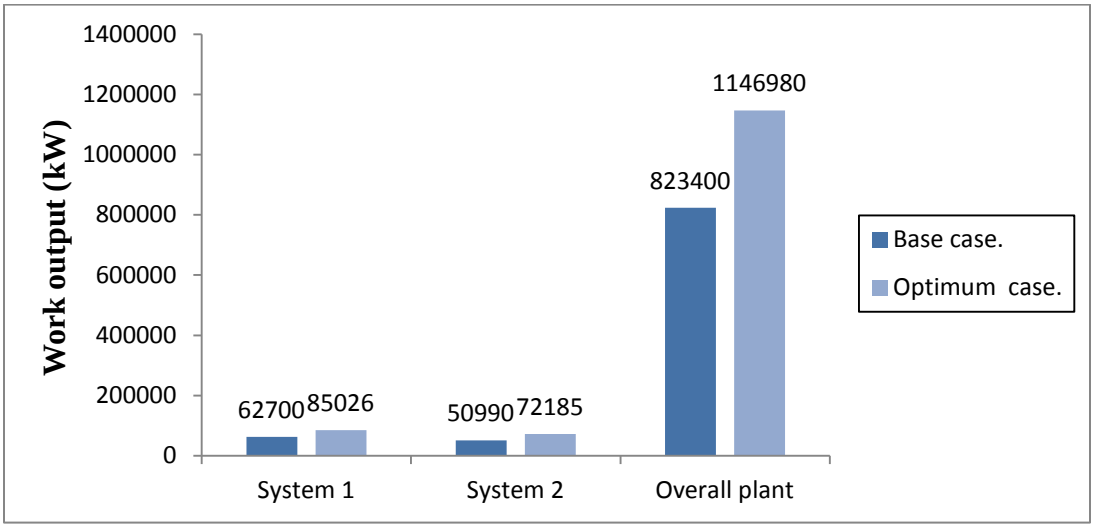

Figure 7.17 Overall plant's work output at base and optimum case.

The achieved improvements in the energetic and exegetic efficiencies of the studied systems, by the application of the optimal operating conditions discussed in Tables 7.15 and Table 7.16 is illustrated in Figures 7.18 and 7.19. It can be observed that the energetic and exergetic efficiencies are increased by approximately 20% and 12% respectively.

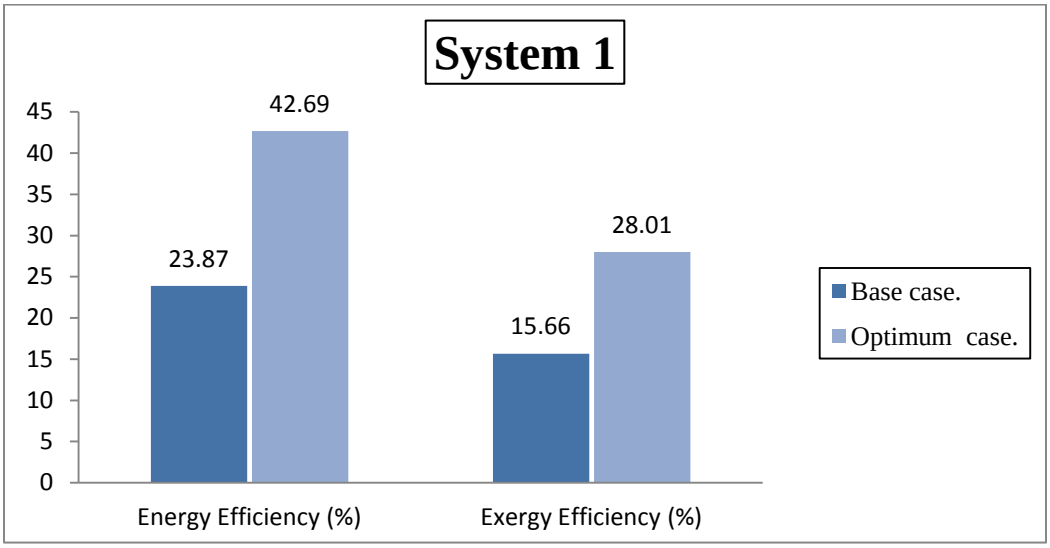

Figure 7.18 Energy and exergy efficiencies of system 1 at base and optimum case.

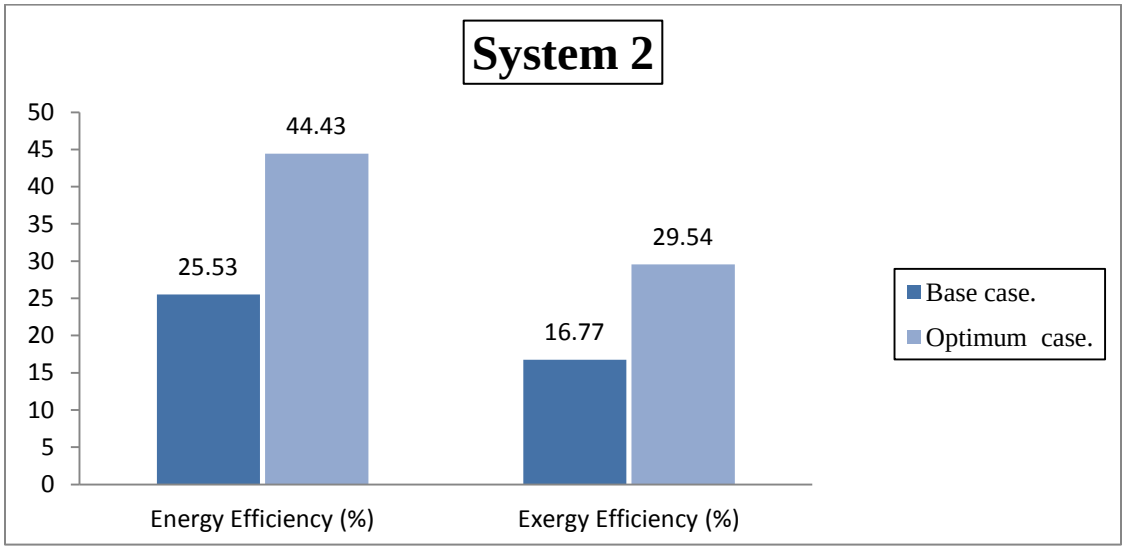

Figure 7.19 Energy and exergy efficiencies of system 2 at base and optimum case.

7.5 Exergy destruction results

Exergy analysis is typically utilized as a tool for the determination of parameters maximizing performance of a system and/or identifying the sites of greatest exergy destruction. The identification of primary sites of exergy destruction, causes of destruction and true magnitude of destruction gives some direction toward potential improvements of the system and its components. Exergy destruction represents major thermodynamic inefficiency and is a quantity that is to be minimized when the overall plant efficiency is to be maximized. In the work carried out by Dincer and Rosen [19], the relation between exergy destruction, exergoeconomic, exergoenvironmental and sustainable development are studied. In their work, they express the concept of exergy destruction as a crucial tool for economic planning, resource optimization and finally

global, regional, and national environmental pollution reduction. Figures 7.20 and 7.21 depict the exergy destructions occurring in systems 1 and 2 respectively.

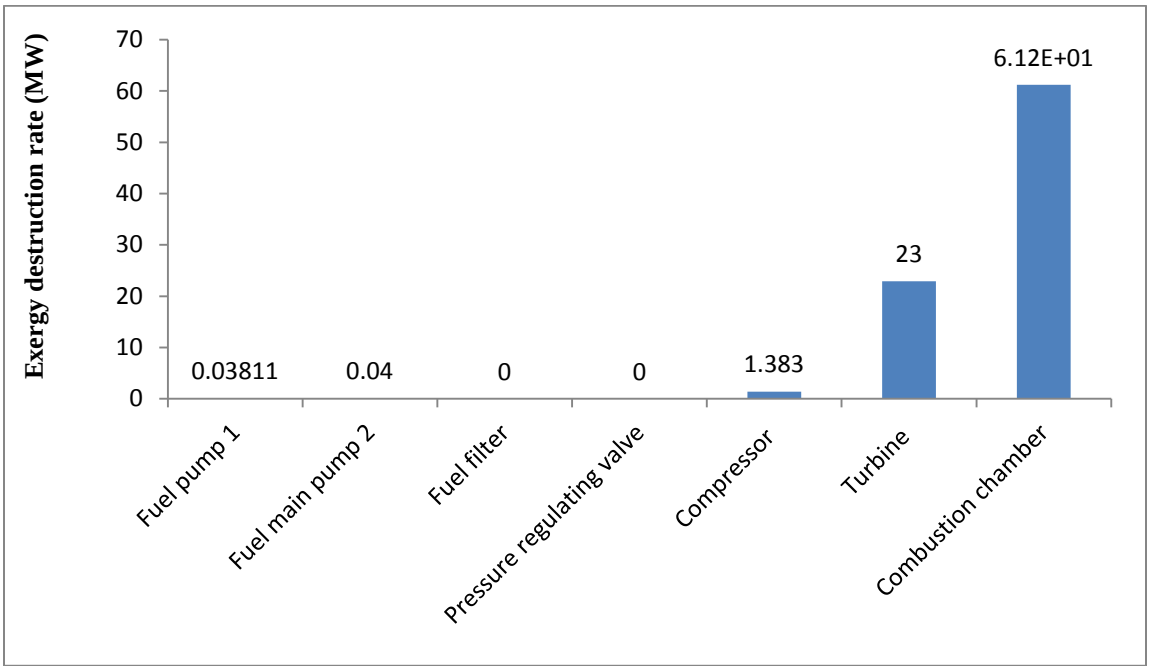

Figure 7.20 Exergy destructions in system 1 and its components.

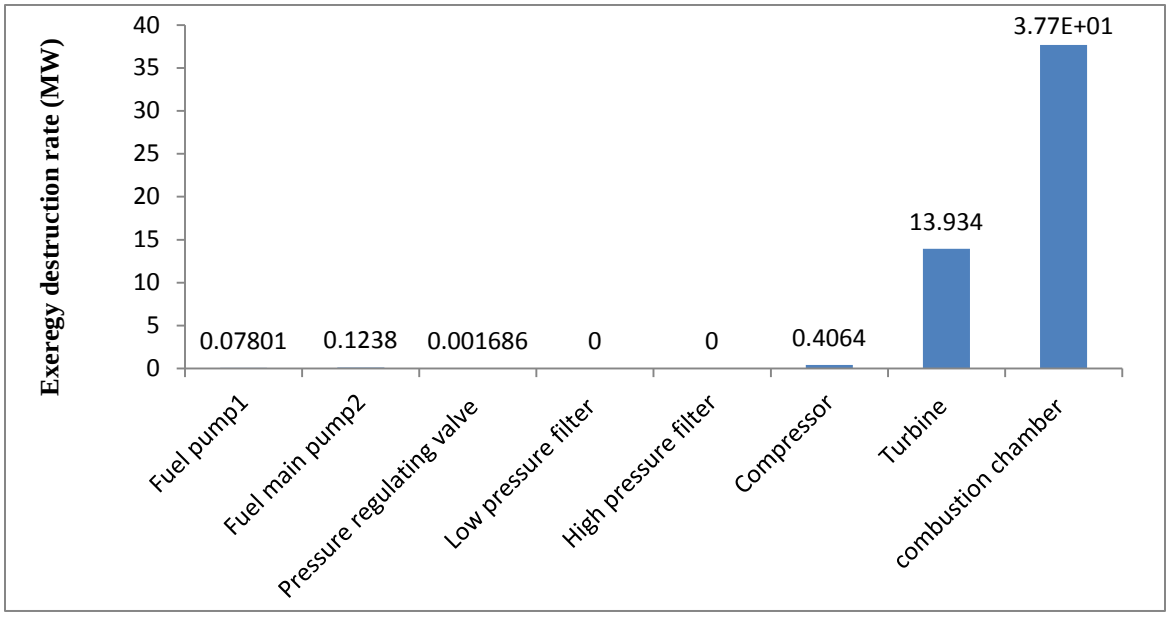

Figure 7.21 Exergy destructions in system 2 and its components.

The preceding two sections of this chapter will investigate the economic and environmental concerns involving the Makkah Power Plant operations. In order to study the aforementioned concerns, it is necessary to investigate the effect of varying several operating parameters on the magnitude of exergy destruction. Varied operating parameters included parameters such as compressor pressure ratio and ambient temperature of some selected components in systems 1 and 2. This study is also intended to shed light on system inefficiencies assisting in the creation of improved accurate modeling. The improved understanding would then empower the future design of superior gas power stations.

As a starting point the compressor pressure ratio is studied. In the compressor and combustion chamber, an increase in pressure ratio is seen to have a positive effect on the exergy destruction production of both systems 1 and 2. This is illustrated in Figures 7.22 and 7.23 respectively. However, it is in the combustion chamber that the highest exergy destruction occurs. Thus, it offers the largest potential for improvement. The chemical reaction and temperature difference between air and fuel are the culprits of the large exergy destruction seen in the combustion chamber.

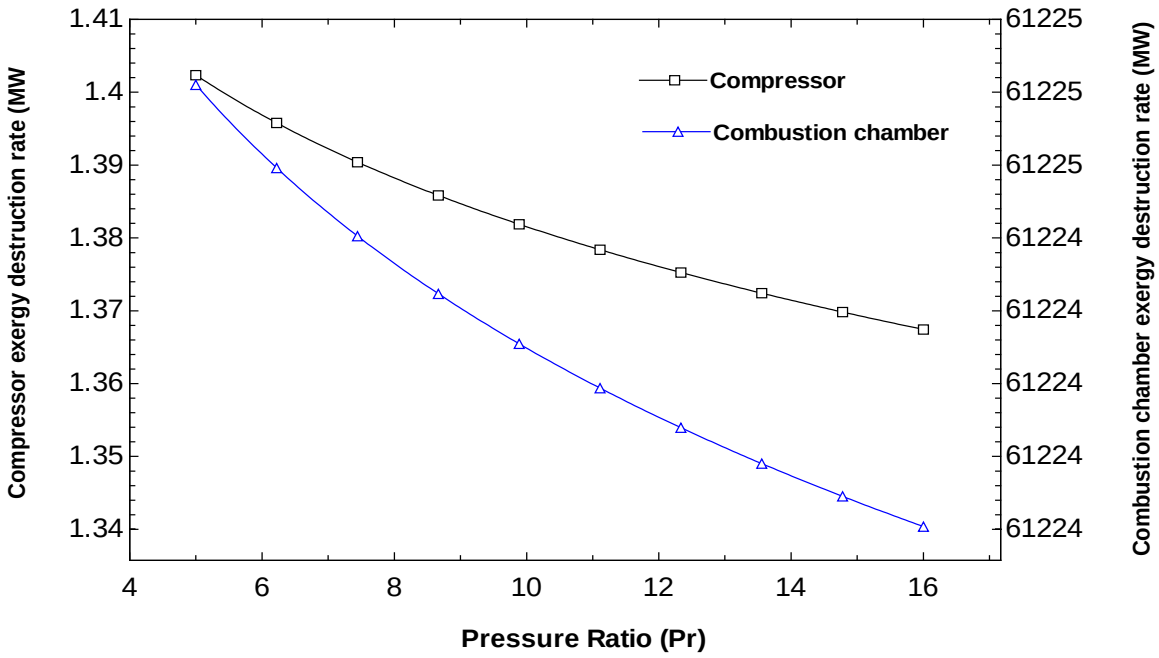

Figure 7.22 Effect of compressor pressure ratio on compressor and combustion chamber exergy destruction rate of system 1.

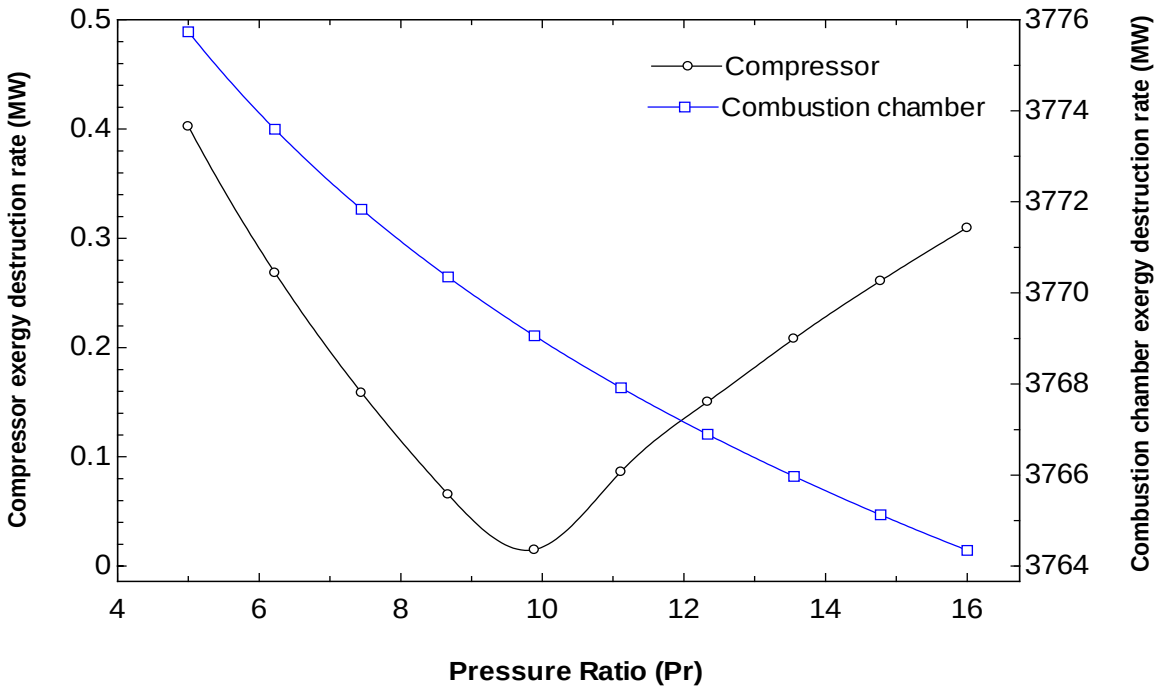

Figure 7.23 Effect of compressor pressure ratio on compressor and combustion chamber exergy destruction rate of system 2.

In this study, it is observed that second largest contributor to exergy destruction is the turbine. It was significant to further investigate the effect of ambient temperature on the rate of exergy destruction occurring in the turbine. Moreover, the exhaust gas stream is an additional source of exergy destruction as it is wasted exergy that is exhausted out of the system. The exergy of the exhaust gas stream can be recovered in some portion by a heat recovery system connected to the bottom cycle in cogeneration or combined cycle systems. The source of turbine irreversibility and exergy destruction come from losses in the flow path of the turbine.

Despite being small contributors to the overall exergy destruction of the system, the fuel pumps used at the Makkah Power Plant are examined for completeness in this thesis. Figures 7.24 and 7.25 depict the effect of ambient temperature on fuel pump exergy destruction rate of system 1 and 2 respectively.

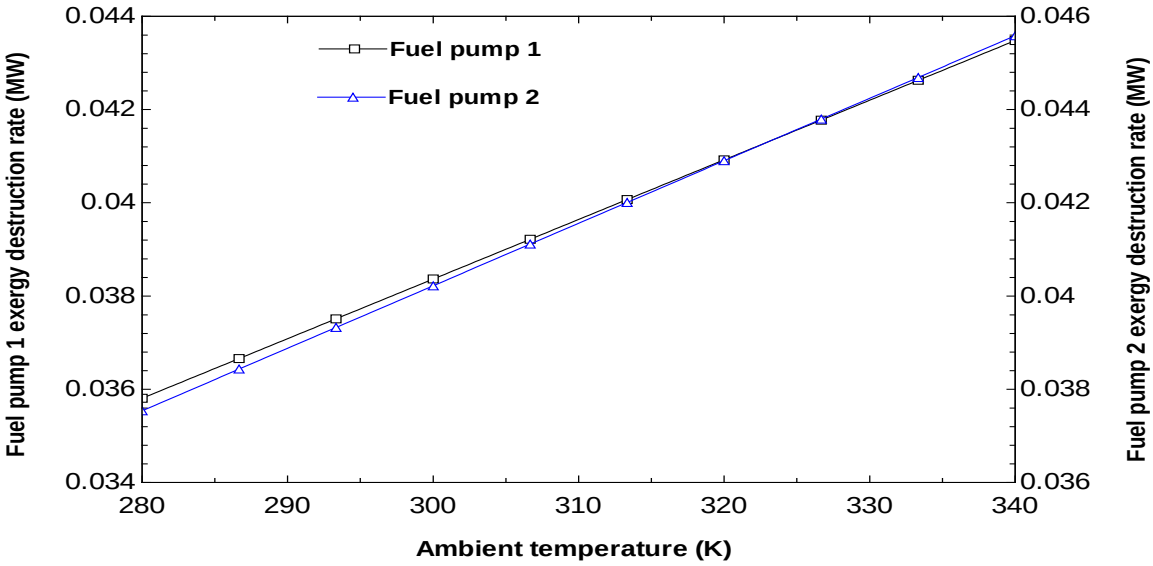

Figure 7.24 Effect of ambient temperature on fuel pump 1 and 2 exergy destruction rate of system 1.

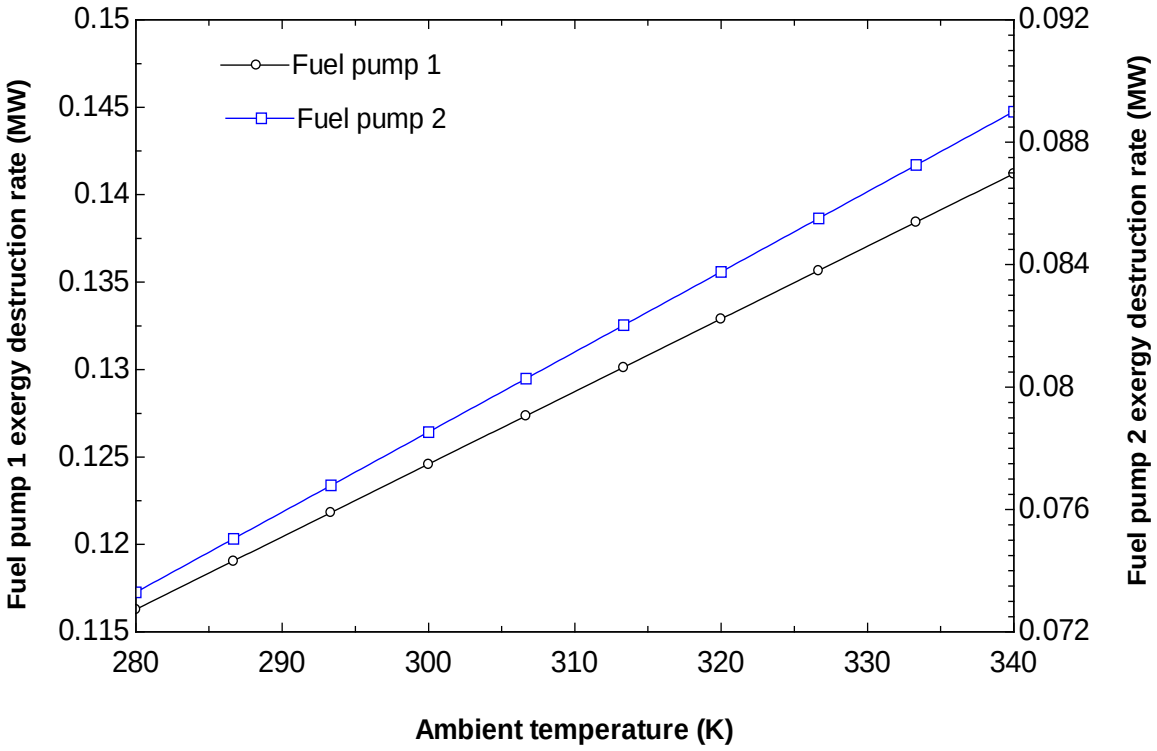

Figure 7.25Effect of ambient temperature on fuel pump 1 and 2 exergy destruction rate of system 2.

An atomizing air compressor is used for only system 2 to break down the jet of fuel that is discharged from the fuel oil nozzle into a fine mist (small particles). This is done to ensure the fuel is completely burned in the combustion chamber. In Figure 7.26, different ambient temperatures and their mutual effect on air atomizing compressor and combustion chamber exergy destruction rate is illustrated.

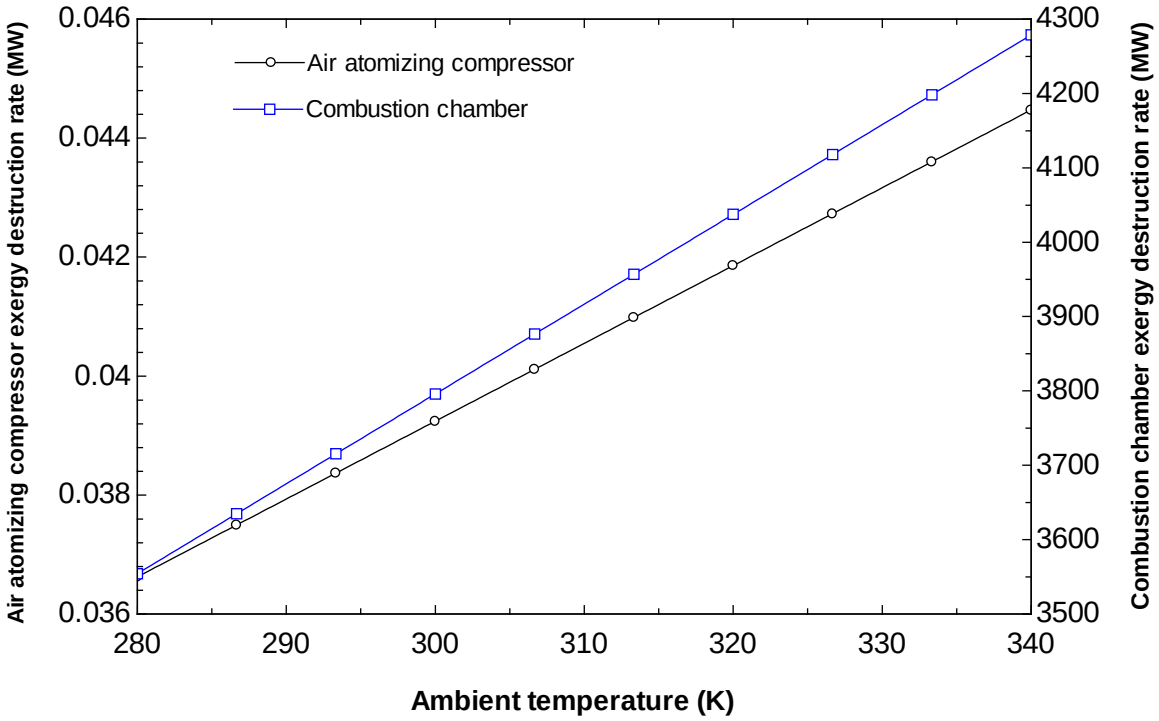

Figure 7.26 Effect of ambient temperature on air atomizing compressor and combustion chamber destruction rate of system 1.

In the investigation of exergy destruction, it is important to note that exergy destructions are due to irreversibility's in plant components. The combustor is the primary contributor of exergy destruction in the respective systems. Therefore, the primary means of keeping the exergy destruction in a combustion process within a reasonable limit is to reduce irreversibility in heat conduction through proper control of physical processes and chemical reactions resulting in a higher flame temperature but lower temperature gradients within the system. The optimum operating condition in this context can be determined from the parametric studies on combustion irreversibility's with operating parameters in different types of flames [78]. The most efficient

performance is achieved when the exergy loss in the process is minimized. This is done by optimizing heat exchangers, fins, the combustor and thermal insulation.

7.6 Results of exergoeconomic analysis

The exergoeconomic performance of the gas turbine of the Makkah Power Plant is investigated considering current conditions such as temperature, pressure, and air/fuel mass flow rate. The variables considered for both systems are as follows: pressure ratio, P_r = 9.5, compressor pressure ratio, $\eta_s c$ = 85%, turbine isentropic efficiency, $\eta_s T$ = 85%, is pump isentropic efficiency, $\eta_s p$ =85% and turbine inlet temperature T_t = 1273^{o}K. The plant life is considered to be 20 years and an interest rate of 10% is considered for all exergoeconomic calculations. In addition, heat losses from the combustion chamber are assumed to be 3% of the energy input to the combustion chamber. The objective of the work performed is to determine the sum of $\dot{Z} + \dot{C}_D$, note that tables and analyses are conducted for a single turbine unit of each respective manufacturer.

The exergoeconomic parameters for each of the components of the system 1 for the actual operating conditions are summarized in Table 7.17 and the cost of the streams is tabulated in Table 7.18 where unit cost of electricity produced is 5.73 cents/kWh in the base case. System 1's schematic is shown in Figure 5.1. In analytical terms, the components with the highest value of $\dot{Z} + \dot{C}_D$ are considered the most significant components from an exergoeconomic perspective. Components are arranged according to their value of $\dot{Z} + \dot{C}_D$ in descending order. This provides a means of determining the level of priority a component should be given with respect to the improving of the

system. The highest value of $\dot{Z} + \dot{C}_D$ correspond to the combustion chamber. Moreover, the low value of exergoeconomic factor, f, associated with the combustion chamber suggests that the cost rate of exergy destruction is the dominate factor influencing the component. Hence, it is implied that the component efficiency is improved by increasing the capital investment. This can be achieved by increasing gas turbine inlet temperature (GTIT). The maximum GTIT is limited by metallurgical concerns.

Table 7.17 Exergoeconomic parameters of the system 1 at the base case.

Component	Exergy Destruction Cost Rate ($/h) $\dot{C}_D$	Capital Cost Rate ($/h) $\dot{Z}$	Total Cost Rate ($/h) $\dot{Z} + \dot{C}_D$	Exergoeconomic Factor f
Fuel Pump 1	1.4	1.65	3.05	0.54
Fuel Main Pump 2	1.9	7.39	9.29	0.79
Combustion Chamber	1053.28	14.47	1067.75	0.013
Main Compressor	78.74	35.21	113.95	0.30
Turbine	395.02	49.72	444.74	0.11
Overall System	1530.34	108.44	1638.78	0.07

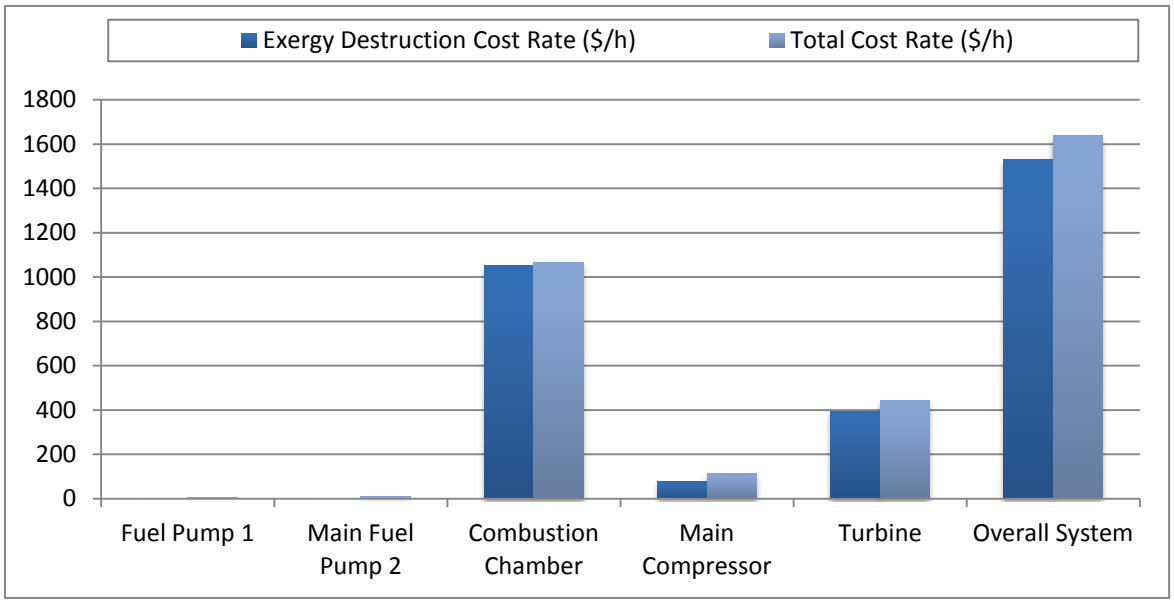

Figure 7.27 Cost rate of exergy destructions and total cost rates for system 1 and its components.

Figure 7.27 depicts the exergy destruction cost rate and the total cost rate for each component in system 1 and shows that the combustion chamber exhibits the greatest exergy destruction cost, followed by the turbine. As the combustion chamber and turbine have the highest value of the total cost rate, this suggests that the cost rate of exergy destruction dominates

Table 7.18 Cost of the streams in the system 1.

State Point	Cost Per Exergy Unit (cent/kWh) C	Cost Rate ($/h) $\dot{C}$
1	1.85	1.4
2	1.91	2.1
3	3.6	2947
4	6.7	1104
5	4	4642
6	2.03	511
7	0	0
W_1	5.73	5.3
W_2	5.73	7.8
W_7	5.73	1030
W_5	5.73	3497

Table 7.19 and Table 7.20 summarize the exergoeconomic parameters for each of the components of system 2 and the cost of the each stream respectively in which the unit cost of electricity produced is 6.3 cents/kWh in the base case. The schematic of system 2 is shown in Figure 5.2. The results of the exergoeconomic study show that the combustion chamber (CC) exhibits the greatest exergy destruction cost. The next highest

source of exergy destruction cost is the turbine. In comparing the results of exergy and exergoeconomic analyses, similar trends are revealed. In the work of Ahmadi et al [40], the gas turbine inlet temperature (GTIT) is proven to have a significant effect on CC and overall cycle exergy destruction. Increasing gas turbine inlet temperature effectively decreases the cost associated with exergy destruction. Further comparisons between related results are consistent with those reported by Ahmadi et al. [40] and proved that the most significant parameter in the plant is GTIT. The finding solidifies the concept that the exergy loss in the combustion chamber is associated with the large temperature difference between the flame and the working fluid. Reducing this temperature difference reduces the exergy loss. Furthermore, cooling compressor inlet air allows the compression of more air per cycle, effectively increasing the gas turbine capacity.

Table 7.19 Exergoeconomic parameters of the system 2 at the base case.

Component	Exergy Destruction Cost rate ($/h) $\dot{C}_D$	Capital Cost Rrate ($/h) $\dot{Z}$	Total Cost Rate ($/h) $\dot{Z} + \dot{C}_D$	Exergoeconomic Factor f
Fuel Transfer Pump 1	5.23	1.23	6.46	0.19
Fuel Main Pump 2	9.63	3.49	13.12	0.26
Combustion Chamber	783.05	12.33	795.38	0.016
Main Compressor	25.15	49.04	74.19	0.66
Atomizing Compressor	6.03	1.88	7.91	0.24
Turbine	168.18	14.62	182.8	0.08
Heat Exchanger	47.72	32.74	80.46	0.4
Overall System	1045	115.33	1160.32	0.1

Figure 7.28 shows the exergy destruction cost rate and the total cost rate for each component in system 2 and shows that the combustion chamber exhibits the greatest exergy destruction cost, followed by the turbine. As the combustion chamber and turbine have the highest value of the total cost rate, this suggests that the cost rate of exergy destruction dominates.

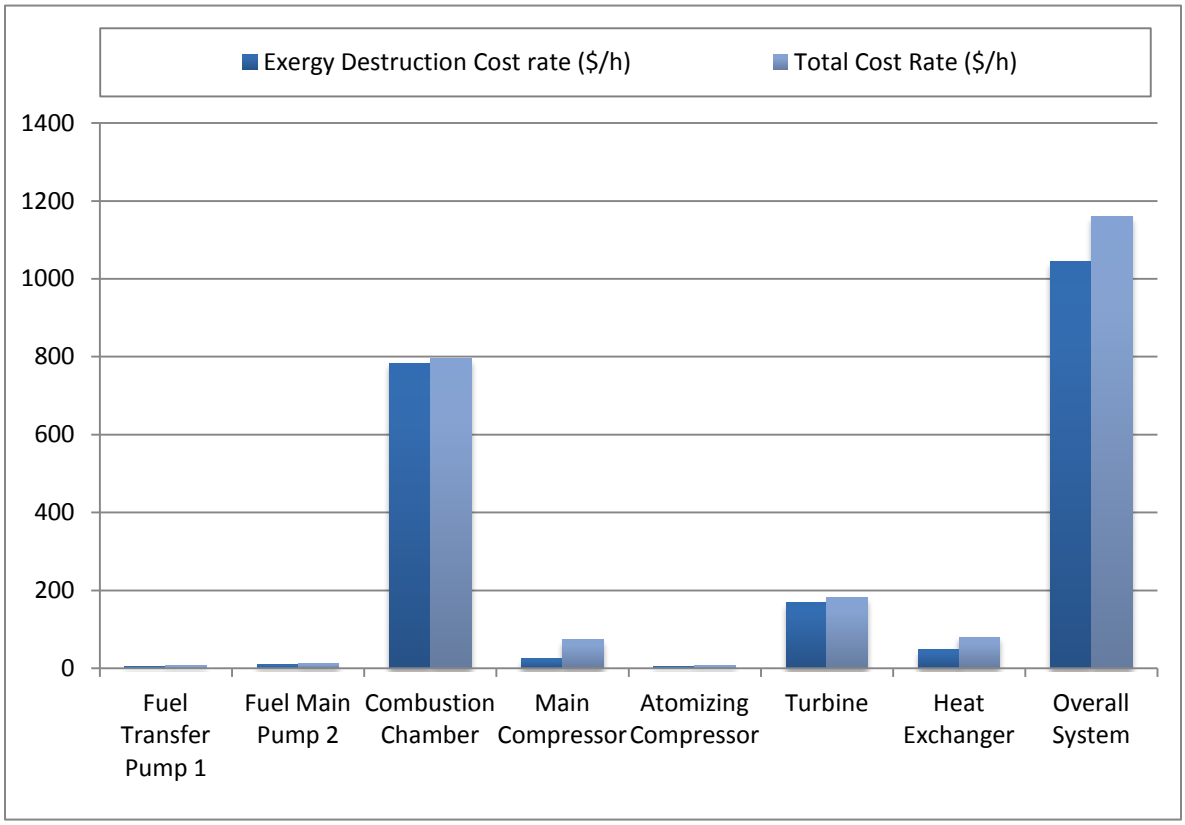

Figure 7.28Cost rate of exergy destructions and total cost rate for system 2 and its components.

Table 7.20 Cost of the streams in the system 2.

State Point	Cost Per Exergy Unit (cent/kWh) C	Cost Rate ($/h) $\dot{C}$
1	2.49	1.81
2	1.34	1.41
3	3.1	2751
4	4.64	4402
5	1.06	428
6	0	0
7	5.9	982
8	1.5	58.1
9	3.7	450
10	2.1	737
11	2.8	503
W_1	6.3	6.8
W_2	6.3	9.04
W_6	6.3	911
W_{10}	6.3	351
W_4	6.3	3948

7.7 Results of exergoenvironmental analysis

Increased energetic and exergetic efficiencies are directly linked to improved environmental impact of a system, and often result in a decrease in fuel consumption. Figure 7.29 illustrates that increasing exergetic efficiency results in CO_2 emission reduction. The increase of exergetic efficiency is related to reduction of ambient inlet air temperature into the compressor. The reduction and the means of reducing compressor

air inlet temperature is an important target in this study. Additionally, as a secondary objective, plant CO_2 emission minimization per MWh is of concern in this study.

Improvement of a system's efficiency is twofold. By improving the most inefficient components (e.g. reducing compressor inlet air temperature) of the system and utilizing the minimum adequate fuel flow rate ensuring maximum burn, the work output of systems 1 and 2 were increased by 27% and 29% respectively. As a consequence of the output increase due to improved efficiencies, there is also a positive influence in the environmental impact of the system. The reduction in wasted unburned fuel and the reduction in overall system inefficiencies results in net CO_2 emissions reduction.

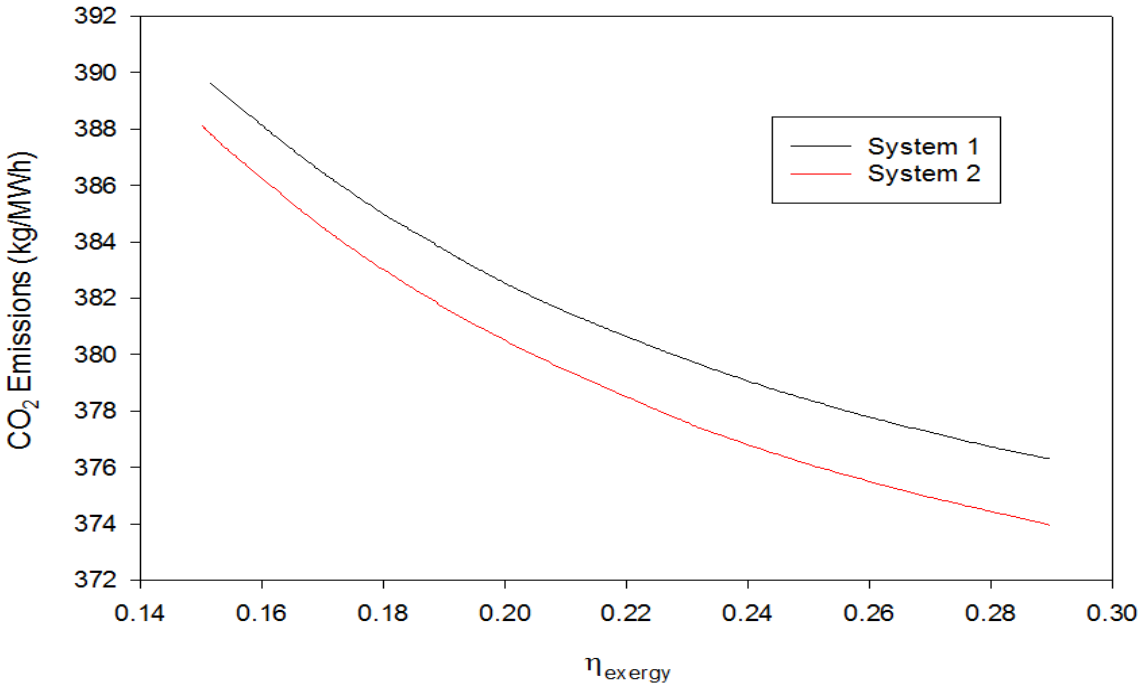

Figure 7.29 Variation of CO_2 emissions with exergetic efficiency.

Figure 7.30 shows the effect of increasing exergy efficiency of systems 1 and 2 on the sustainability index of the whole system. The efficiencies of the individual systems are directly linked the entire system. However, it is apparent that the overall exergy destruction of the cycle decreases, while the sustainability index increases with decreasing compressor inlet temperature. Moreover, Exergy efficiency, exergy destruction, environmental impact and sustainability are apparently linked in such systems, and thus supporting the utility of exergo-environmental analyses.

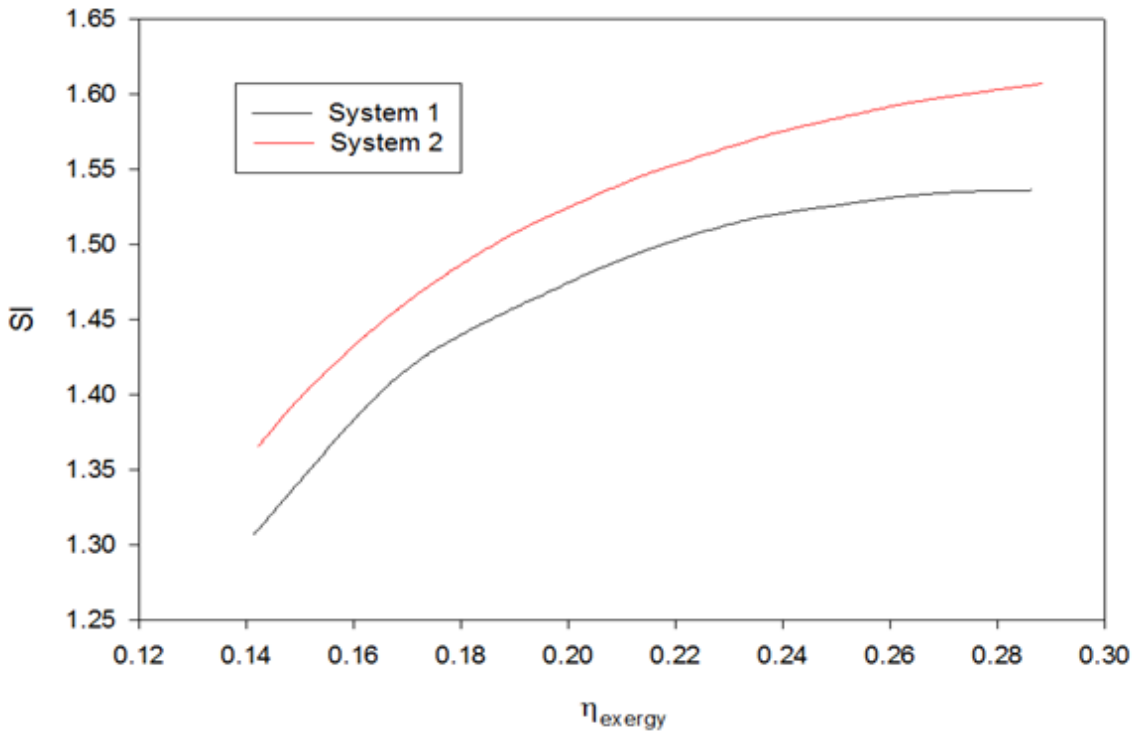

Figure 7.30 Variation of sustainability index with exergetic efficiency.

7.8 Gas turbine inlet cooling conceptual design

As discussed in Chapter 3, section 3, gas turbine inlet air-cooling technology (GTIAC) is a promising commercially available method for improving the efficiency of an existing gas turbine. The technological method is versatile in that it can be applied in various configurations. This makes the instillation of a GTIAC system on a gas turbine nearly possible for almost any turbine model currently in production.

It is well documented the relation between the factors of ambient temperature, humidity and pressure on gas turbine performance. Through thermodynamic analyses, it is exposed that thermal efficiency among other specific outputs decrease with an increase in humidity and ambient temperature as was observed by Tsujikawa and Sawada [79]. El-Hadik [80] performed a parametric study of the effects of ambient temperature, pressure, humidity and turbine inlet temperature on the outputs power and thermal efficiency. He came to the conclusion that the ambient temperature demonstrated the greatest effect on gas turbine performance. He observed that increases in turbine inlet temperature and pressure ratio reduced turbine performance. He further deduced that reductions of power and efficiency due to a 1K temperature growth were found to be around 0.6 and 0.18% respectively. In the work of Dincer and Rosen [81], in a case study they propose the use of an energy thermal storage to cool down the gas turbine inlet air temperature. They state that, “output power is directly linked to the rate of fuel that they can consume efficiently. This in turn is a function of air mass flow, which is a function of air density. Moreover, it can be inferred that if the air density can be increased, it is likely the turbine would be capable of burning more fuel fully and therefore produce more power.

All methods mentioned to cool down turbine inlet air temperature have a similar concept of using air water heat exchangers. In this research, it is the aim to propose a conceptual design of shell and tube heat exchanger that is to be installed before the filter houses prior to the compressor inlet. These heat exchangers would be primarily used during the summer season in which the ambient temperature can reach 50^{o}C. The target is to cool down the compressor inlet air to a temperature of 10^{o}C. However, based on system 1 optimum operation condition discussed in Table 7.15, cooling down inlet air temperature to 10^{o}C would be resultant of increasing the system 1 output by 29%, virtually from 62.700 MW to 85.026 MW. Similarly, based on system 2 optimum operation condition discussed in Table 7.16, cooling down inlet air temperature to 10^{o}C would be resultant of increasing the system 2 turbine output by 27%, practically from 50.990 MW to 72.185 MW.

The design parameters of the proposed heat exchanger are illustrated in Table 7.21. Cross flow fluid arrangement is selected for maximum heat transfer between air and water. The temperatures are known and Log Mean Temperature Difference (LMTD) is used. Tubular Exchanger Manufacture Association (TEMA) standards are followed for design purpose. According to TEMA front head A, shell type E and rare head type P was used. A copper tube with outside diameter of 1 inch is used according to “Tube counts for 3/4-in. OD tubes on 15/16-in. Triangular Pitch Specifications” presented by Serth, Robert W [81].

Table 7.21 Design parameters of the proposed heat exchanger.

Tube outside diameter (m)	0.0254
Tube inside diameter (m)	0.0212
Shell inside diameter (m)	3.048
Number of tubes	14,459
Number of shell passes	4
Number of tube passes	2 each shell
Air inlet temperature (K)	330
Water inlet temperature (K)	280
Air outlet temperature (K)	283
Water outlet temperature (K)	325
Tube side fluid	Water
Shell side fluid	Air
Mass flow rate of air (kg/s)	307.5
Mass flow rate of water (kg/s)	77.14
Length of exchanger (m)	22

As mentioned earlier, the proposed design heat exchanger consists of two fluids, air and cold water. Cold water is provided from a gas refrigerated cycle such as the one shown in Figure 7.31. The gas cycle has four main components, a compressor, turbine, condenser and evaporator. The surroundings are at an ambient temperature, T_0. The air is compressed during process between states 1-2. After which the high-pressure, high-temperature gas at state 2 is cooled at constant pressure to T_0 by rejecting heat to the surroundings. Following the cooling stage is an expansion process in a turbine, during which the gas temperature drops to T_4. Finally, the cool gas absorbs heat from the

refrigerated space until its temperature rises to T_1. All the processes described are internally reversible, and the cycle executed is the ideal gas refrigeration cycle. However, the net work supplied to the refrigeration cycle is subtracted from the total net work of the plant.

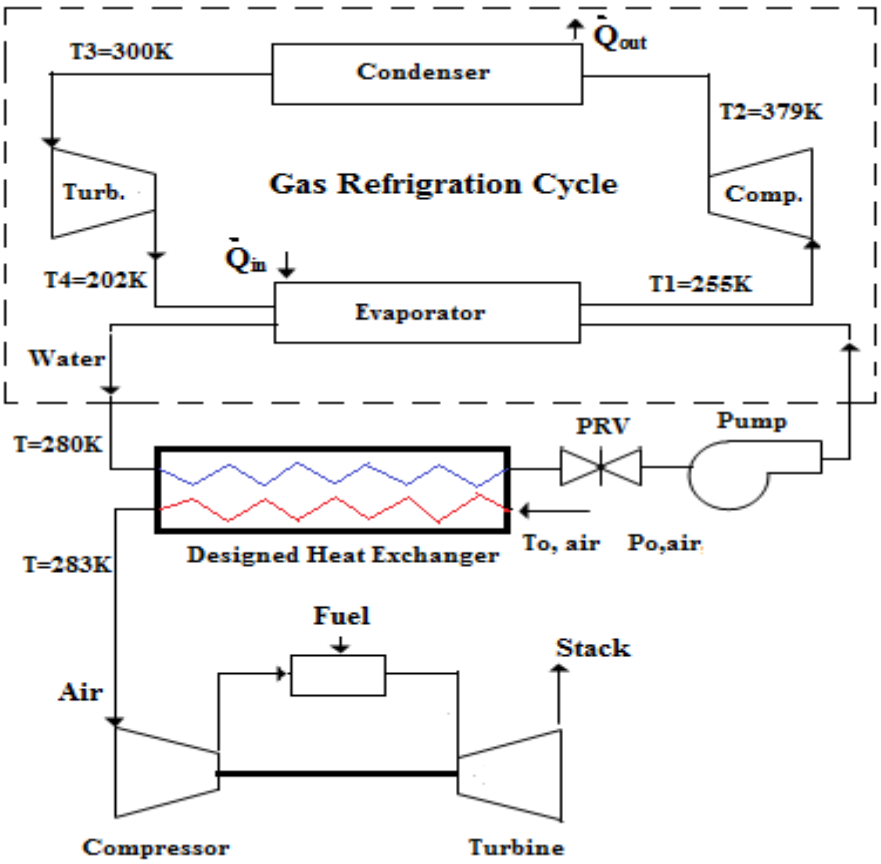

Figure 7.31 The conceptual design.

Chapter 8

CONCLUSIONS AND RECOMMENDATIONS

8.1 Conclusions

An energy, exergy, exergoeconomic and exegoenvironmental analyses are performed for the turbines of the two different manufacturers used at the Makkah Power Plant in Saudi Arabia. From the study and analysis of the power plant in Makkah, several conclusions could be drawn.

- Employing equations of conservation for mass, energy and exergy, a greater understanding of the system components as well as defining their efficiencies are achieved.
- Overall plant energetic and exergetic efficiencies are increased by 20% and 12% respectively.
- Overall plant work output is increased by 28%. From 823.400 MW to 1146.980 MW.
- The cost analysis indicated that combustion chamber exhibits the greatest exergy destruction cost, followed by the turbine.
- Reducing exergy destruction of the power plant components and increasing the energetic and exergetic efficiencies, results in reduced emissions, less environmental impact and enhanced sustainability.

8.2 Recommendations

Further thermodynamic analysis of such systems is required in order to gain the necessary knowledge needed to optimize the performance of gas turbine based systems. Furthermore, using newer versions of Design-Expert® Stat-Ease software or other software, analysis of variance (ANOVA) methods and improvements in heat transfer could be employed to enhance the efficiency of gas turbine based systems.

To have a good thermodynamic and thermo-economic model, the results from the base case simulation code presented in this study could be used or even compared in order to choose optimum design variables in future gas turbine power plants construction. These design parameters can be compressor pressure ratio, compressor isentropic efficiency, gas turbine isentropic efficiency, gas turbine inlet temperature and pump isentropic efficiency or even fuel type. The parameters may be varied in an optimization procedure, but must still be within a reasonable range. However, the improvement in output capacity has to be balanced against additional costs of the enhancements to the system. Hence, the implementation of an air inlet cooling system to increase production capacity is warranted if its cost is less than the costs of new turbine equipment. Finally, improving those efficiencies would reduce emissions, environmental impact and enhanced sustainability. This information should assist efforts to understand the thermodynamic losses in the cycle, and to improve efficiency.

References

[1] Al-Ibrahim, A., Varnham, A., "A review of inlet air-cooling technologies for enhancing the performance of combustion turbines in Saudi Arabia", *Applied Thermal Engineering*, Vol. 30, pp. 1879-1888, 2010.

[2] Hasnain, S., Smiai, M., Al-Ibrahim, A., Al-Awaji S.,"Analysis of electric energy consumption in an office building in Saudi Arabia", *ASHRAE Transactions*, Vol. 106, pp. 4383-439, 2000.

[3] Dincer, I., Al-Rashed, B., "Energy analysis of Saudi Arabia" *International Journal of Energy Research*, Vol. 26, pp. 263–278. 2002.

[4] Saudi Arabia Energy Data, Statistics and Analysis - Oil, Gas, and Electricity. US Energy Information Administration EIA report, pp. 1-2, 2011.

[5] Electricity and Cogeneration Regulatory Authority (ECRA), "Activities and Achievements of the Authority" Annual Report, pp. 19-42. 2010, (Arabic text)

[6] Dincer, I., Hussain, M., Alzaharnah, I., "Energy and exergy utilization in transportation sector of Saudi Arabia", *International Journal of Energy Research*, Vol. 24, Issue 4, pp. 525-538, 2004.

[7] Dincer, I., Hussain, M., Alzaharnah, I., "Energy and exergy use in the Agriculture sector of Saudi Arabia", *International Journal of Energy Research*, Vol. 33, Issue 11, pp. 1461-1467, 2005.

[8] Dincer, I., Hussain, M., Alzaharnah, I., “Energy and exergy use in public and private sector of Saudi Arabia”, *International Journal of Energy Research,* Vol. 32, Issue 14, pp.1615-1624, 2004.

[9] Dincer, I., Hussain, M., Alzaharnah, I., “Energy and exergy use in the utility sector of Saudi Arabia”, *International Journal of Energy Research,* Vol. 169, Issue 3, pp. 245-255, 2004.

[10] Dincer, I., Hussain, M., Al- Alzaharnah, I. “Analysis of sectoral energy and exergy use of Saudi Arabia”. *International Journal of Energy Research,* Vol. 28, pp. 205–243, 2004.

[11] Independent statistics and analysis, US Energy Information Administration EIA, Saudi Arabia: Country Analysis Briefs, 2008.

[12] Al-Ibrahim, A. Varnham, A., “Combustion turbine inlet air-cooling technologies and in-situ performance in the climate conditions of Saudi Arabia”, Saudi Aramco, Dammam, 2002.

[13] Dincer, I. Rosen, M., “Exergy: Energy, Environment and Sustainable Development” Elsevier, First Edition, pp. 1-14, 2007.

[14] Hermann, W., “Quantifying global exergy resources”, *Energy,* Vol. 31, pp.1685–1702, 2006.

[15] Ganapathy, T., Alagumurthi, N., Gakkharand, R., Murugesan, K., “Exergy Analysis of Operating Lignite Fired Thermal Power Plant” *Journal of Engineering Science and Technology Review 2,* Vol. 1, pp. 123-130, 2009.

[16] Horlock, J., Young, J., Manfrida, G., “Exergy Analysis of Modern Fossil–Fuel Power Plants”, *Journal of Enenrgy for Gas Turbines and Power*, Vol. 122, pp. 1–7, 2000.

[17] Orhan, F., Dincer, I., Rosen, M., “Exergo-economic analysis of a thermo-dynamical copper-chlorine cycle for hydrogen production production using specific exergy cost (SPECO) method”, *Thermochimica Acta*, Vol. 497, pp. 60-66, 2010.

[18] Orhan, F., Dincer, I., Rosen, M., “An exergy–cost-energy-mass analysis of a hybrid copper-chlorine thermochemical cycle for hydrogen production”, *International Journal of Hydrogen Energy*, Vol. 35, Issue 10, pp. 4831-4838, 2010.

[19] Rosen, M., Dincer, I., Kanoglu, M., “Role of exergy in increasing efficiency and sustainability and reducing environmental impact”, *Energy Policy*, Vol. 36, Issue 1, pp. 128-137, 2008.

[20] Dincer, I. Hussain, M. Al-Zaharnah, M.” Energy and exergy use in public and private sector of Saudi Arabia”, *Energy Policy*, Vol. 32, Issue 14, pp. 1615-1624, 2004.

[21] Ozgener, L., Hepbasli, A., Dincer, I., “Energy and exergy analysis of the Gonen geothermal district heating system”, Turkey, *Geothermics*, Vol. 34, Issue 5, pp. 632-645, 2005.

[22] Dincer, I., “Exergy as a potential tool for sustainable drying systems”, *Sustainable Cities and Society*, Vol. 1, pp. 91–96, 2011.

[23] Haseli, Y., Dincer, I., Naterer, G., “Optimum temperatures in a shell and tube condenser with respect to exergy”, *International Journal of Heat and Mass Transfer*, Vol. 51, Issue 9-10, pp. 2462-2470, 2008.

[24] Deng-Chern S., Chia-Chin C., “Engineering design and exergy analyses for combustion gas turbine based power generation system”, Vol. 29, Issue 8, pp. 1183-1205. 2004.

[25] Haseli, Y. Dincer, I. Naterer, G., “Thermodynamics analysis of a combined gas turbine power system with a solid oxide fuel cell through exergy”, *Thermochimica Acta*, Vol. 480, Issues 1 -2, pp. 1-9, 2008.

[26] Bonnet, S., Alaphilippe, M., Stouffs, P., “Energy, exergy and cost analysis of a micro-cogeneration system based on an Ericsson engine”, Elsevier publisher, *International Journal of Thermal Sciences*, Vol. 44, pp. 1161-1168, 2005.

[27] Camdali, U., Erisen, A., Celen, F.,“Energy and exergy analyses in a rotary burner with pre-calcinations in cement production”, Elsevier publisher, *Energy Conversion and Management*, Vol. 45, pp. 3017-3031, 2004.

[28] Oladiran, M., Meyer, J., “Energy and exergy analyses of energy consumptions in the industrial sector in South Africa”, Elsevier publisher, *Applied Energy*, Vol. 84, pp.1056-1067, 2007.

[29] Tatiana, M., Tsatsaronis, G, “Advanced Exergy Analysis for Chemically Reacting Systems – Application to a Simple Open Gas-Turbine System”, *International Journal of Thermodynamics*, Vol. 12, pp. 105-111, 2009.

[30] Rosen, M., “Energy and exergy analyses of electrolytic hydrogen production”, *International Journal of Hydrogen Energy*, Vol. 20, pp. 547-553, 1995.

[31] Azouma, Y. Blin, J. Daho, T., “Exergy efficiency applied for the performance optimization of a direct injection compression ignition (CI) engine using biofuels”, *Renewable Energy*, Vol. 34, pp. 1494–1500, 2009.

[32] Rivero, R., Garfias, M., “Standard chemical exergy of elements updated”, *Energy*, Vol. 31, pp. 3310-3326, 2006.

[33] Ertesvag, I.S., “Sensitivity of chemical exergy for atmospheric gases and gaseous fuels to variations in reference-environment conditions”, *Energy Conversion and Management*, Vol. 48, pp. 1983-1995, 2007.

[34] Gao, L., Jin, H., Liu, Z., Zheng, D., “Exergy analysis of coal-based polygeneration system for power and chemical production”, *Energy*, Vol. 29, pp. 2359-2371, 2004.

[35] Rosen, M., Dincer, I., “Effect of varying dead-state properties on energy and exergy analyses of thermal systems”, *International Journal of Thermal Sciences*, Vol. 43, pp. 121-133, 2004.

[36] Kwak, H., Kim, D., Jeon, J., “Exergetic and thermoeconomic analyses of power plants”, *Energy*, Vol. 28, pp. 343–360, 2003.

[37] Rosen, M., Dincer, I. “Exergoeconomic analysis of power plants operating on various fuels”. Applied Thermal Engineering, Vol. 23, pp. 643-658. 2003.

[38] Tsatsaronis, G., “Definitions and nomenclature in exergy analysis and exergoeconomics”, *Energy*, Vol. 32, pp. 249–253, 2007.

[39] Ameri, M., Ahmadi, P., Hamidi, A., “Energy, exergy and exergoeconomic analysis of a steam power plant: a case study”. *International Journal of Energy Research*, Vol. 33, pp. 499-512, 2009.

[40] Ahmadi, P., Dincer, I., Rosen, M., “Exergy, exergoeconomic and environmental analyses and evolutionary algorithm based multi-objective optimization of combined cycle power plants”, *Energy*, Vol. 36, pp. 5886-5898, 2011.

[41] Cziesla, F., Tsatsaronis, G**.,** Gao Z**.,** “Avoidable thermodynamic inefficiencies and costs in an externally fired combined cycle power plant”, *Energy*, Vol. 31, pp. 1472–1489, 2006.

[42] Sahoo, P., “Exergoeconomic analysis and optimization of a cogeneration system using evolutionary programming”, *Applied Thermal Engineering*, Vol. 28, Issue.13, pp.1580-1588, 2008.

[43] Tsatsaronis**,** G**.,** Moran M**.,** “Exergy-aided cost minimization”, *Energy Conversion and Management*, Vol. 38, pp. 1535-1542, 1997.

[44] Toffolo, A., Lazzaretto, A., “Evolutionary algorithms for multi-objective energetic and economic optimization in thermal system design”. *Energy*, Vol. 27, pp. 549-567. 2002.

[45] Ozgener, L**.,** Hepbasli**,** A**.,** Dincer, I., Rosen, M., "Exergoeconomic analysis of geothermal district heating systems: A case study", *Applied Thermal Engineering*, Vol. 27, pp. 1303–1310, 2007.

[46] Sayyadali, H., Sabzaligol, T., "Exergoeconomic optimization of a 1000 MW light water reactor power generation system". *International Journal of Energy Research*, Vol. 33, Issue 4, pp. 378-395, 2009.

[47] Uhlenbruck, S., Lucas, K., "Exergoeconomically—aided evolution strategy applied to a combined cycle power plant", *International Journal of Thermal Sciences*, Vol. 43, pp. 289–296, 2004.

[48] Al-Jeelani, H., "Evaluation of Air Quality in the Holy Makkah during Hajj Season 1425 H", *Journal of Applied Sciences Research*, Vol. 5, No. 1, pp. 115-121, 2009.

[49] "Economic Impact Analysis of the Proposed Stationary Combustion Turbines NESHAP", *Environmental Protection Agency*, Final Report, pp. 2-4, 2002.

[50] Al-Jeelani, H., "Air quality assessment at Al-Taneem area in the Holy Makkah City, Saudi Arabi", *Environmental Monitoring and Assessment*, Vol. 156**,** pp. 211-222, 2009.

[51] Hermann, W., "Quantifying global exergy resources", *Energy*, Vol. 31, pp. 1685–1702, 2006.

[52] Szargut, J., Morris, D., Steward, F., "Exergy analysis of thermal, chemical, and metallurgical processes". Hemisphere Publishing, *International Journal of Heat and Fluid Flow*, Vol. 10, No. 1, 1989.

[53] Moran, M., Shapiro, H., “Fundamentals of Engineering Thermodynamics”, Fifth edition, Chapter 9, pp. 389-390, Wiley, 2006.

[54] Langston, L., Opdyke, G., Dykewood, E., “Introduction to Gas Turbines for Non Engineers”, *The Global Gas Turbine News*, University of Connecticut, Vol. 37: 1997.

[55] Cengel, Y., Boles, M., “Thermodynamics: an engineering approach”, Sixth edition, Chapter 9, Mc Graw Hill, New York, 2008.

[56] Sonntag, B., Van W., “Fundamentals of Thermodynamics”, 6th Edition, pp. 411. 2003.

[57] Kakaras, E., Doukelis, A., Karellas, S., “Compressor intake-air cooling in gas turbine plants”, *Energy* 29, pp. 2347–2358, 2004.

[58] MacCracken, C., “Overview of the progress and the potential of thermal storage in off-peak turbine inlet cooling”. ASHRAE Transactions. Vol. 100
pp. 569-571, 1994.

[59] Kitchen, B., Ebeling, J., “Qualifying combustion turbines for inlet air cooling capacity enhancement”, in: International gas turbine and aero engine congress and exposition, June 5-8, Houston, Texas, 1995.

[60] Giourof, A., “Gas-turbine inlet-air cooling: you can almost pick your payback”, Journal Vol. 139, Issue: 5, pp. 56-58, 1995.

[61] De Lucia, M., Lanfranchi, C., Boggio, V., "Benefits of compressor inlet air cooling for gas turbine cogeneration plants". *Journal of Engineering for Gas Turbines and Power* Vol. 118, pp. 598-603, 1996.

[62] ASHRAE, "Hand book HVAC Systems and Equipment", Chapter 17, pp. 17.1-17.5, 2008.

[63] Andrepont, J., "Combustion turbine inlet air cooling (CTIAC): fuels and technology options in district energy applications", *American Society of Heating Refrigerating, and Air Conditioning Engineers*, Vol. 107, pp. 892-902, 2001.

[64] Stewart, W., "Design Guide: Combustion Turbine Inlet Air Cooling System" ASHRAE, Atlanta, GA, Technical Report No. 902, pp. 165–173, 1999.

[65] Google Maps, "http://maps.google.com/maps?hl=en&tab=il"

[66] Makkah Power Plant's Manual and Layout.

[67] Dincer I., Zamfirescu C. "Sustainable energy and applications", Springer: New York. In press. 2011.

[68] Roosen, P., Uhlenbruck, S., Lucas, K., "Pareto optimization of a combined cycle power system as a decision support tool for trading off investment vs. operating costs", *International Journal of Thermal Sciences*, Vol. 42, pp. 553–560, 2003.

[69] Design Expert, State Ease , Version 8.1.6

[70] Lind , I., "Regressor and structure selection: uses of ANOVA in system Identification", *Linkopings university*,, pp. 4-48. 2006.

[71] Burdick, R., Borror, C., Montgomery, D., "Design and Analysis of Gauge R&R Studies: Making Decisions with Confidence Intervals in Random and Mixed

Anova Models (ASA-SIAM Series on Statistics and Applied Probability" *Society for Industrial Applied Mathematics*, Arizona State University, US, 2005.

[72] Montgomery, D., "Design and Analysis of Experiments", 5th Edition, John Wiley & Sons Inc., UK, 2001.

[73] Doncaster, C. Patrick. Davey, Andrew J. H."Analysis of Variance and Covariance: How to Choose and Construct Models for the Life Sciences", *Cambridge University Press*, UK, 2007.

[74] Quinn, Gerry P. Keough, Michael J. "Experimental Design and Data Analysis for Biologists", *Cambridge University Press*, UK, 2002.

[75] Khuri, Andre I. "Response Surface Methodology and Related Topics", *World Scientific Publishing Company*, US, 2006.

[76] Khuri, Andre I. "Linear Model Methodology", *Chapman & Hal*, US, 2009.

[77] Derringer, G., Suich, R., "Simultaneous Optimization of Several Response Variables", Journal of Quality Technology, Vol. 12, Issue. 4, pp. 214-219, 1980.

[78] Saidur, R., Ahamed, J., Masjuki, H., "Energy, exergy and economic analysis of industrial boilers" *Energy Policy*, Vol. 38, pp. 2188–2197, 2010.

[79] Tsujikawa, Y., Sawada, T., "Characteristics of hydrogen-fueled gas turbine cycle with intercooler, hydrogen turbine and hydrogen heater", *International Journal of Hydrogen Energy*, Vol. 10, No. 10, pp. 677-683, 1985.

[80] El-hadik, A., "The Impact of Atmospheric Conditions on Gas Turbine Performance" *Journal of Engineering for Gas Turbines and Power*, Vol. 112, Issue. 4, pp. 590, 1990.

[81] Dincer, I., Rosen, M., “Thermal Energy Storages Systems and Applications”, John Wiley and Sons Ltd., First Edition, Chapter 9, 2011.

[82] Serth, R., “Process Heat Transfer principles and Applications” *Elsevier Science & Technology Books*, pp. 730, 2007.

Appendix A

Actual operating parameters for system 1

State Point	BBC-1			BBC-2		
	Pressure (bar)	Temperature (C^0)	Mass flow rate (l/s)	Pressure (bar)	Temperature (C^0)	Mass flow rate (l/s)
1	1.0	45	5.3	1.0	45	5.3
2	4.5	50	5.3	4.5	50	5.3
3	4.5	50	5.3	4.5	50	5.3
4	90-100	55-60	5.3	90-100	55-60	5.3
5	90	55-60	5.3	90	55-60	5.3
6	1	45	232000	1	45	232000
7	8-9.5	300	N/A	8-9.5	300	N/A
8	N/A	1000	232000	N/A	1000	232000
9	N/A	560	232000	N/A	560	232000
10	9	300	232000	9	300	232000

State Point	BBC-3			BBC-4 & BBC-5		
	Pressure (bar)	Temperature (C^0)	Mass flow rate (l/s)	Pressure (bar)	Temperature (C^0)	Mass flow rate (l/s)
1	1.0	45	5.3	1.0	45	5.3
2	4.5	50	5.3	4.5	50	5.3
3	4.5	50	5.3	4.5	50	5.3
4	90-100	55-60	5.3	90-100	55-60	5.3
5	90	55-60	5.3	90	55-60	5.3
6	1	45	232000	1	45	232000
7	8-9.5	300	N/A	8-9.5	300	N/A
8	N/A	1000	232000	N/A	1000	232000
9	N/A	560	232000	N/A	560	232000
10	9	300	232000	9	300	232000

Appendix B

Actual operating parameters for system 2

State Point	GE-B1			GE-B2		
	Pressure (bar)	Temperature (C^0)	Mass flow rate (l/s)	Pressure (bar)	Temperature (C^0)	Mass flow rate (l/s)
1	10-20	40-50	4.75	10-20	40-50	4.75
2	120	50-60	4.75	120	50-60	4.75
3	75	50-60	4.75	75	50-60	4.75
4	75	50-60	4.75	75	50-60	4.75
5	350	70	4.75	350	70	4.75
6	350	70	4.75	350	70	4.75
7	350	70	4.75	350	70	4.75
8	180	80	N/A	180	80	N/A
9	350	70	0.475	350	70	0.475
10	N/A	1004	194442	N/A	1004	194442
11	N/A	575	194442	N/A	575	194442
12	14.7	40-50	194442	14.7	40-50	194442
13	108	350	194442	108	350	194442
14	108	350	N/A	108	350	N/A
15	108	80	N/A	108	80	N/A
16	180	N/A	N/A	180	N/A	N/A
17	40	40-45	N/A	40	40-45	N/A
18	22	50-55	N/A	22	50-55	N/A

Appendix B (Continued)

State Point	GE-B3			GE-B4		
	Pressure (bar)	Temperature (C^0)	Mass flow rate (l/s)	Pressure (bar)	Temperature (C^0)	Mass flow rate (l/s)
1	10-20	40-50	4.75	10-20	40-50	4.75
2	120	50-60	4.75	120	50-60	4.75
3	75	50-60	4.75	75	50-60	4.75
4	75	50-60	4.75	75	50-60	4.75
5	350	70	4.75	350	70	4.75
6	350	70	4.75	350	70	4.75
7	350	70	4.75	350	70	4.75
8	180	80	N/A	180	80	N?A
9	350	70	0.475	350	70	0.475
10	N/A	1004	194442	N/A	1004	194442
11	N/A	575	194442	N/A	575	194442
12	14.7	40-50	194442	14.7	40-50	194442
13	108	350	194442	108	350	194442
14	108	350	N/A	108	350	N/A
15	108	80	N/A	108	80	N/A
16	180	N/A	N/A	180	N/A	N/A
17	40	40-45	N/A	40	40-45	N/A
18	22	50-55	N/A	22	50-55	N/A

Appendix B (Continued)

State Point	GE-E1			GE-E2		
	Pressure (bar)	Temperature (C^0)	Mass flow rate (l/s)	Pressure (bar)	Temperature (C^0)	Mass flow rate (l/s)
1	10-20	40-50	5.44	10-20	40-50	5.44
2	120	50-60	5.44	120	50-60	5.44
3	75	50-60	5.44	75	50-60	5.44
4	75	50-60	5.44	75	50-60	5.44
5	450	70	5.44	450	70	5.44
6	450	70	5.44	450	70	5.44
7	450	70	5.44	450	70	5.44
8	220	80	N/A	220	80	N/A
9	450	70	0.544	450	70	0.544
10	N/A	1085	240693	N/A	1085	240693
11	N/A	580	240693	N/A	580	240693
12	14.7	40-50	240693	14.7	40-50	240693
13	120	360	240693	120	360	240693
14	120	360	N/A	120	360	N/A
15	120	80	N/A	120	80	N/A
16	120	N/A	N/A	120	N/A	N/A
17	120	40-45	N/A	120	40-45	N/A
18	120	50-55	N/A	120	50-55	N/A

Appendix B (Continued)

State Point	GE-E3			GE-E4		
	Pressure (bar)	Temperature (C^0)	Mass flow rate (l/s)	Pressure (bar)	Temperature (C^0)	Mass flow rate (l/s)
1	10-20	40-50	5.44	10-20	40-50	5.44
2	120	50-60	5.44	120	50-60	5.44
3	75	50-60	5.44	75	50-60	5.44
4	75	50-60	5.44	75	50-60	5.44
5	450	70	5.44	450	70	5.44
6	450	70	5.44	450	70	5.44
7	450	70	5.44	450	70	5.44
8	220	80	N/A	220	80	N/A
9	450	70	0.544	450	70	0.544
10	N/A	1085	240693	N/A	1085	240693
11	N/A	580	240693	N/A	580	240693
12	14.7	40-50	240693	14.7	40-50	240693
13	120	360	240693	120	360	240693
14	120	360	N/A	120	360	N/A
15	120	80	N/A	120	80	N/A
16	120	N/A	N/A	120	N/A	N/A
17	120	40-45	N/A	120	40-45	N/A
18	120	50-55	N/A	120	50-55	N/A

Appendix B (Continued)

State Point	GE-E5			GE-E6		
	Pressure (bar)	Temperature (C^0)	Mass flow rate (l/s)	Pressure (bar)	Temperature (C^0)	Mass flow rate (l/s)
1	10-20	40-50	5.44	10-20	40-50	5.44
2	120	50-60	5.44	120	50-60	5.44
3	75	50-60	5.44	75	50-60	5.44
4	75	50-60	5.44	75	50-60	5.44
5	450	70	5.44	450	70	5.44
6	450	70	5.44	450	70	5.44
7	450	70	5.44	450	70	5.44
8	220	80	N/A	220	80	N/A
9	450	70	0.544	450	70	0.544
10	N/A	1085	240693	N/A	1085	240693
11	N/A	580	240693	N/A	580	240693
12	14.7	40-50	240693	14.7	40-50	240693
13	120	360	240693	120	360	240693
14	120	360	N/A	120	360	N/A
15	120	80	N/A	120	80	N/A
16	120	N/A	N/A	120	N/A	N/A
17	120	40-45	N/A	120	40-45	N/A
18	120	50-55	N/A	120	50-55	N/A